

# 中性子星連星合体からの 重力波と電磁波

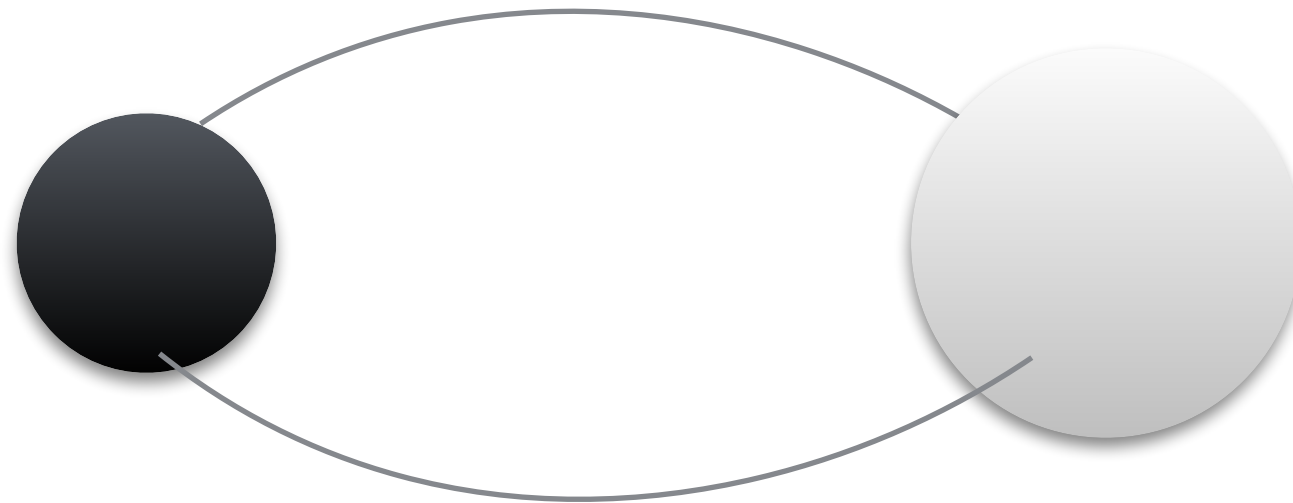
川口 恭平

2020.01.29 @HEAコロキウム

# Introduction



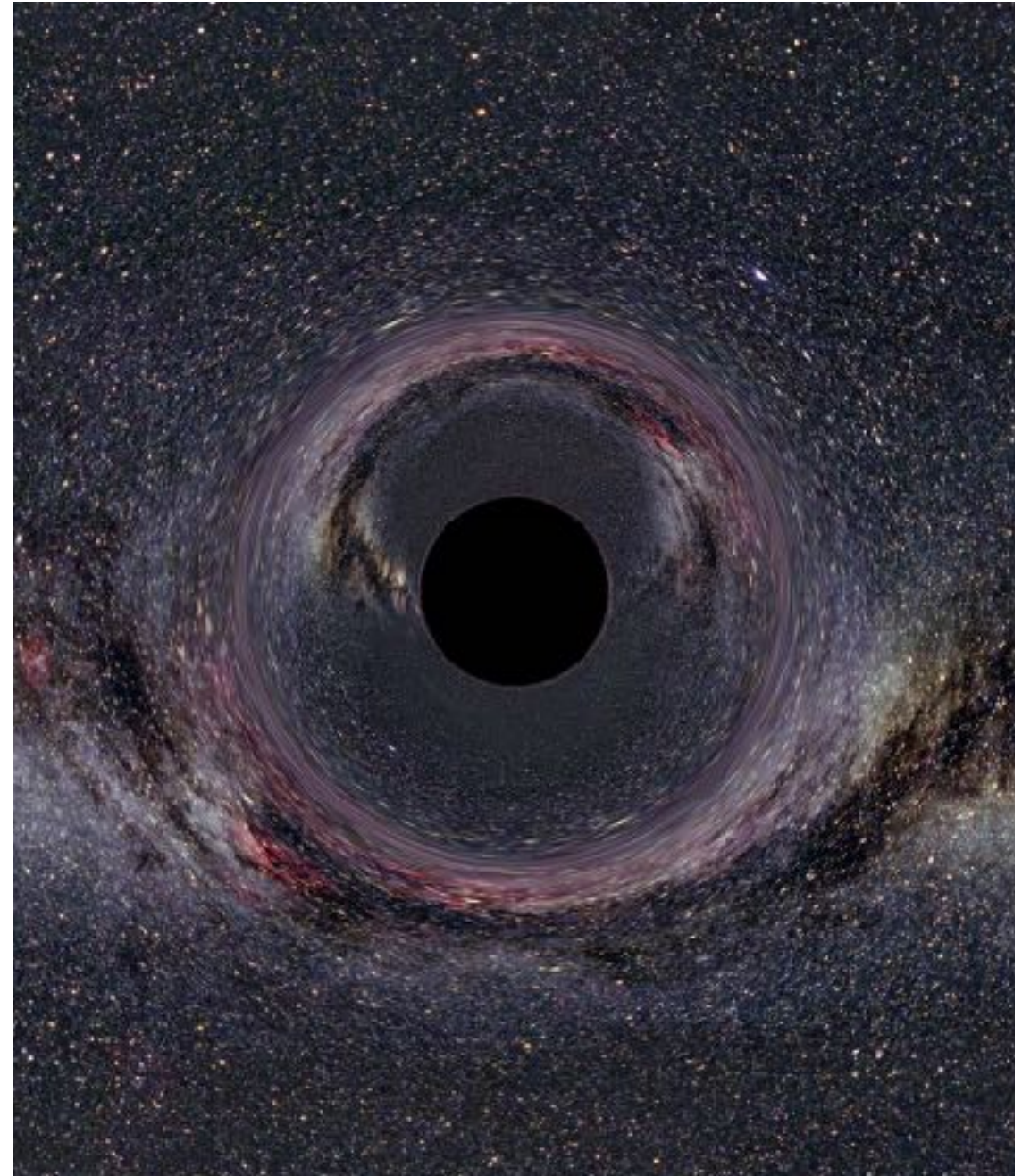
# Compact Binary



- A compact binary: A binary system composed of **compact objects**, such as a black hole (BH), a neutron star (NS), (and/or a white dwarf)

# Black hole

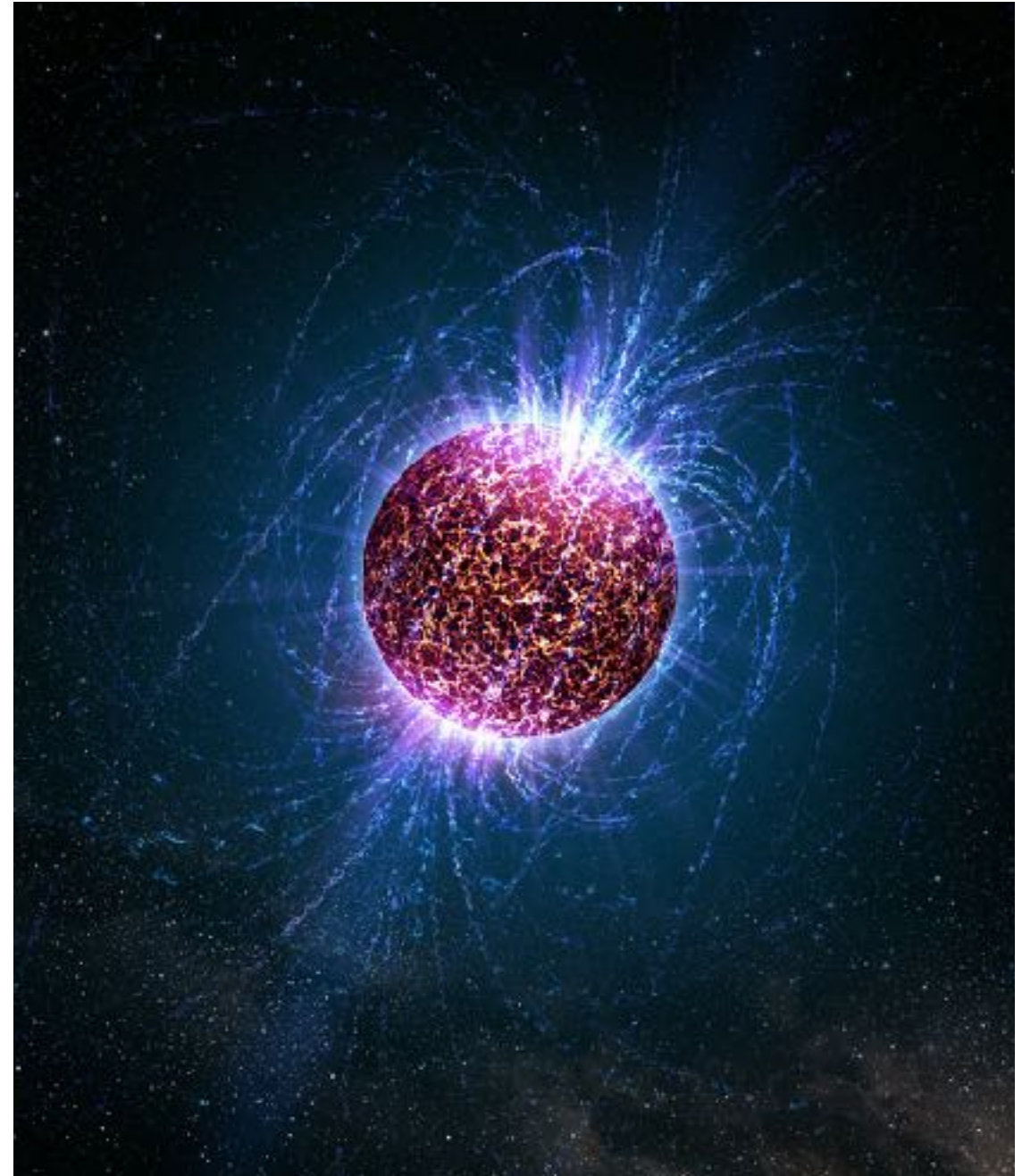
- A region of the space-time where anything, including lights, can not escape for its strong gravity. The surface of the region is called the Event horizon.
- Black hole can have only three physical parameters;  
The **mass**,  
**spin angular momentum**,  
and **charge**.  
For astronomical situations, the charge is consider to be neutralized.



ref) U. Kraus (2014)

# Neutron star

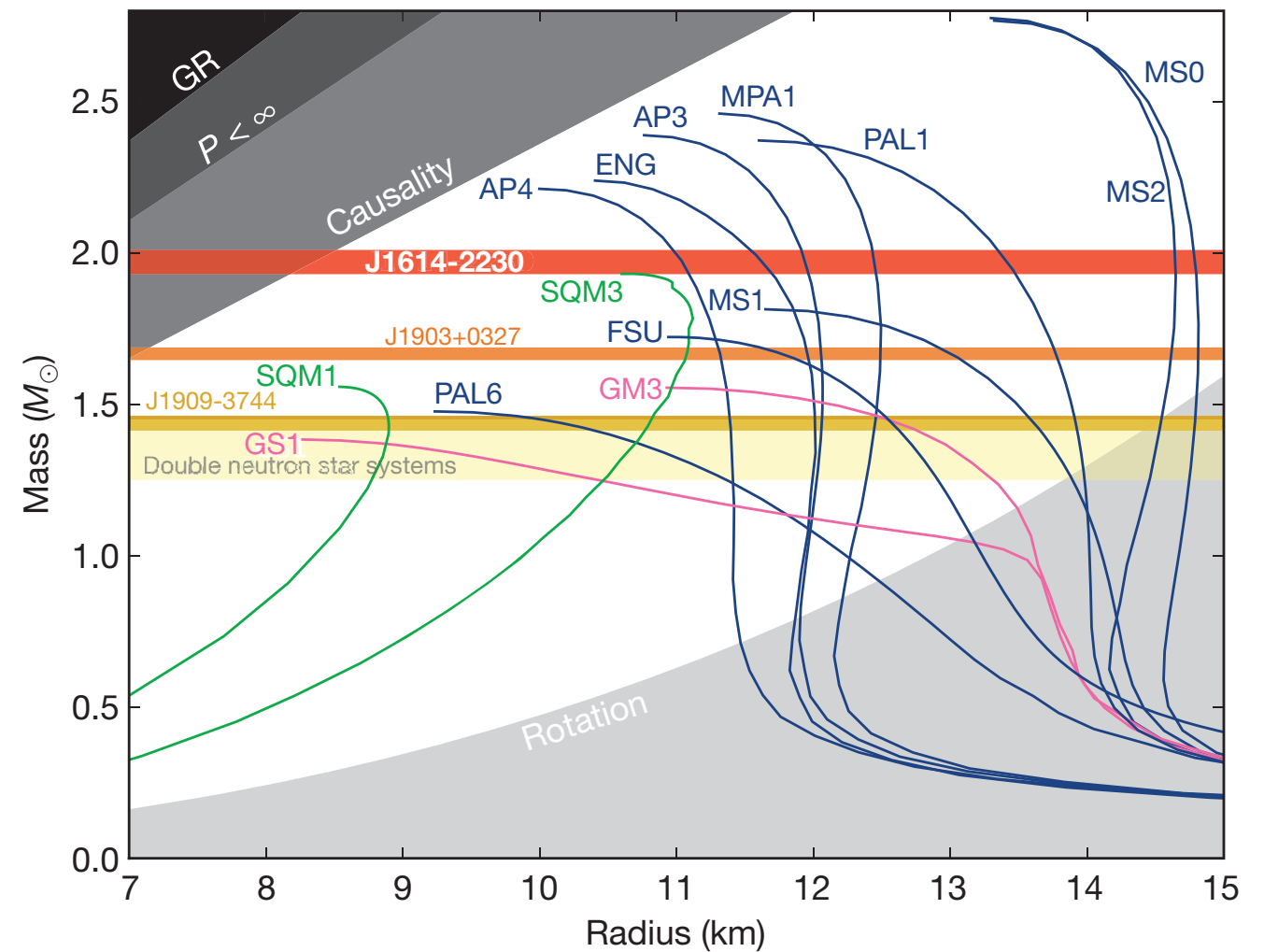
- A neutron star is an extremely dense star formed as the result of the collapse of a massive star.
- Most of them are observed as pulsars, which are rapidly rotating, highly magnetized neutron stars, emitting a strong beams.
- 1-2Msun, typically  $\sim 1.4$  Msun,  $\sim 10$  km





# NS equation of state (EoS)

- The NS radius / maximum NS mass is sensitive to the equation of state (EoS) of NS, which is still not comprehended yet.
- Precise measurement of the NS radius / maximum NS mass provides us the information of the NS EoS.

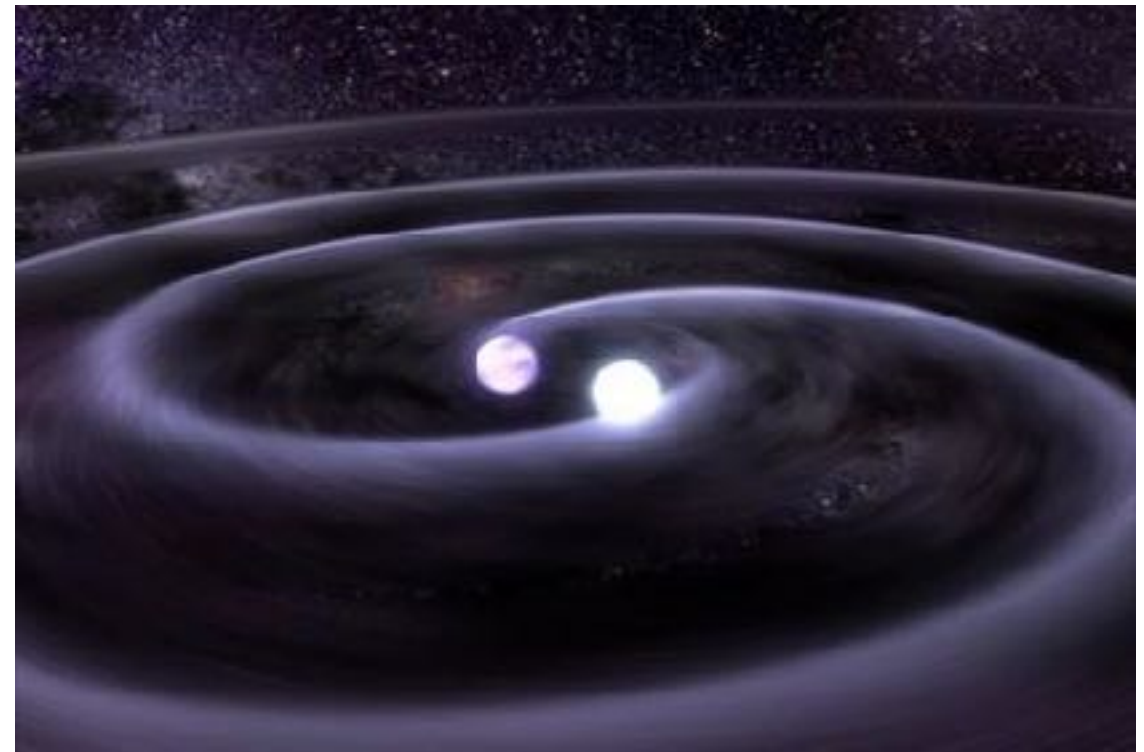


ref) P. Demorest et. al. (2010)



# Gravitational waves (GWs)

- Gravitational waves are the ripples of curvature that propagate at the speed of light, and their existence is predicted by general relativity.
- The binary system composed of compact objects, such as NS-NS, BH-NS and BH-BH binary, are the efficient sources of gravitational waves.



<http://www.amnh.org/>

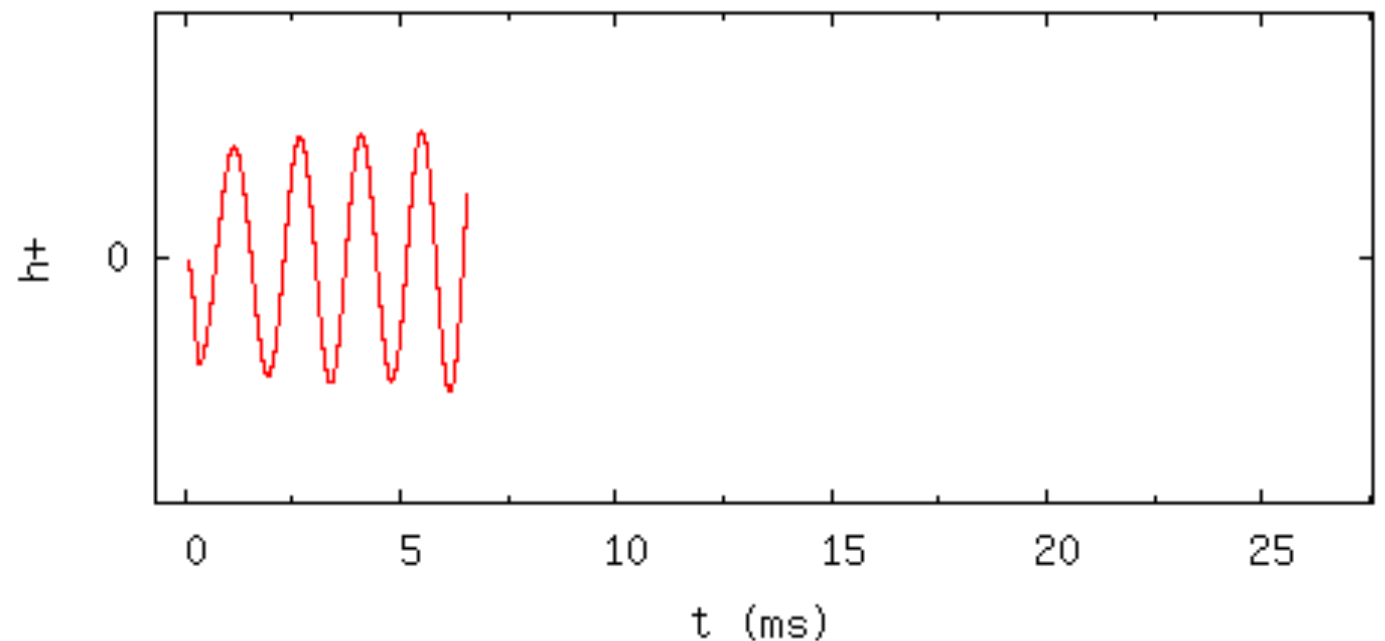
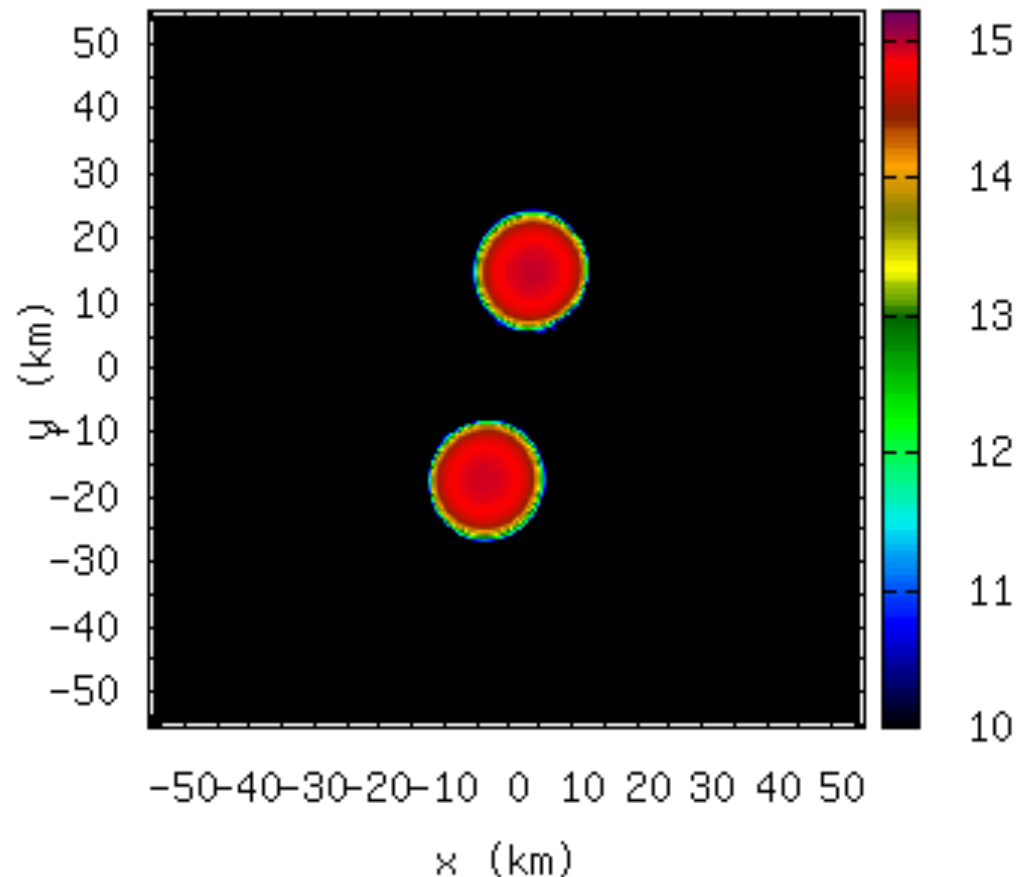
$$g_{\mu\nu} = \eta_{\mu\nu} + h_{\mu\nu} + \mathcal{O}(h^2)$$

$$\left( \frac{\partial^2}{\partial t^2} - \nabla^2 \right) h_{\mu\nu} = 0$$

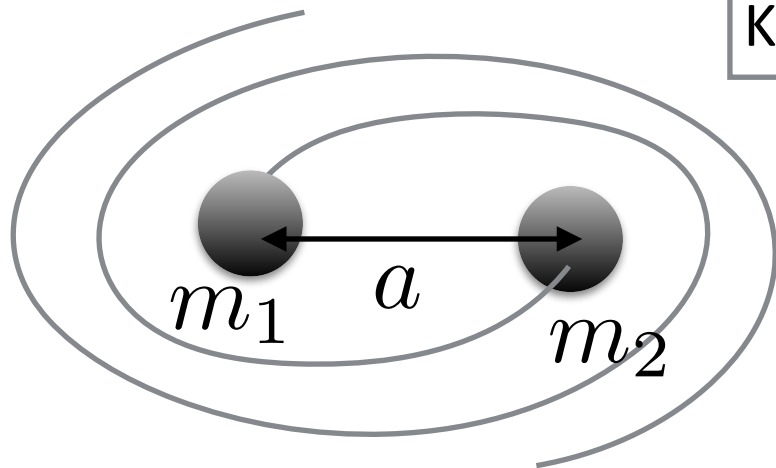
# Compact binary mergers

- Compact binaries efficiently emit gravitational waves shrinking their orbital separation, and the objects eventually merge  
→ **compact binary mergers**
- Gravitational waveform from a binary merger contains rich physical information of the source (masses, spins, distance, inclination, etc...)

t=6.2523 ms



# Gravitational waves from a compact binary merger (leading order)



Kepler's law

$$m = m_1 + m_2$$

:total mass

$$\eta = \frac{m_1 m_2}{(m_1 + m_2)^2}$$

:symmetric mass ratio

$$E = -\frac{\eta m^2}{a}$$

:total energy

$$f = \frac{\Omega}{2\pi} = \frac{1}{2\pi} \sqrt{\frac{m}{a^3}}$$

:orbital frequency

Quadrupole formula

$$\Rightarrow |h| \approx \frac{2\pi^{2/3} \mathcal{M}^{5/3}}{D} f_{\text{GW}}^{2/3} \quad \dot{E}_{\text{GW}} = -\frac{32\eta}{5} \left(\frac{m}{a}\right)^5$$

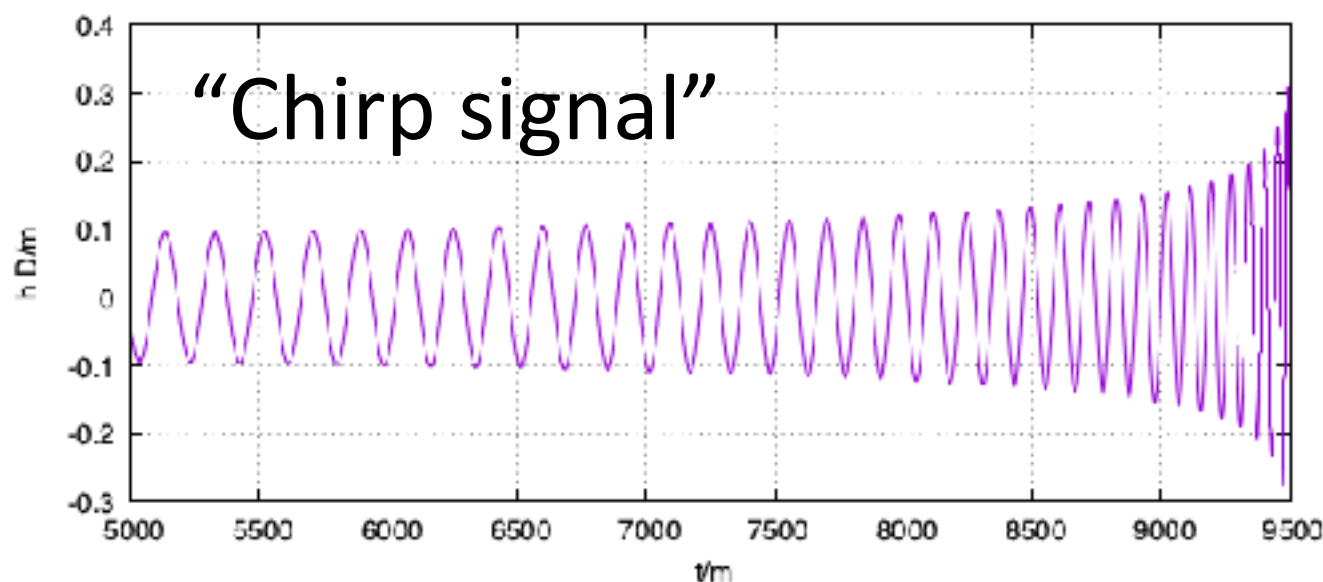
:energy loss via GW emission

$$\frac{df_{\text{GW}}}{dt} = \frac{96}{5} \pi^{8/5} \mathcal{M}_{\text{chirp}}^{5/3} f_{\text{GW}}^{11/3}$$

$$f_{\text{GW}} = 2f \quad \text{:GW frequency}$$

$$\mathcal{M}_{\text{chirp}} = m\eta^{3/5} \quad \text{:chirp mass}$$

$$D \quad \text{:luminosity distance}$$



# PostNewtonian expansion

PostNewtonian expansion:

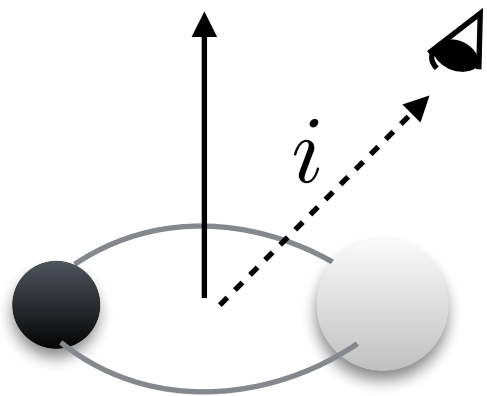
$$A(x) = \frac{2m\eta}{D} x (A_0 + A_{0.5}x^{0.5} + A_1x + A_{1.5}x^{1.5} + A_2x^2 + \dots)$$

$$h = Ae^{i\phi_{\text{GW}}}$$

$$\frac{dx}{dt} = \frac{64\eta}{5} x^5 (1 + a_1x + a_{1.5}x^{1.5} + a_2x^2 + \dots)$$

PostNewtonian Parameter:  $x := (\pi m f_{\text{GW}})^{2/3} \approx \left(\frac{m}{a}\right)$

※Note that amplitude factors depend on the inclination angle



$$A_0^+ = -(1 + \cos^2 i)$$

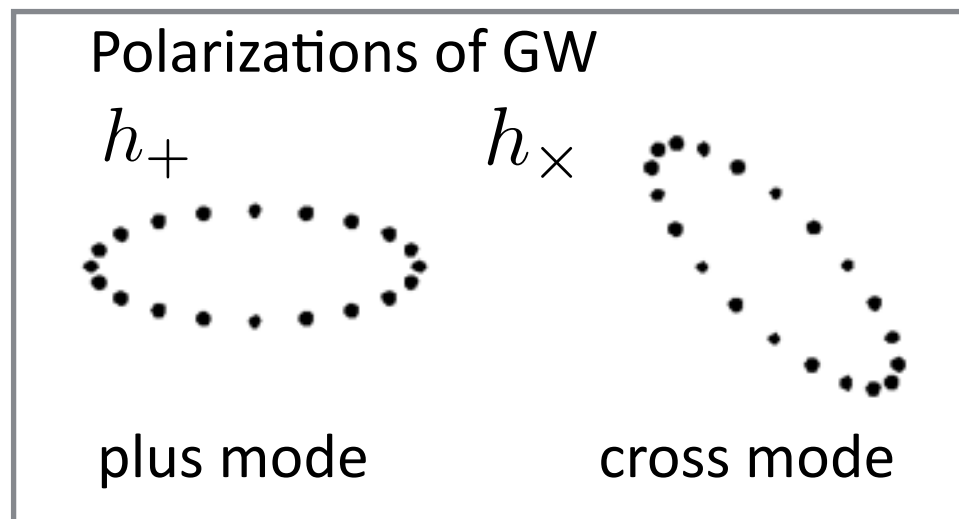
$$A_0^\times = -2\cos^2 i$$

- 0PN: chirp mass:  $\mathcal{M}_{\text{chirp}} = m\eta^{3/5}$
- 1PN: symmetric mass:  $\eta = \frac{m_1 m_2}{(m_1 + m_2)^2}$
- 1.5PN: spin:  $\chi_i = \frac{S_i}{m_i^2}$
- **5PN: tidal deformability:**  $\Lambda_i$



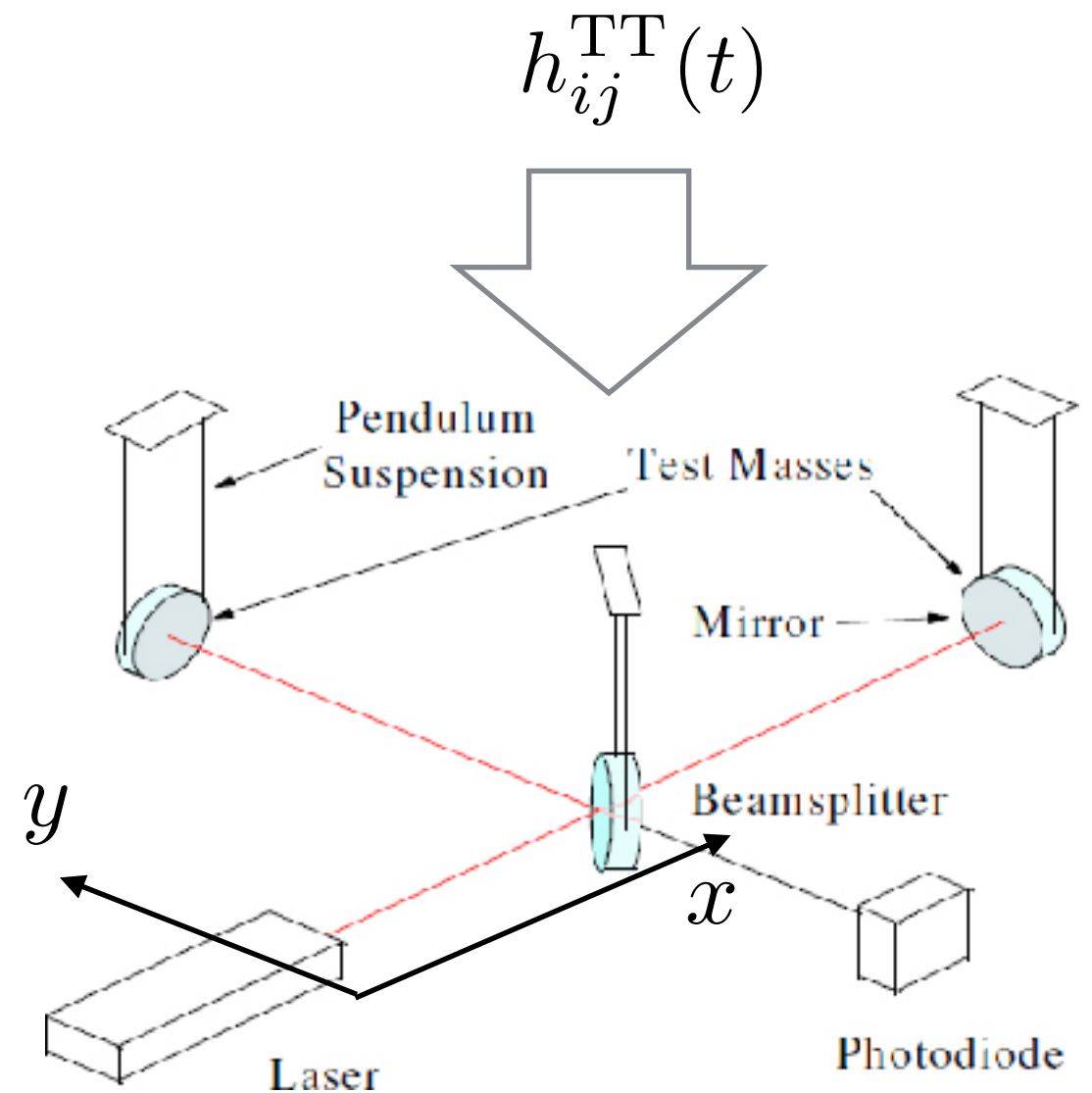
# Detecting gravitational waves

- Gravitational waves are detected by measuring the change of the distance by laser interferometer



Transverse-Traceless gauge:

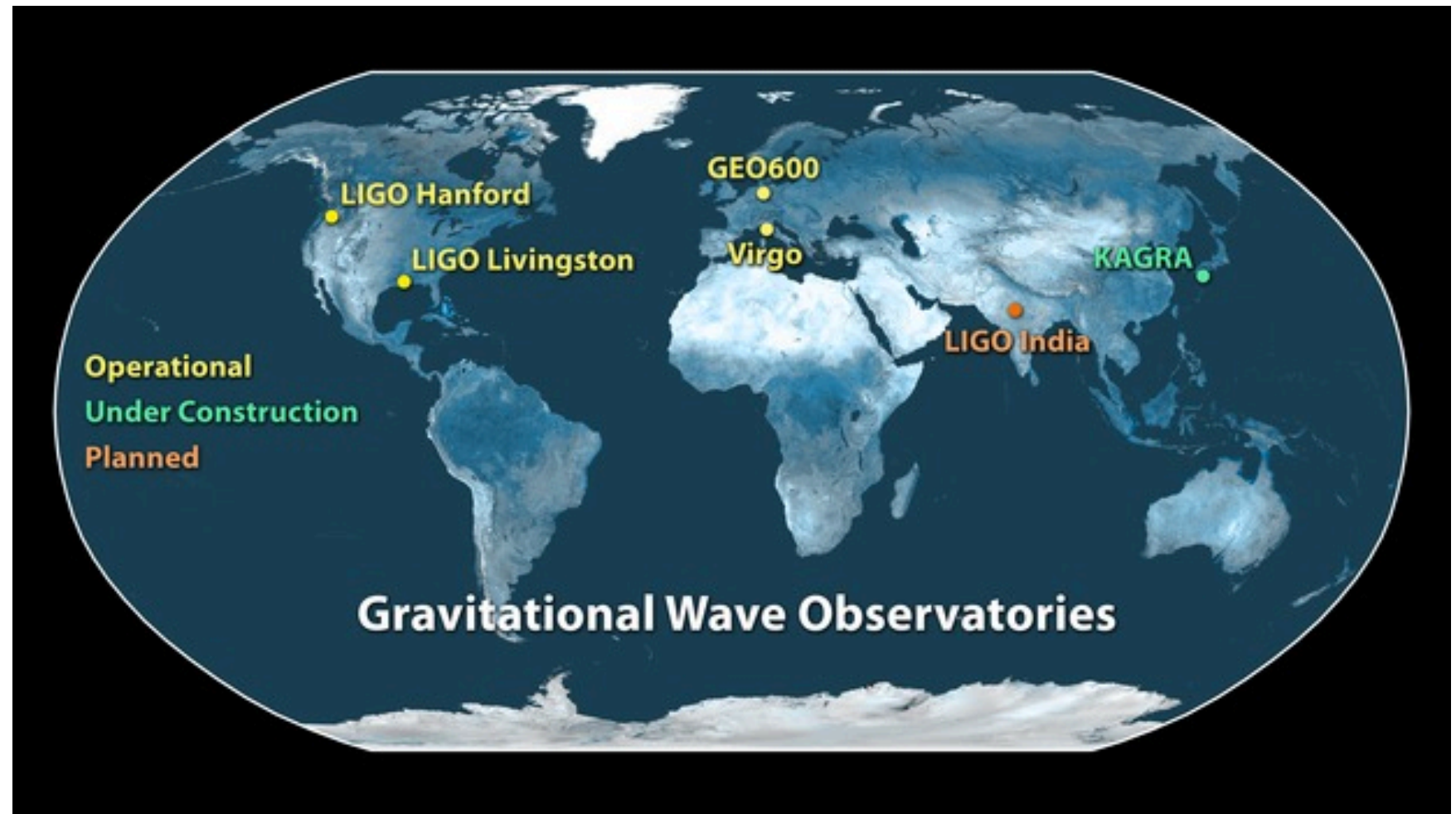
$$h_{\mu\nu}^{TT} = \begin{pmatrix} 0 & 0 & 0 & 0 \\ 0 & h_+ & h_{\times} & 0 \\ 0 & h_{\times} & -h_+ & 0 \\ 0 & 0 & 0 & 0 \end{pmatrix}$$



For face-on waves:  $\frac{d^2 X^i}{dt^2} \approx \frac{1}{2} \ddot{h}_{ij}^{TT} X^j$

# Gravitational wave detectors

## advanced LIGO



<https://www.ligo.caltech.edu/>

- GW sources for ground-based GW detectors

- **Compact binary mergers**
- Core collapse Super Novae
- Rotating Neutron stars
- Primordial GW (Inflation)
- Cosmic Strings



<http://www.virgo-gw.eu/>



<http://gwcenter.icrr.u-tokyo.ac.jp/>

# Gravitational wave events

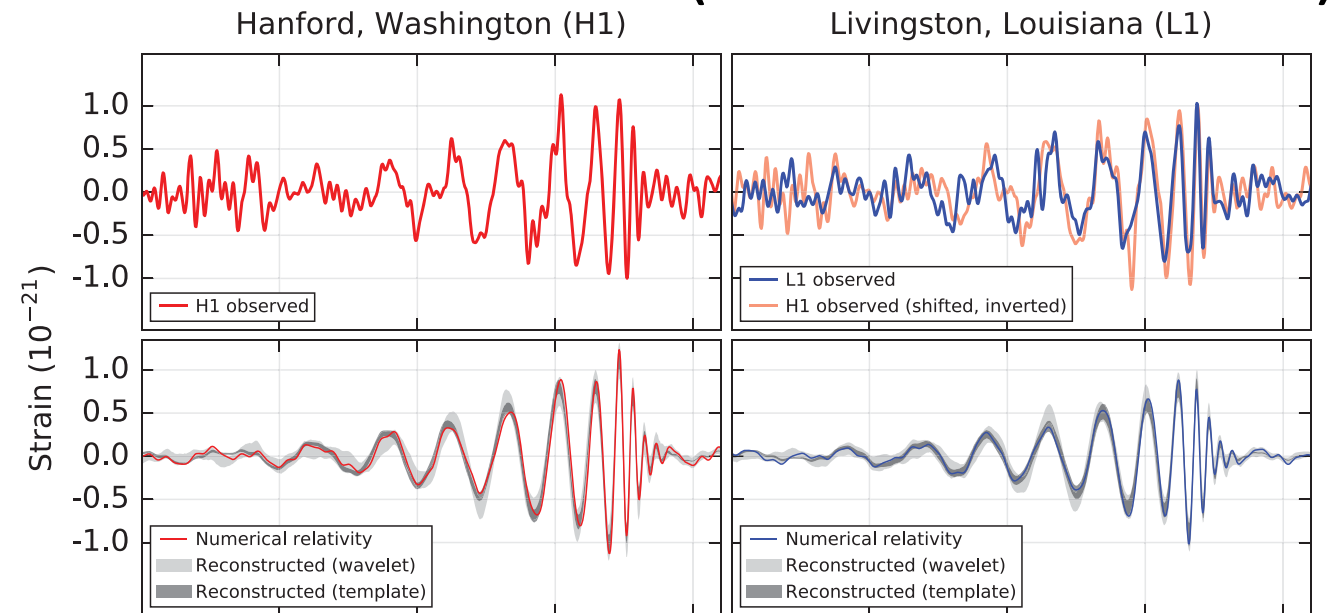
- Compact binary mergers are among the main targets of ground-based gravitational-wave detectors, such as **LIGO**, **Virgo**, and **KAGRA**
- Since 14th of September 2015, many GW events have been detected

- Binary BH (BBH; BH-BH)

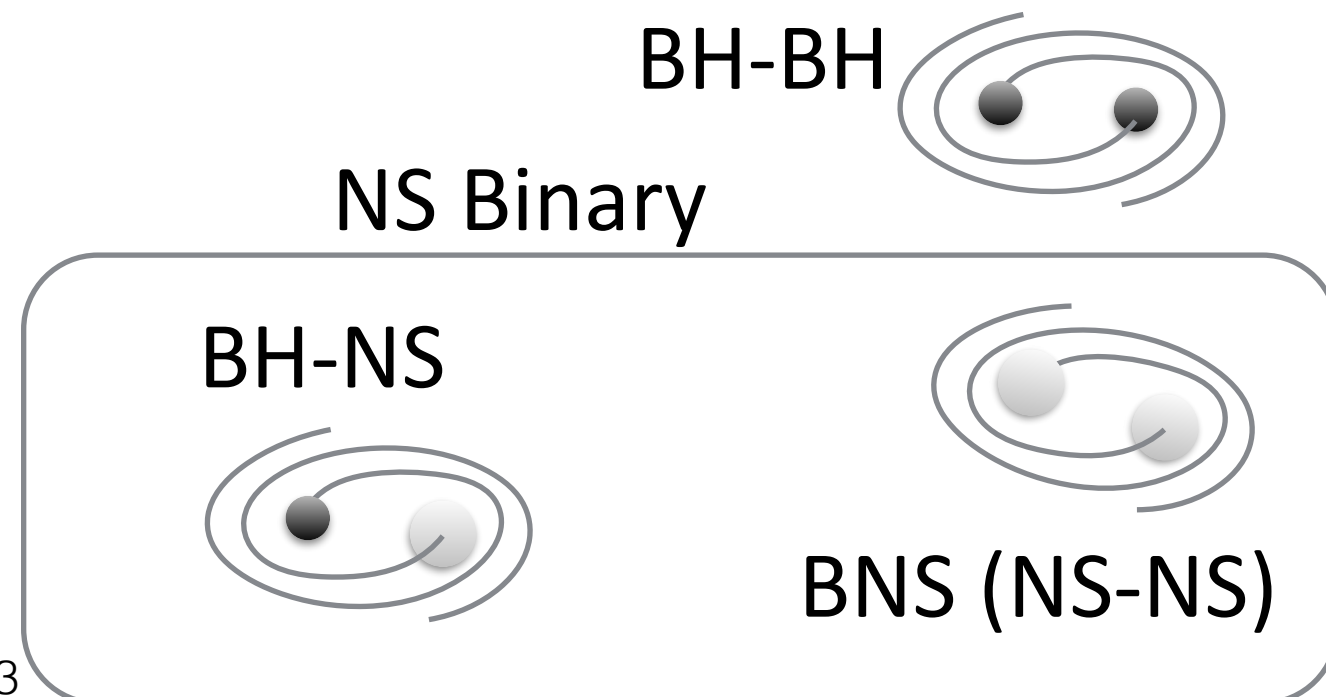
- GW150914, GW151012, GW151226, GW170104, GW170608, GW170809, GW170814, GW170817, GW170818, GW170823

- **Binary NS (BNS; NS-NS)**  
**GW170817**

## • GW150914 (The first GW event)

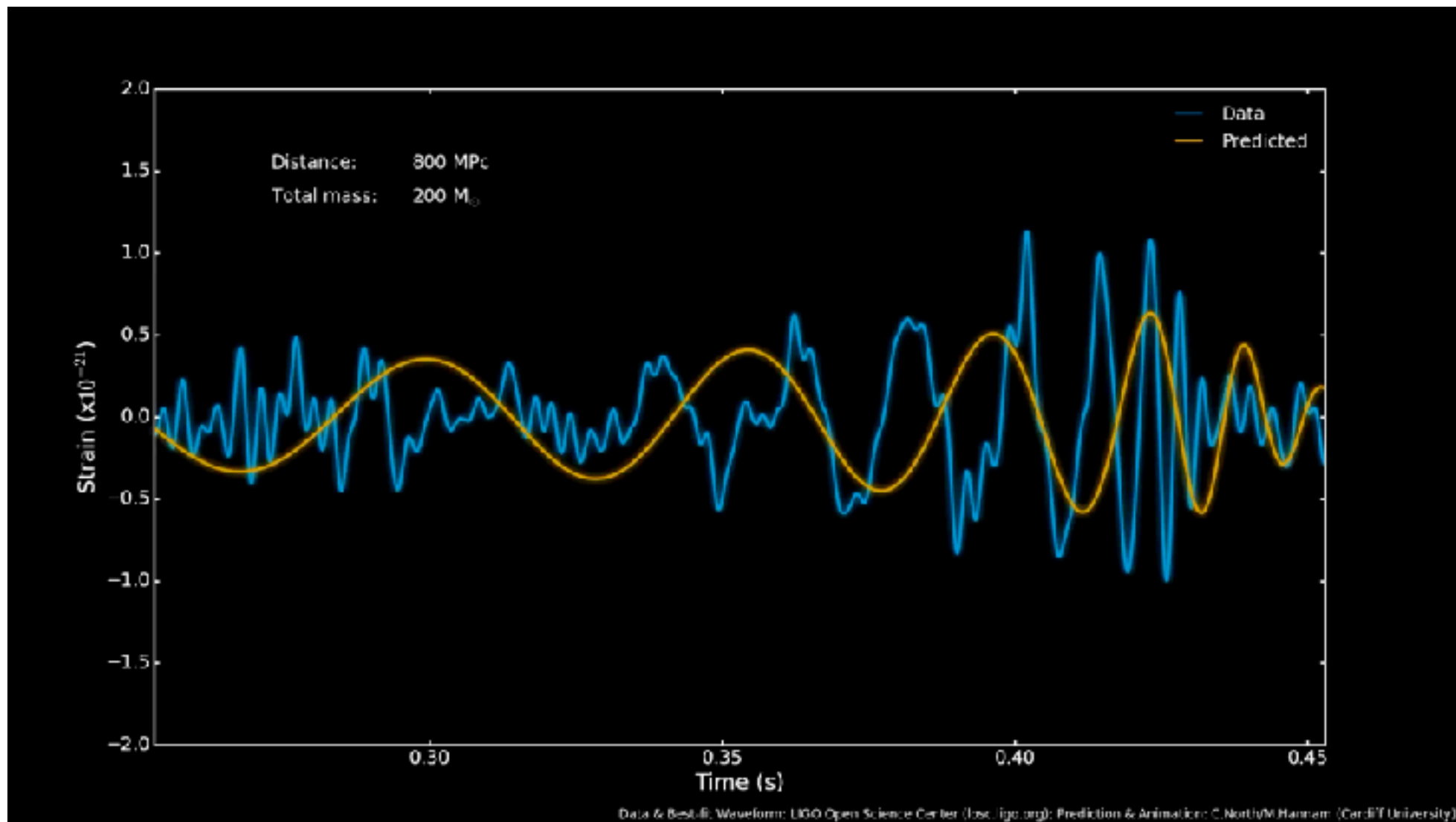


Ref: B.P. Abbot et al. 2016





# Parameter estimation (intuitive picture)



Ref: Gravitational Wave Open Science Center (<https://www.youtube.com/watch?v=fiQtwPn6kfw>)

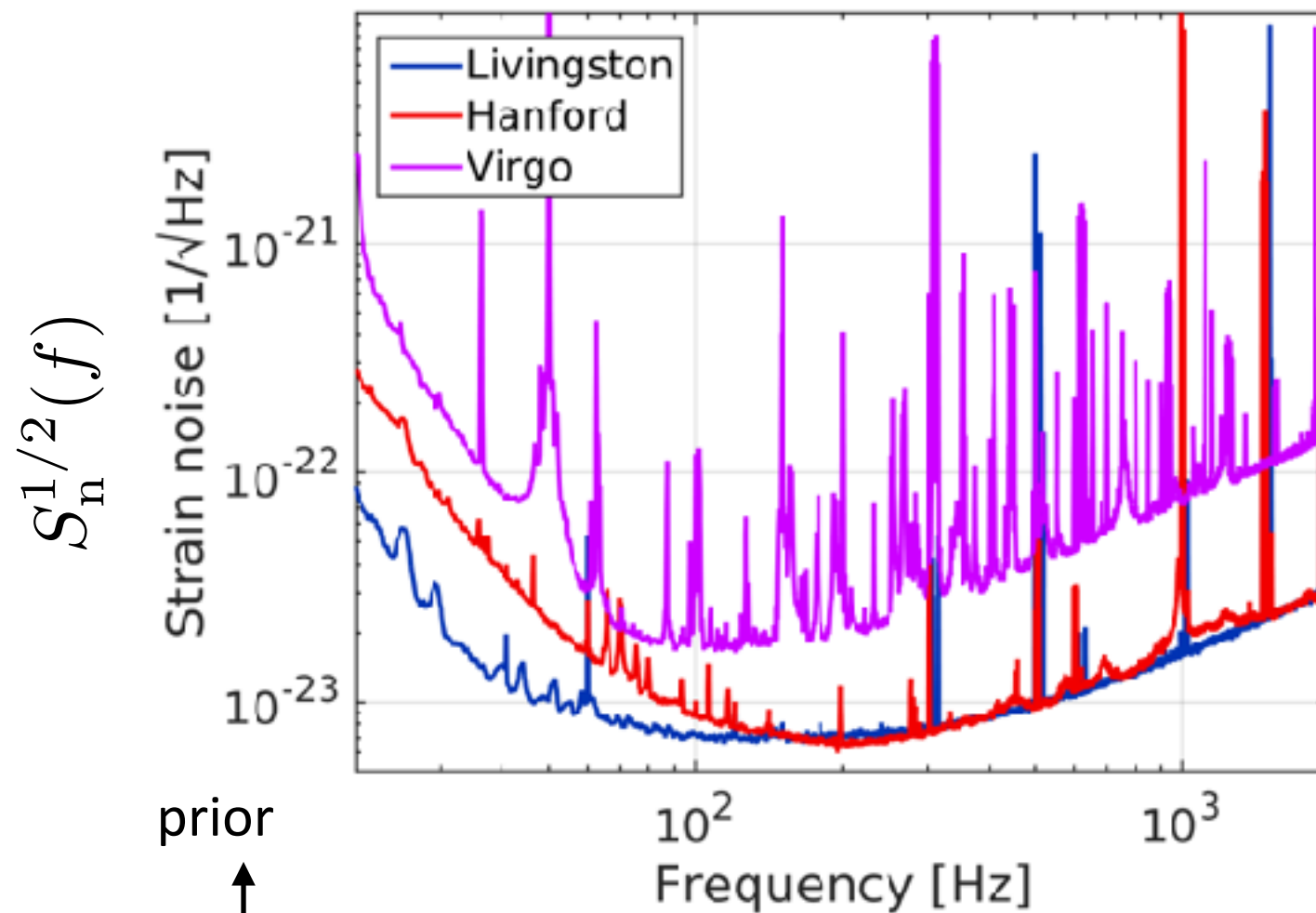
- Physical information is extracted from the signal by the comparison with theoretical waveform templates



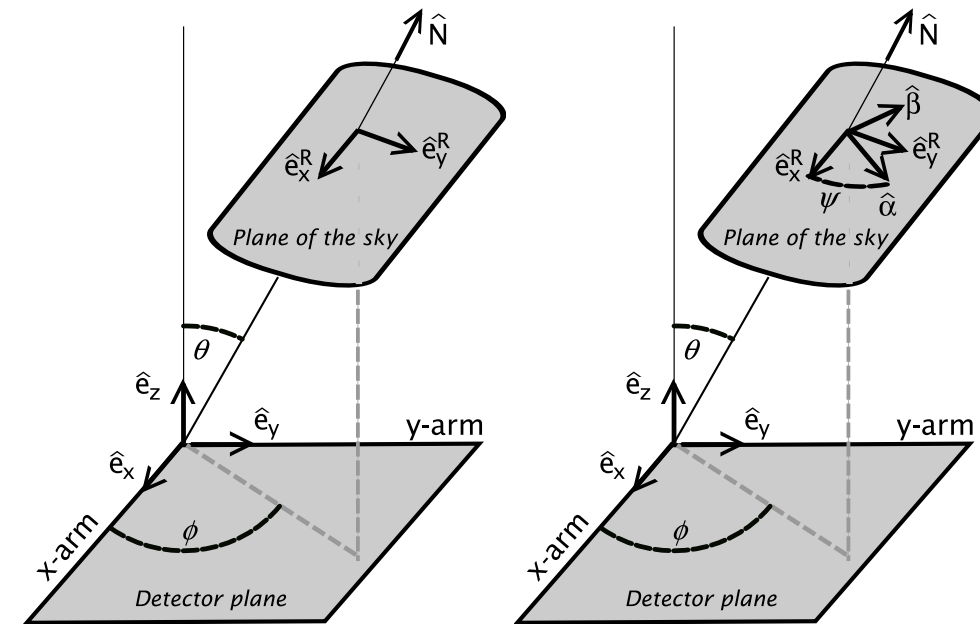
# Parameter estimation

Detector sensitivity

Ref: B.P.Abbot et al. 2017



Ref: Sathyaprakash & Schutz 2009



posterior

prior

likelihood

$$p(\vec{\theta}|\vec{d}) \propto p(\vec{\theta}) \prod_{\text{det}} \mathcal{L}_{\text{det}}(\vec{d}|\vec{\theta}) \quad \mathcal{L}_{\text{det}}(\vec{d}|\vec{\theta}) = \exp \left[ -2 \int_0^\infty \frac{|d(f) - \tilde{h}(f; \vec{\theta})|^2}{S_{n,\text{det}}(f)} df \right]$$

signal

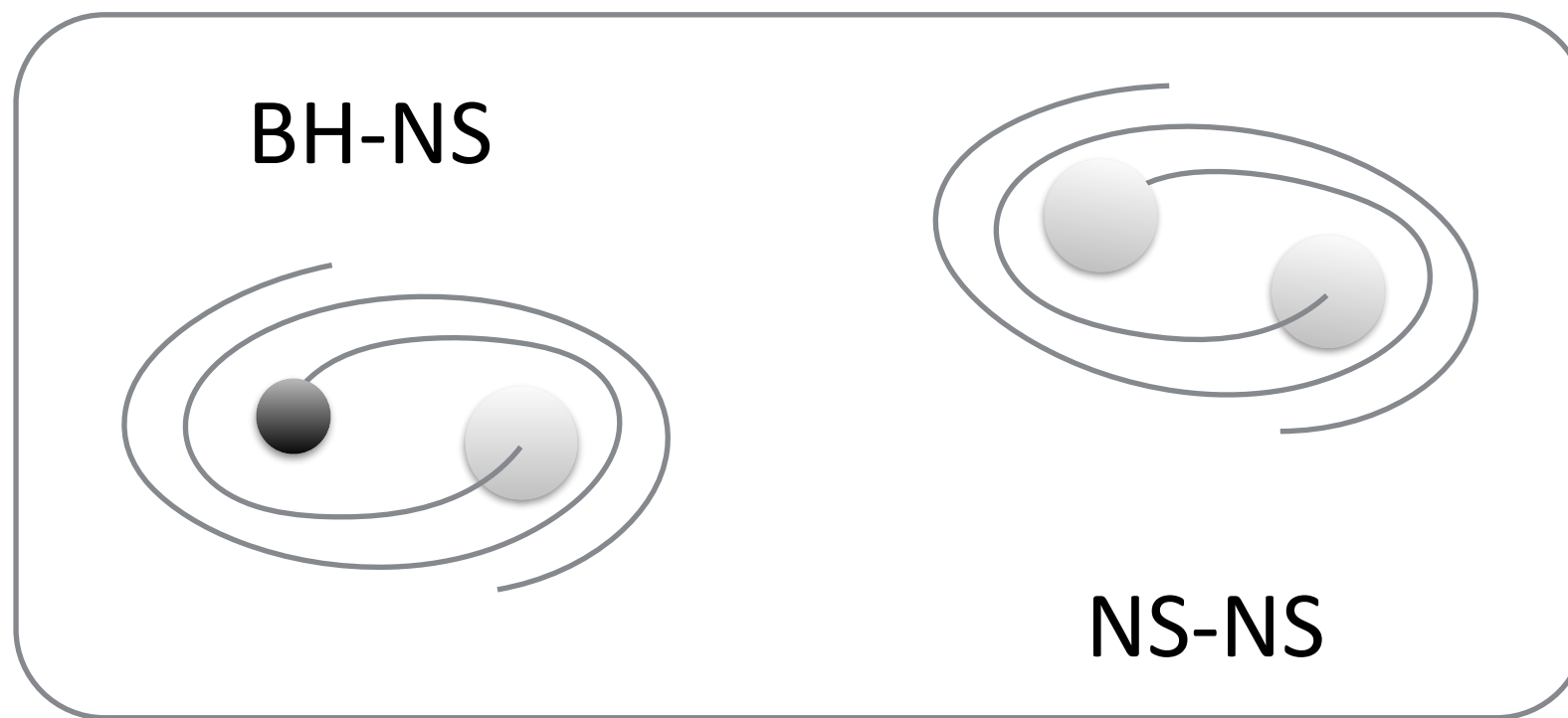
waveform template

$\vec{\theta} = (m_1, m_2, \chi_1, \chi_2, \Lambda_1, \Lambda_2, \dots$  :intrinsic parameters  
 $, d_L, \theta, \phi, \psi, i \dots)$  :extrinsic parameters

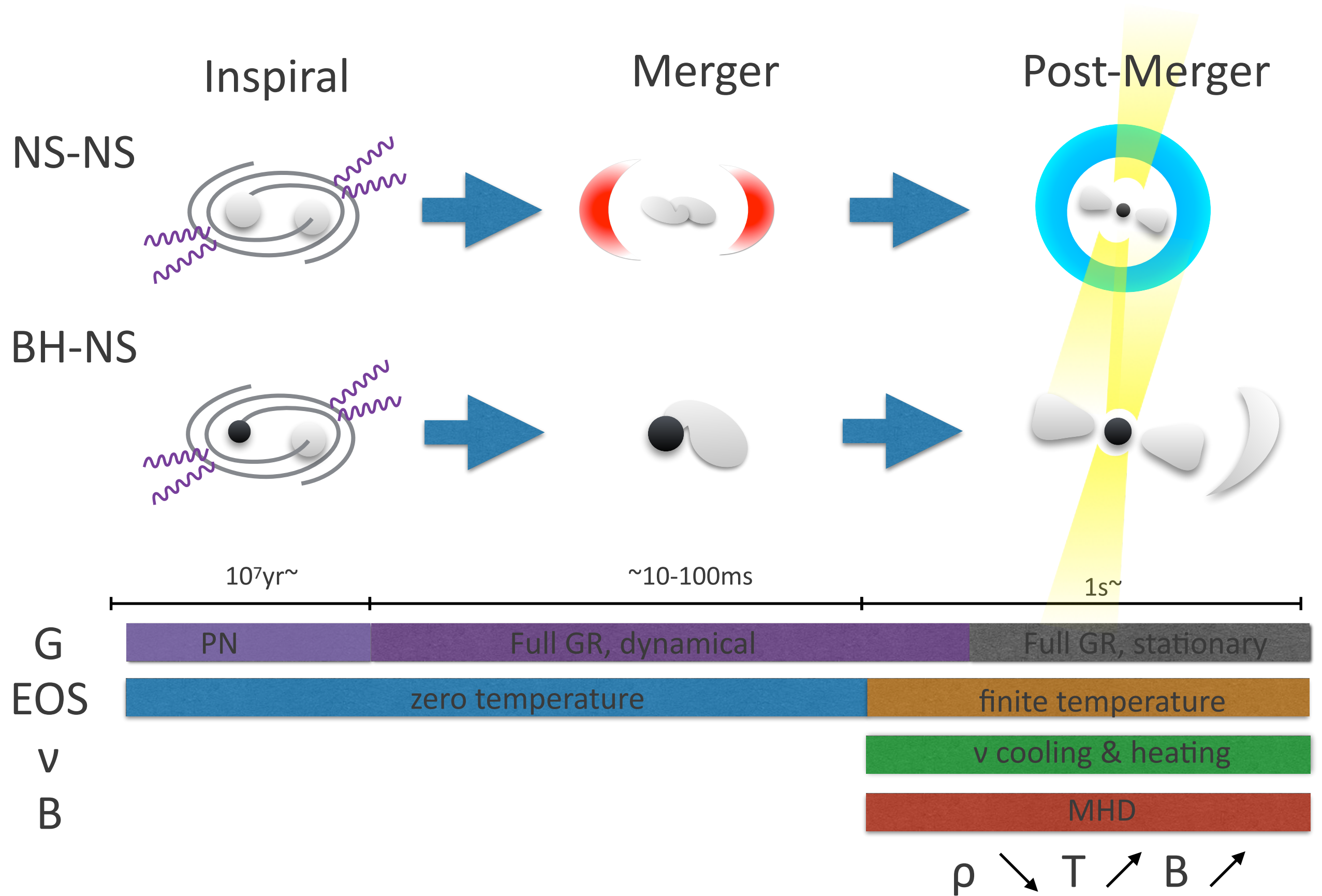
detector noise spectrum

# NS binary mergers

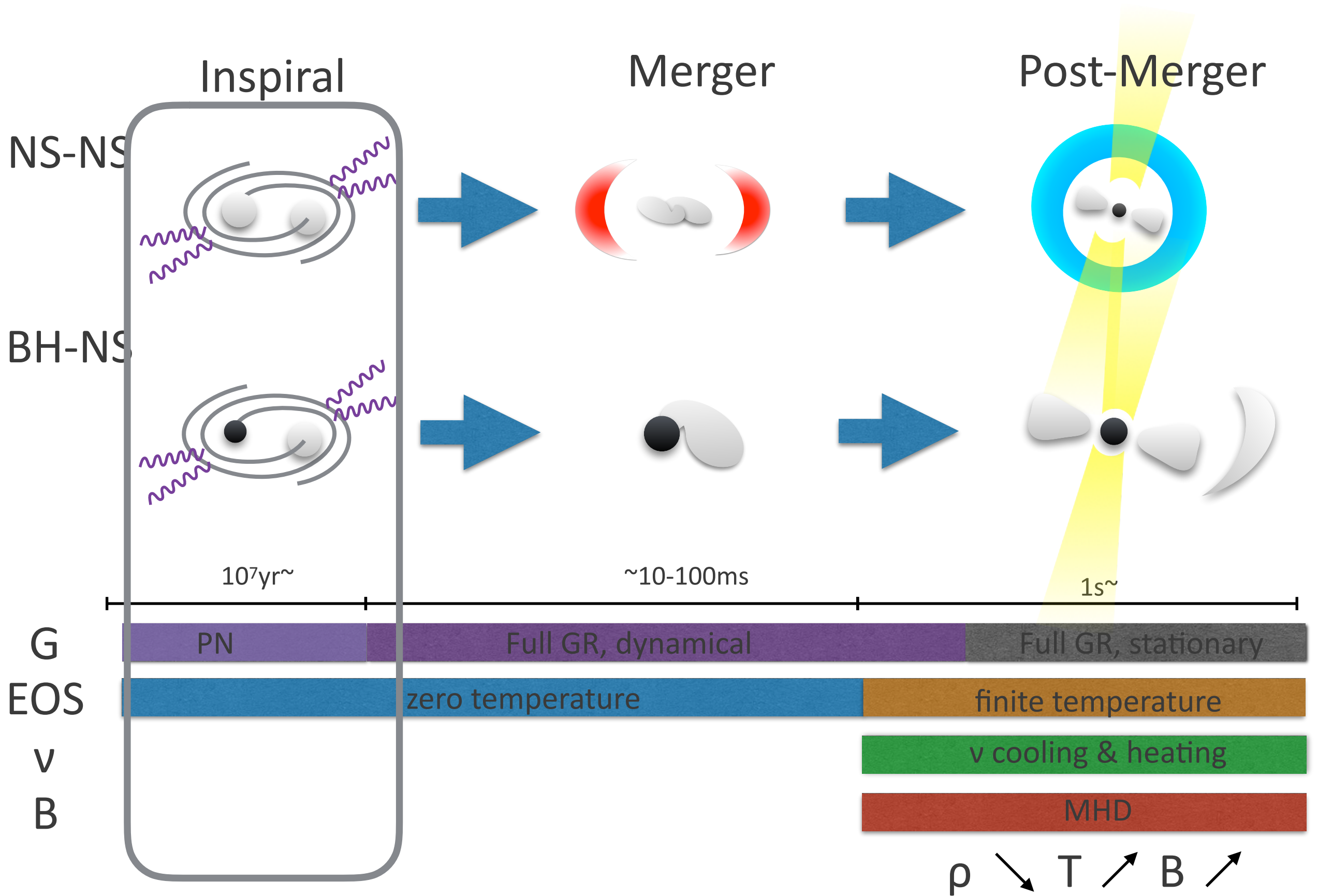
NS Binary



# General picture



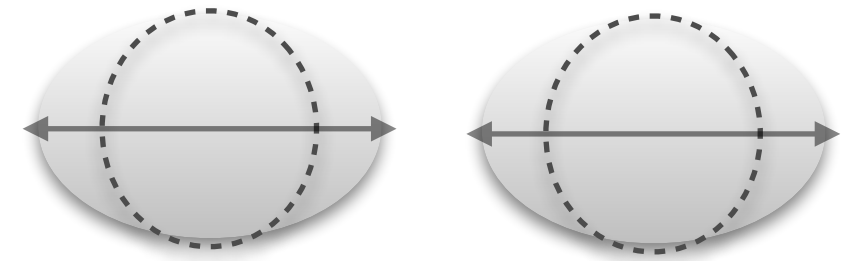
# General picture



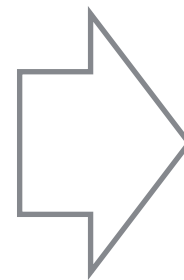


# Inspiral phase: Tidal deformation

- Gravitational waveform from a binary merger contains rich physical information of the source (masses, spins, distance, inclination, etc...)
- In particular, **if the binary contains a NS**, the information of the internal structure of the NS can be extracted
- During the inspiral, a NS is deformed by the tidal force of the companion object. Deformation of a NS (s) accelerates the orbital shrinking, and modifies gravitational waveforms



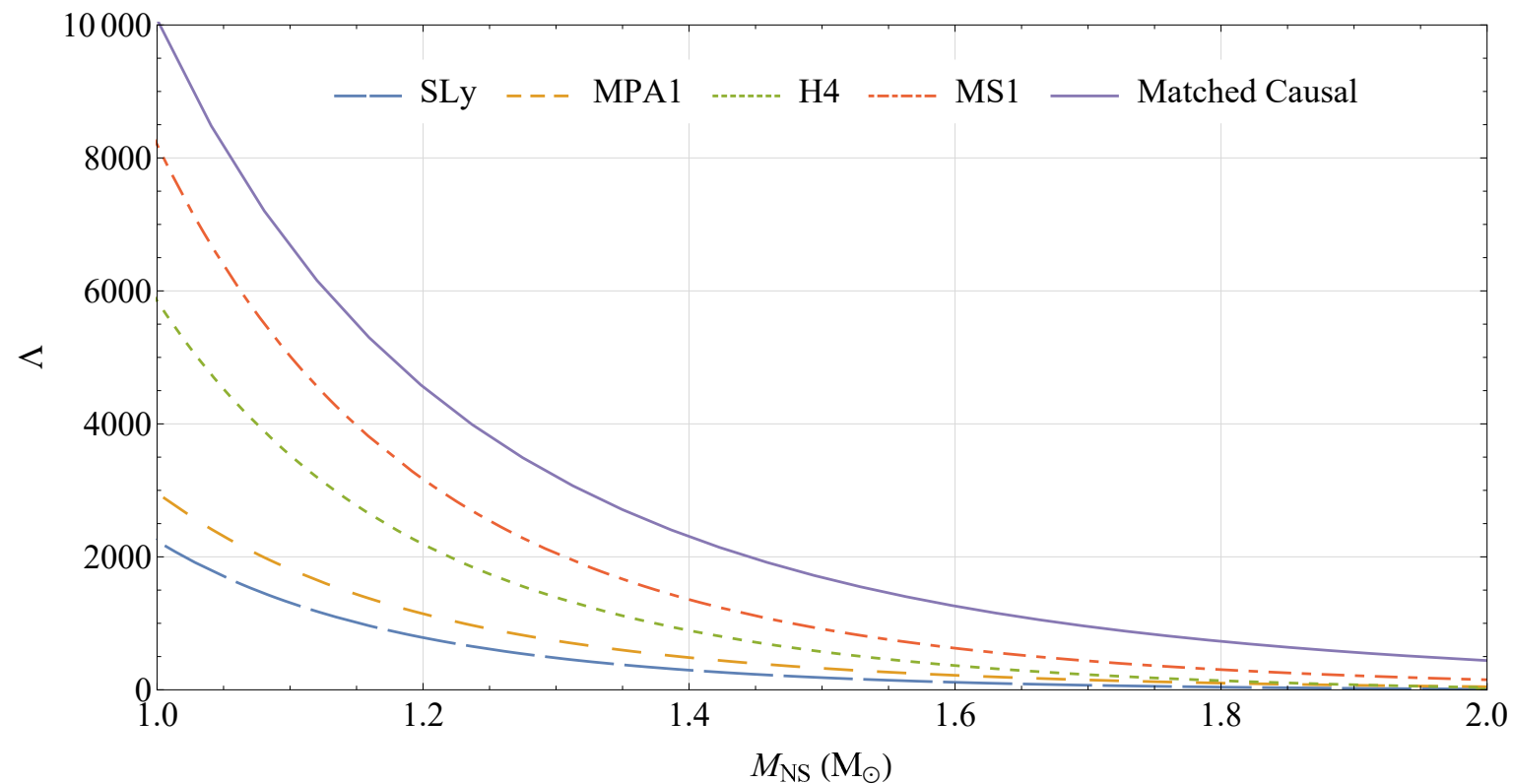
Tidal deformation



$$\Delta\Phi_{\text{GW}}^{\text{Tidal}}(t)$$

Modification in the GW phase

# Tidal deformability



Ref) Oeveren & Friedman 2017

$$\Lambda = G\lambda \left( \frac{c^2}{GM_{\text{NS}}} \right)^5 \sim \left( \frac{c^2 R_{\text{NS}}}{GM_{\text{NS}}} \right)^5$$

(dimensionless) tidal deformability

$$Q_{ij} = -\lambda \mathcal{E}_{ij} = -\lambda \partial_i \partial_j \Phi$$

Quadrupole moment      tidal field

- From the observed waveforms, *the tidal deformability* of a NS can be extracted
- The tidal deformability reflects the internal structure of a NS, and its measurement can be used to constrain **the NS equation of state (EOS)**

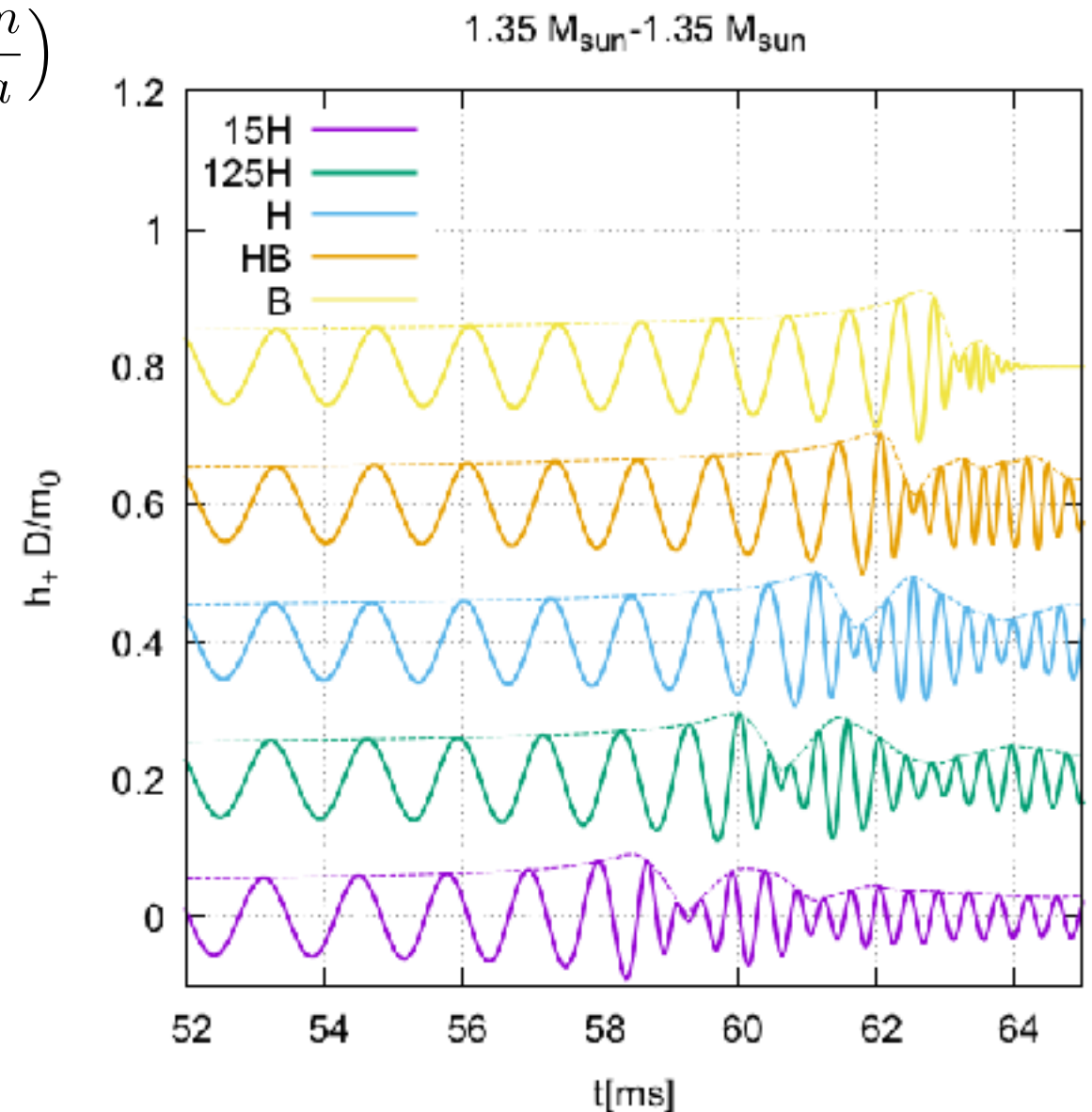
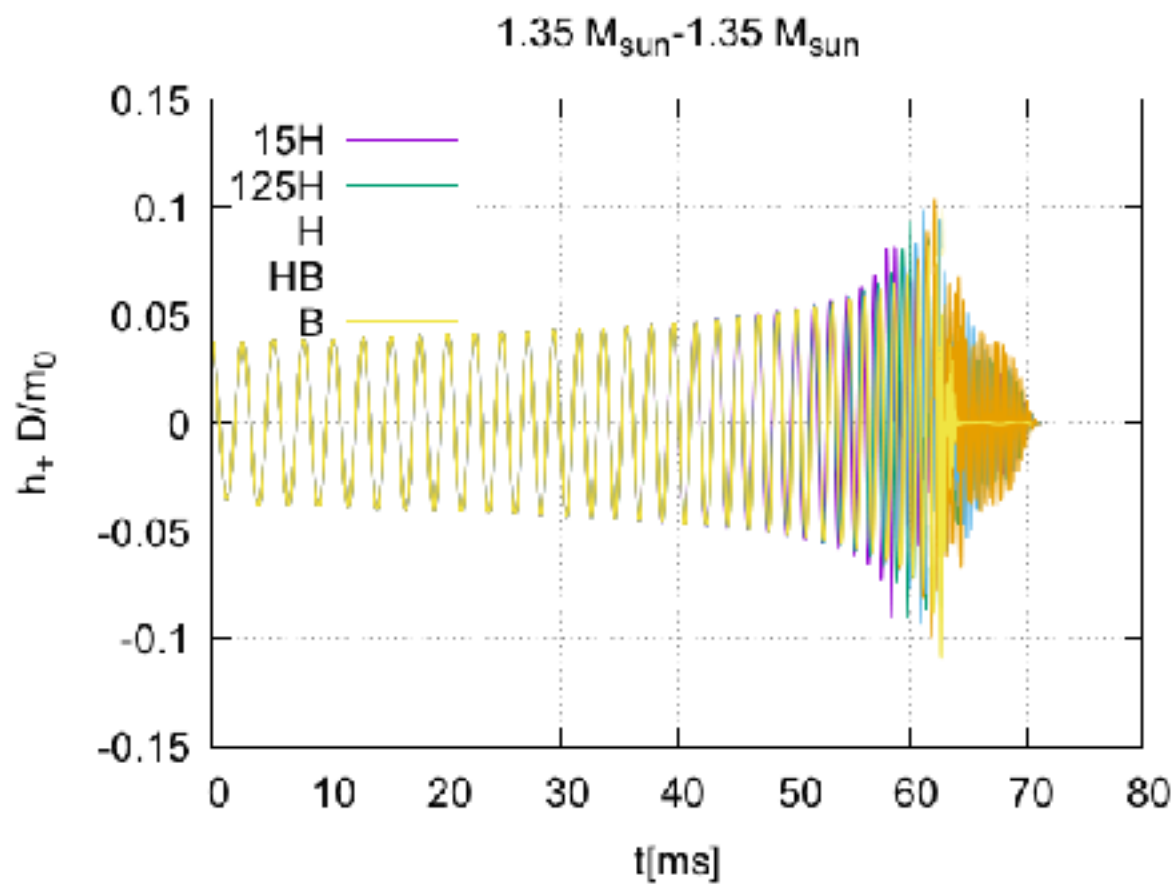
# Effect of tidal deformation

quadrupole formula

tidal correction

$$\frac{dx}{dt} = \frac{64\eta}{5m_{\text{tot}}} x^5 \left[ 1 + \dots + 6 \left( 12 \frac{m_2}{m_1} + 1 \right) \left( \frac{1}{1 + m_2/m_1} \right)^5 \Lambda_1 x^5 + (1 \leftrightarrow 2) + \dots \right]$$

PostNewtonian Parameter:  $x := (\pi m f_{\text{GW}})^{2/3} \approx \left( \frac{m}{a} \right)$

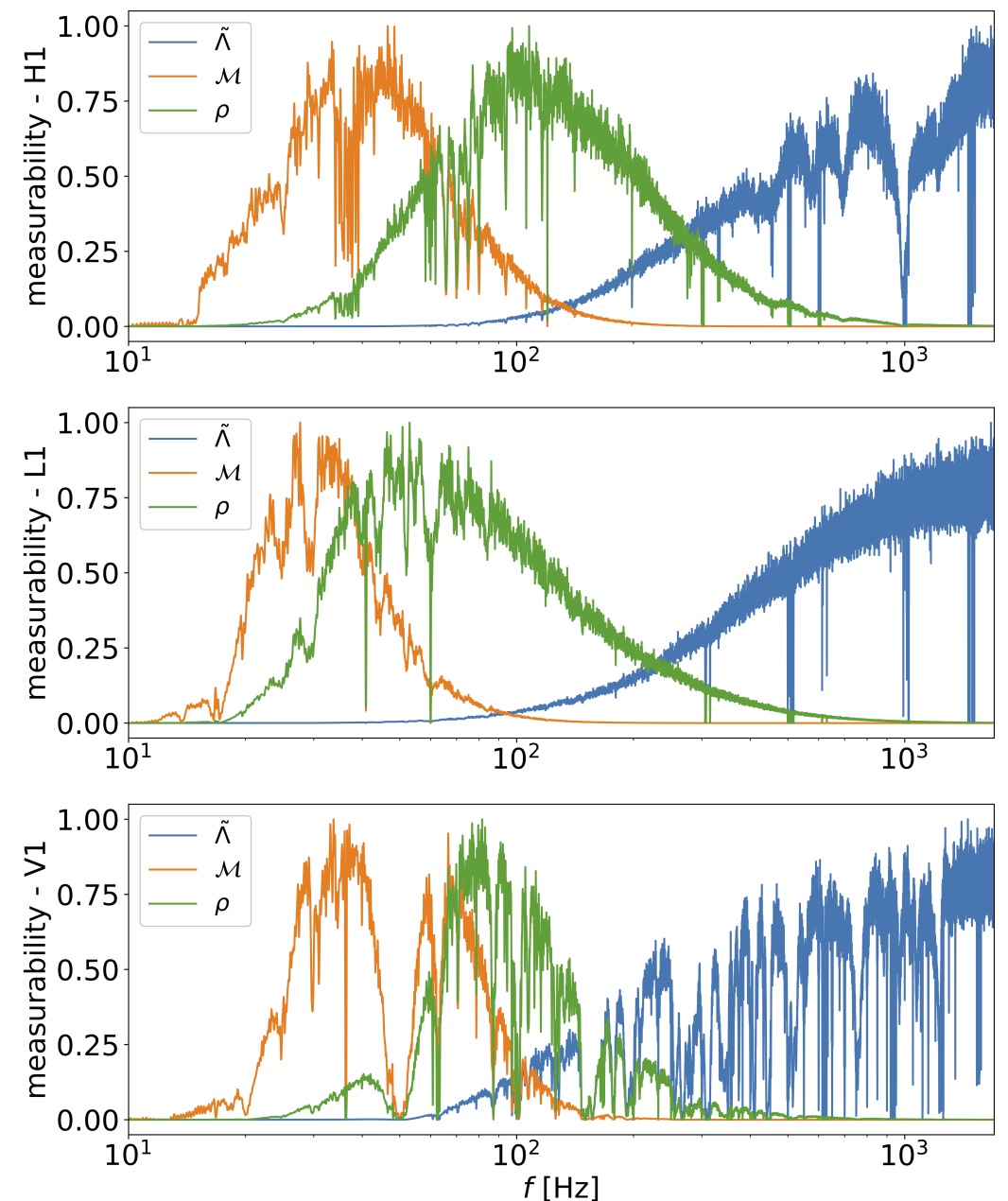


- Radius & Tidal deformability  
15H > 125H > H > HB > B

# GW templates for NS binaries

- Physical information is extracted from observed gravitational waves by the comparison with theoretical templates  
→ **an accurate waveform templates are crucial for parameter estimation**
- The waveforms **including the tidal effects** are analytically derived by post-Newtonian (PN) calculation (and by the Effective-One-Body formalism)
  - Newtonian (Flanagan et al. 2008)
  - 1 PN (Vines et al. 2011)
  - 2.5 PN (Damour et al. 2012)
  - Self force informed resum. (Bernuzzi et al. 2015, 2018)
  - Dynamical tide (Hinderer et al. 2016, Lackey et al. 2018)
- **Tidal effects become significant in the last part of the inspiral. However, the model based on PN calculation would not be accurate just before the merger.**

ref) De et al. 2018



Prediction by numerical simulations is important for modeling the tidal correction  
(at least needed to be checked)



# Numerical Relativity simulations

- **Numerical-relativity (NR) simulation** is the unique method to predict dynamics and gravitational waves in the late inspiral & merger phase.

Einstein's equation

$$G_{\mu\nu} = \frac{8\pi G}{c^4} T_{\mu\nu}$$

Euler equation

$$\nabla_{\mu}(\rho u^{\mu}) = 0 \quad \nabla_{\mu} T^{\mu\nu} = 0$$

Equation of state (EOS)

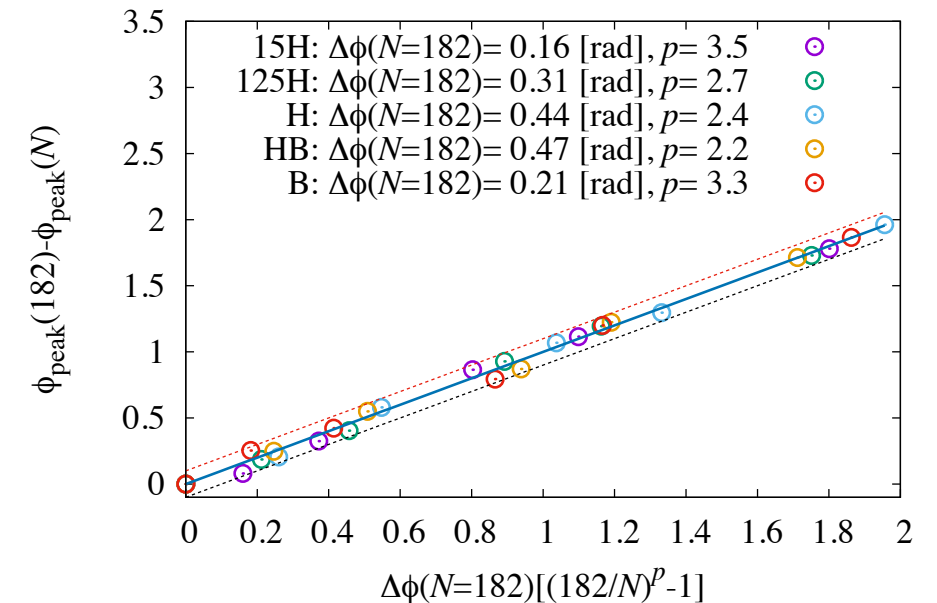
$$P = P(\rho)$$

\*neither MHD nor neutrino radiation are not considered in these simulations

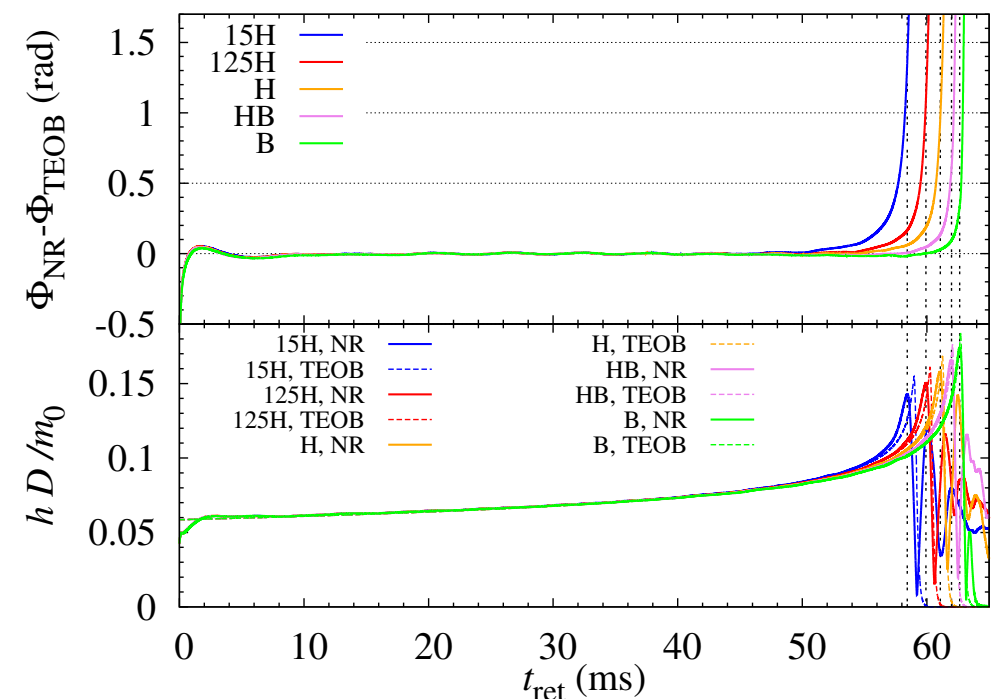
- **Performing high-resolution NR simulations, waveforms calculation with sub-radian phase errors are achieved.**
- The phase difference larger than  $\sim 1$  rad is found between recent TEOB waveforms (SEOBNRv2T) and NR results for the case that  $\Lambda \sim 850$
- See also Dietrich et al. 2016, Foucart et al. 2018, Haas et al. 2016 for recent high precision NR simulations for NS binary mergers

phase at the time of the peak amplitude

1.21-1.51  $M_{\text{sun}}$

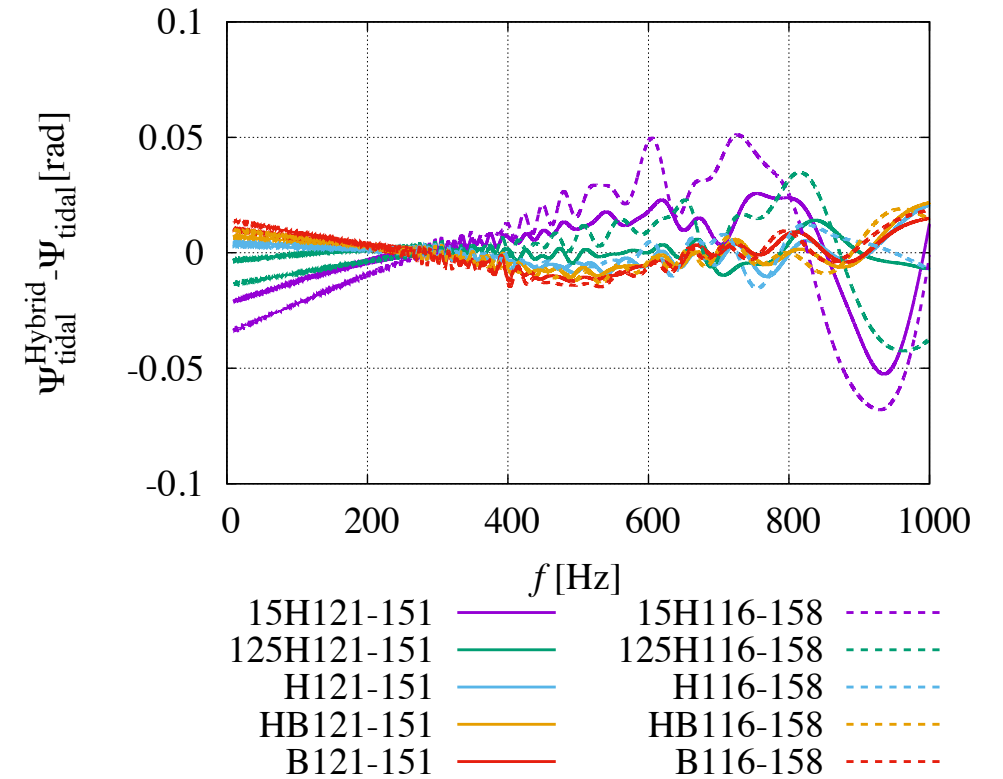


Ref: Kiuchi et al. 2017, KK et al. 2018



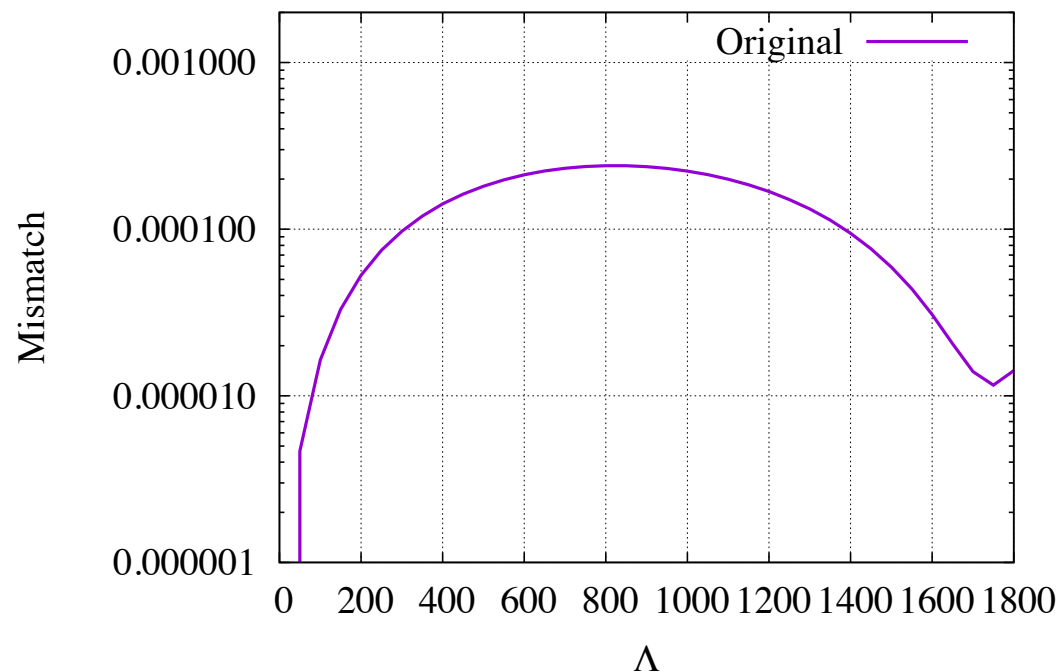
# NS-NS waveform model

- Based on our latest numerical-relativity waveforms, a waveform model for NS-NS mergers is derived
- A NS-NS GW model is also derived in Dietrich et al. 2017, 2019 based on different NR waveforms and TidalEOB waveforms
- Though their and our models are derived independently, two models give almost consistent results



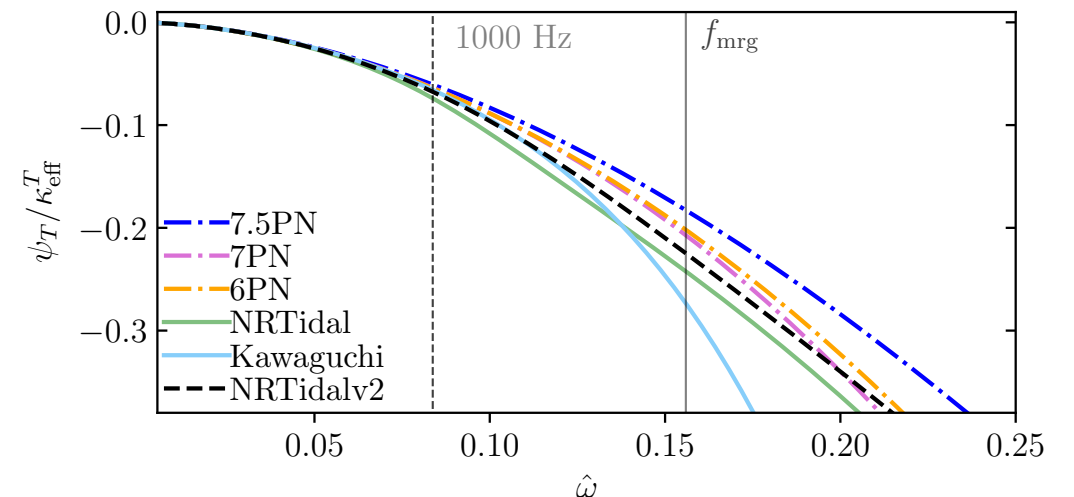
Ref: KK et al. 2018, K. Kiuchi, KK et al. 2019  
Comparison with Dietrich+17

$$f_{\min} = 10 \text{ Hz}, f_{\max} = 1000 \text{ Hz}, \\ m_1 = m_2 = 1.35 M_{\text{sun}}$$



$$\Psi_{\text{tidal}} = \frac{3}{128\eta} \left[ -\frac{39}{2} \tilde{\Lambda} \left( 1 + a\tilde{\Lambda}^{2/3} x^p \right) \right] x^{5/2} \quad \begin{matrix} a = 12.55, \\ p = 4.240. \end{matrix} \\ \times \left[ 1 + \frac{3115}{1248} x - \pi x^{3/2} + \frac{28024205}{3302208} x^2 - \frac{4283}{1092} \pi x^{5/2} \right]$$

Ref: Dietrich et al. 2017, 2019



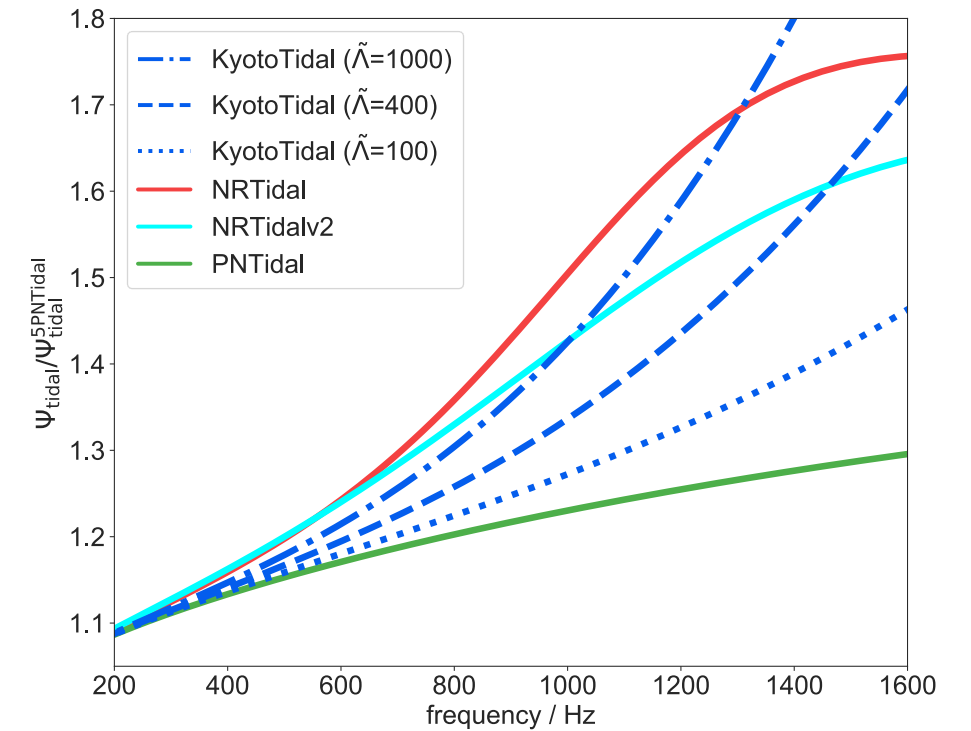
# Comparison with Dietrich et al. 2017,2019

- A BNS GW model is also derived in Dietrich et al. 2017 , 2019 based on different NR waveforms and TidalEOB waveforms

$$P_{\text{NRTidalv2}}(x) = \frac{1 + n_1 x + n_{3/2} x^{3/2} + n_2 x^2 + n_{5/2} x^{5/2} + n_3 x^3}{1 + d_1 x + d_{3/2} x^{3/2} + d_2 x^2}$$

- Though their and our models are derived independently, two models give almost consistent results**

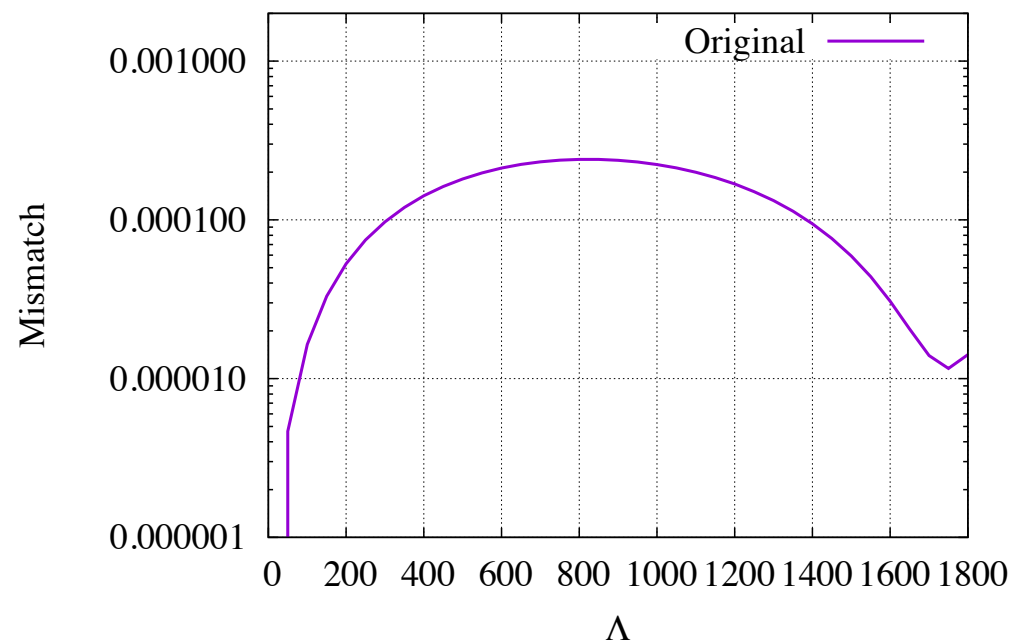
Ref: Narikawa, KK et al. 2019



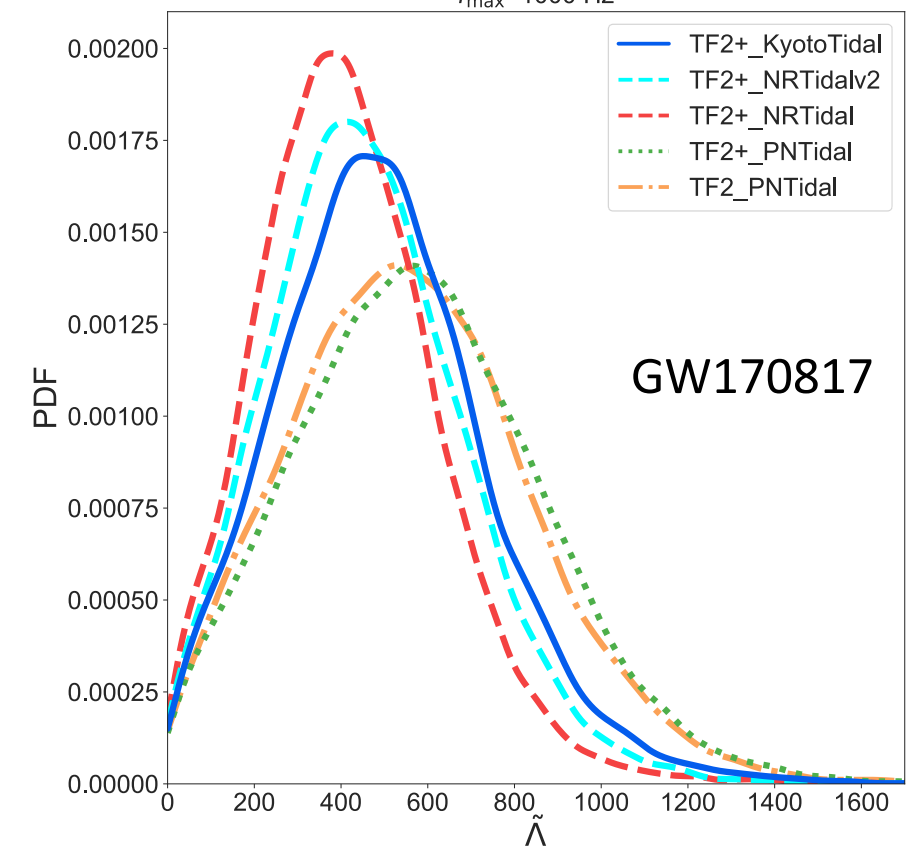
$$\langle \tilde{h}_1 | \tilde{h}_2 \rangle = 4\text{Re} \left[ \int_{f_{\min}}^{f_{\max}} \frac{\tilde{h}_1(f) \tilde{h}_2^*(f)}{S_n(f)} df \right] \quad \|\tilde{h}\| = \sqrt{\langle \tilde{h} | \tilde{h} \rangle} \quad \text{Mismatch: } \bar{F} = 1 - \max_{\phi_0, t_0} \frac{|\langle \tilde{h}_1 | \tilde{h}_2(\phi_0, t_0) \rangle|}{\|\tilde{h}_1\| \|\tilde{h}_2\|}$$

Comparison with Dietrich+17

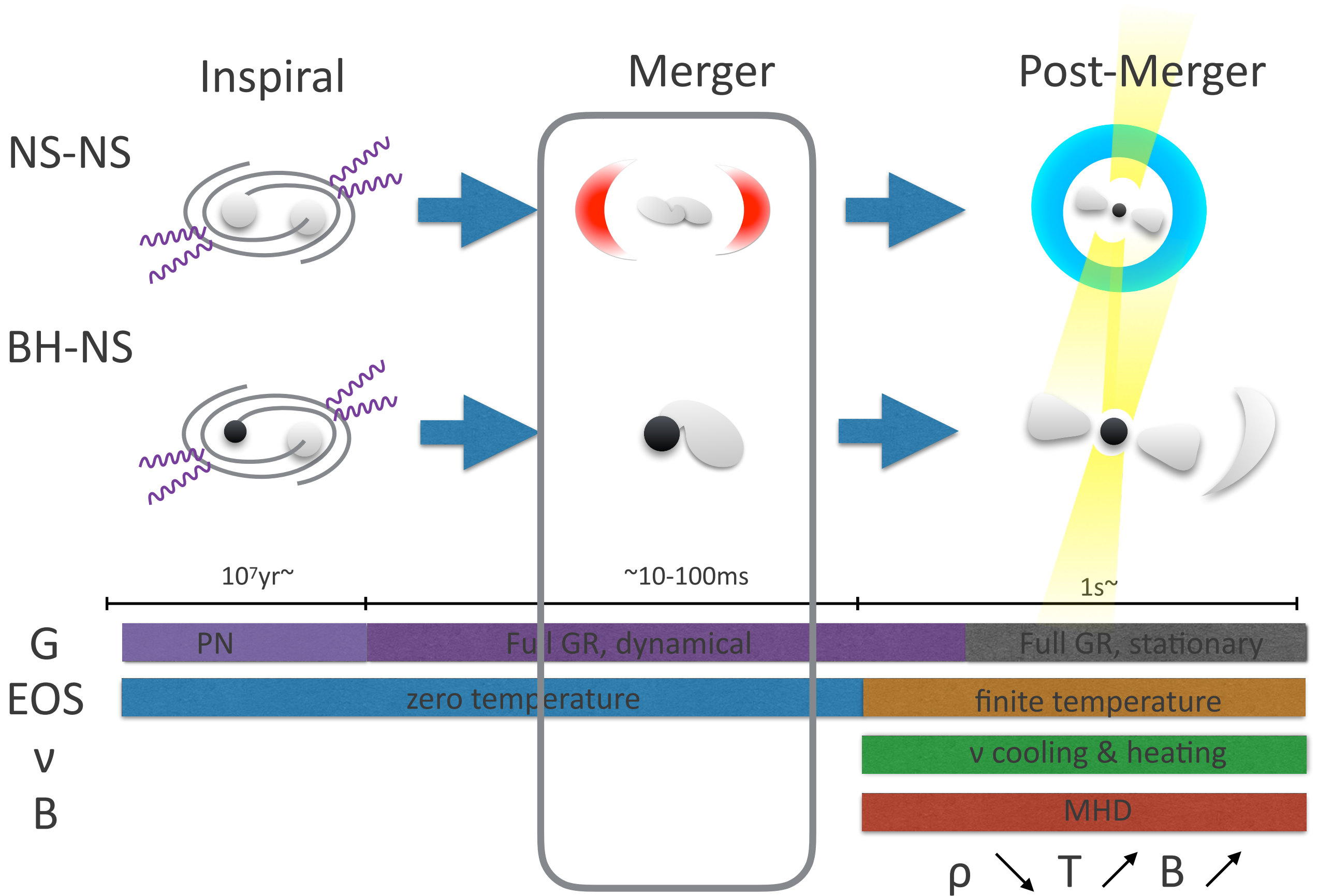
$$f_{\min} = 10 \text{ Hz}, f_{\max} = 1000 \text{ Hz}, \\ m_1 = m_2 = 1.35 M_{\text{sun}}$$



$f_{\max}=1000 \text{ Hz}$



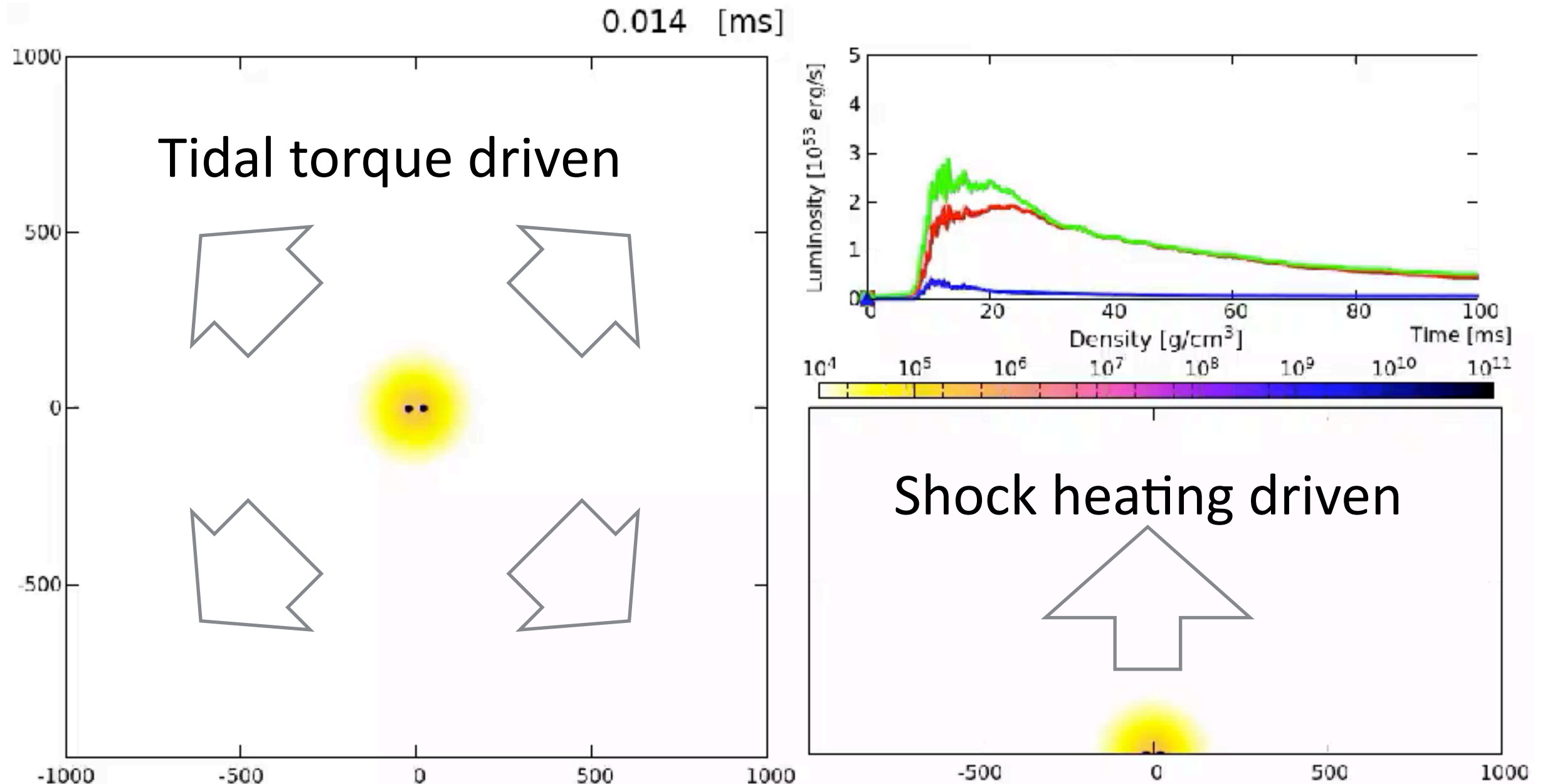
# General picture





# Mass ejection (NS-NS)

Ref: Y. Sekiguchi et al. 2015

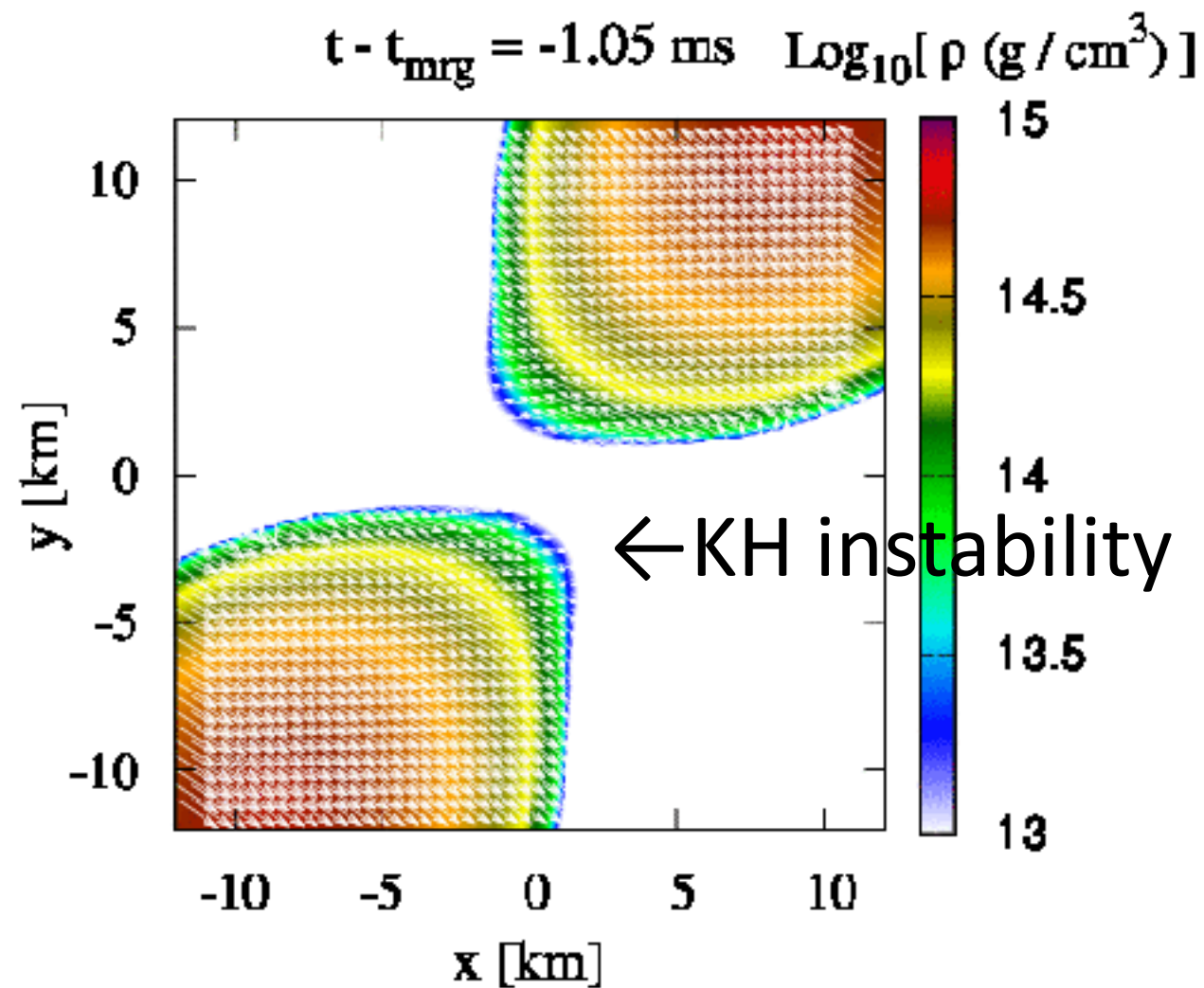


A fraction of NS material would be ejected from the system during the merger.

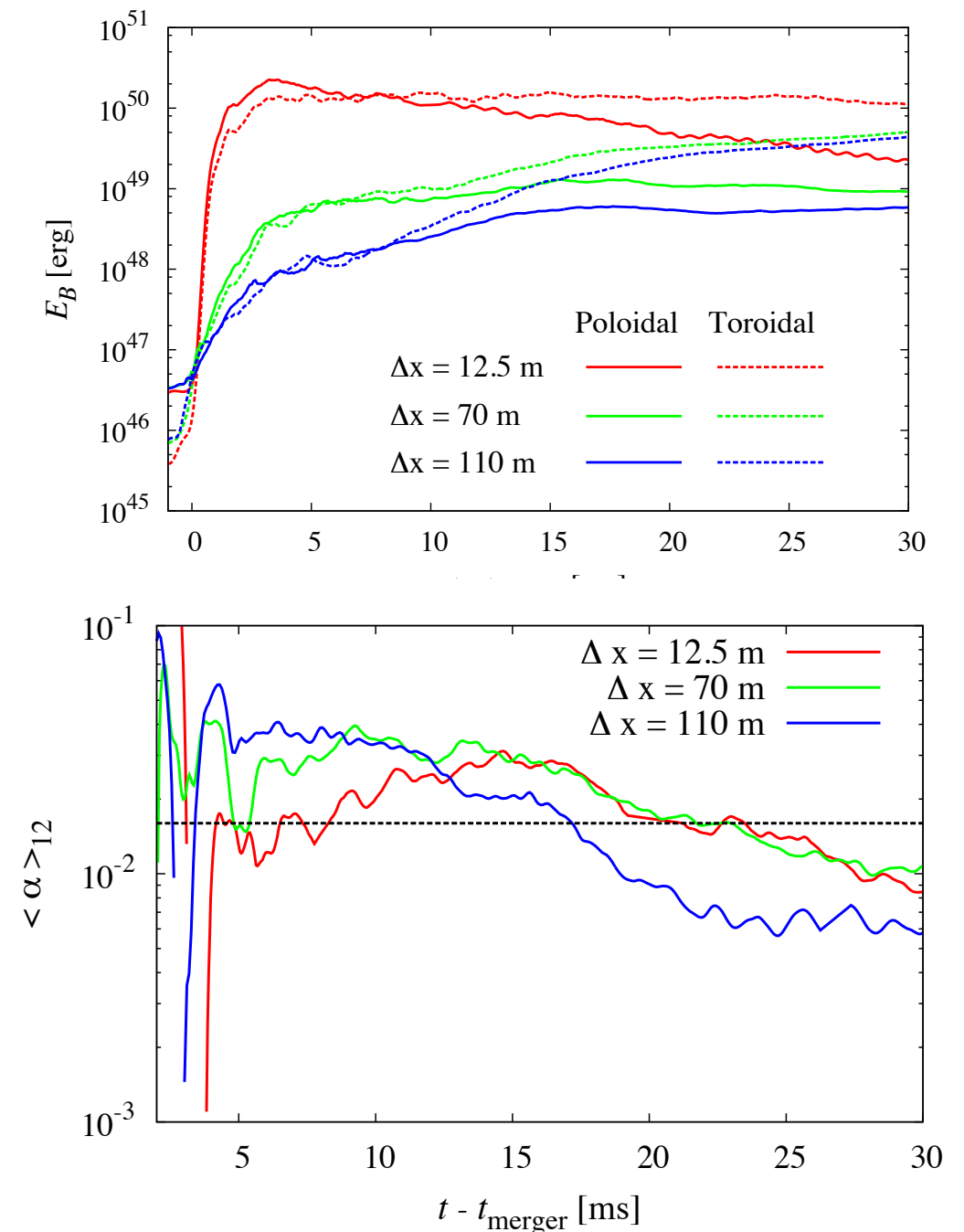
(e.g. Hotokezaka et al. 2013; Bauswein et al. 2013; Sekiguchi et al. 2016; Radice et al. 2016; Dietrich et al. 2017; Bovard et al. 2017)

# Remnant NS & torus

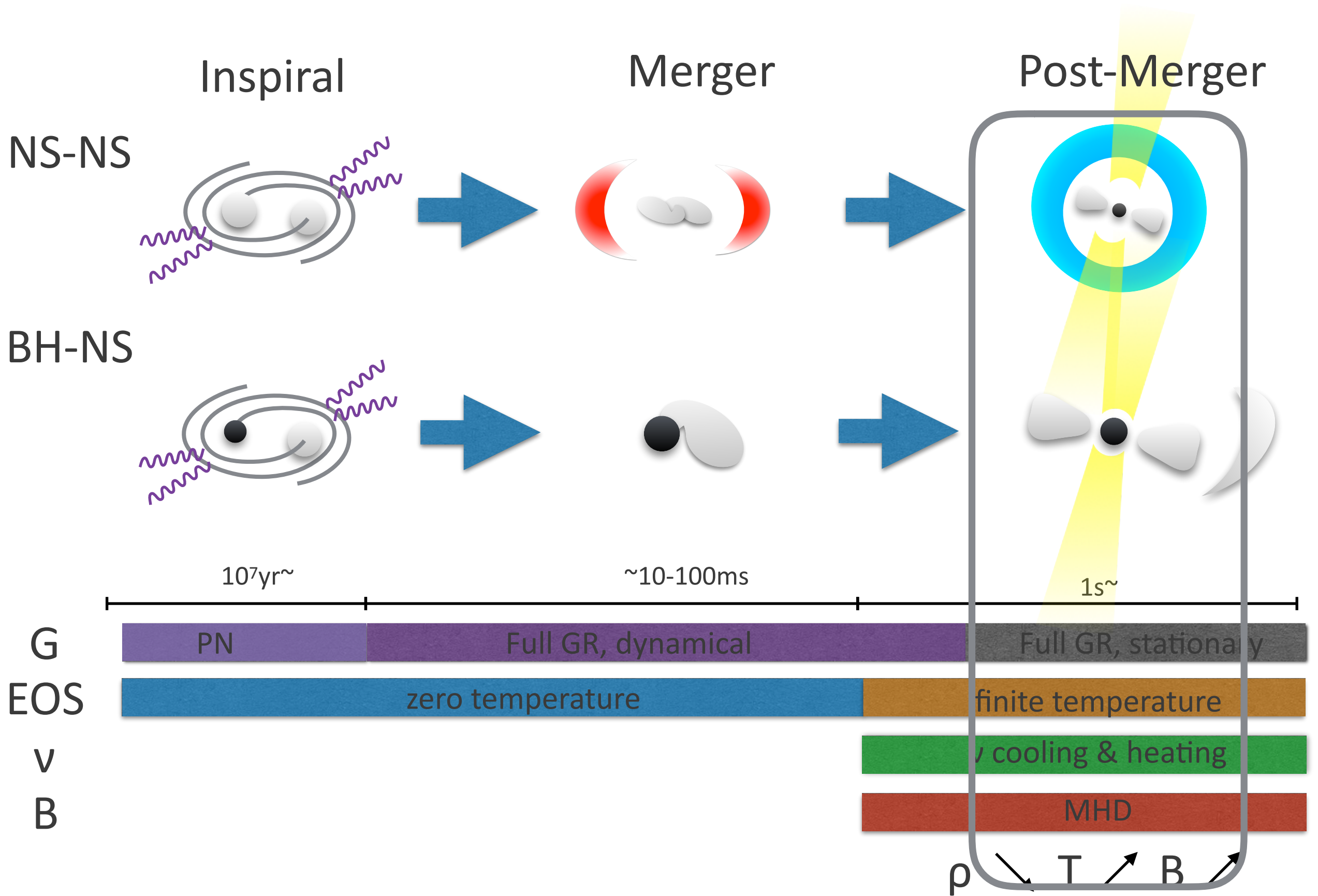
Turbulence in the contact surface → amplification of magnetic field  
→ **The remnant NS and accretion torus would be highly magnetized.**



Ref: K. Kiuchi et al. 2015, 2017

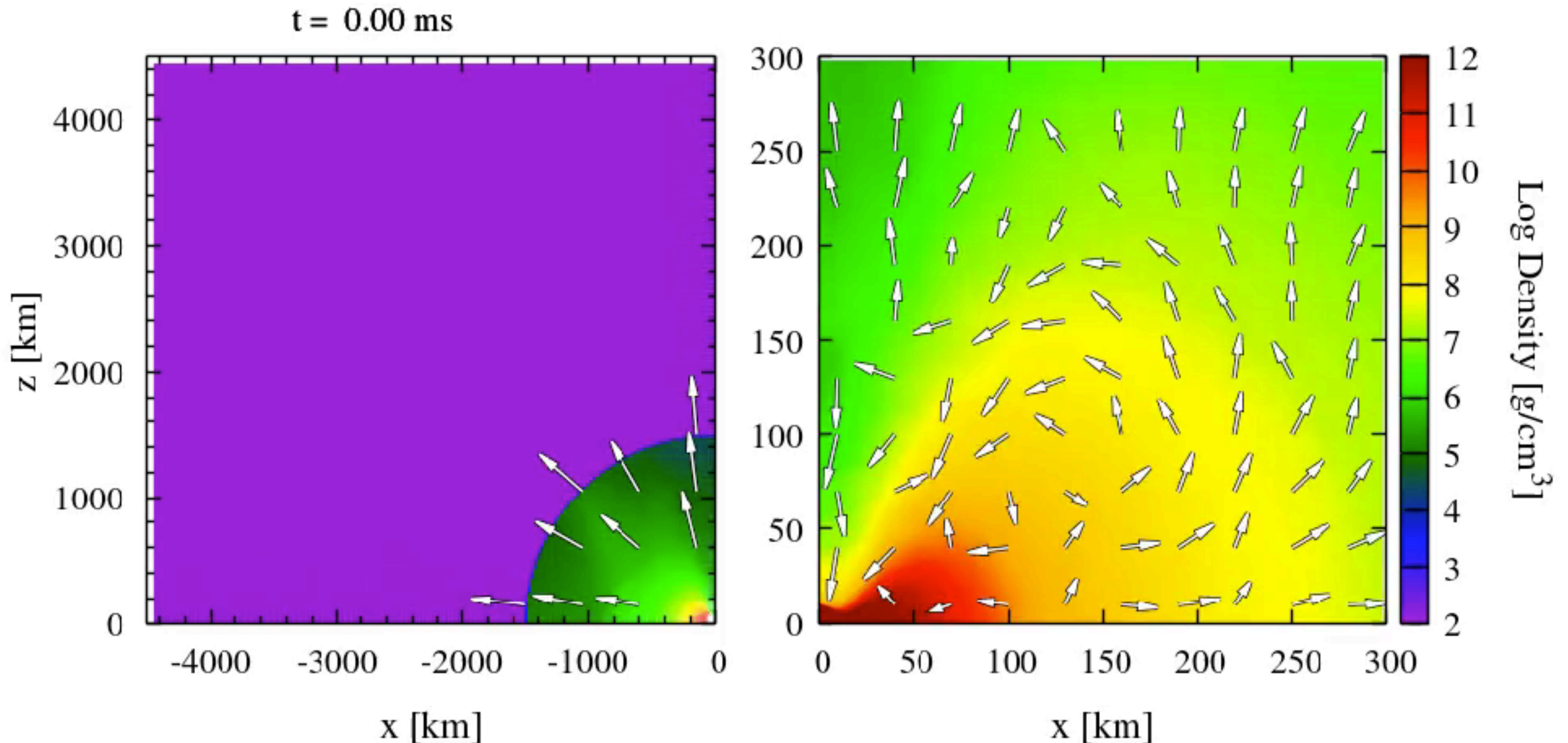


# General picture



# Post-merger mass ejection

Viscous GRRHD simulation for merger remnant  
(Ref: S. Fujibayashi et al. 2018)



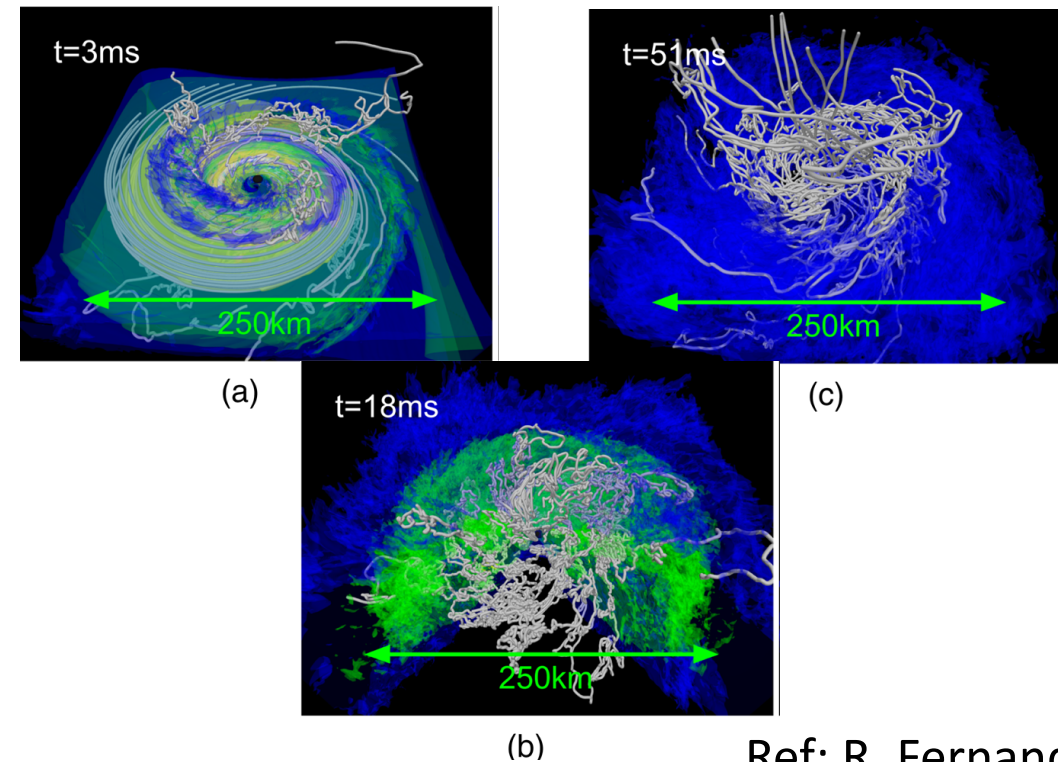
Mass ejection from the remnant torus would occur  
driven by amplified magnetic fields or effective viscous heating due to magnetic turbulence  
(see also e.g. Siegel et al. 2018, Fernandez et al. 2018 for GRMHD simulations)



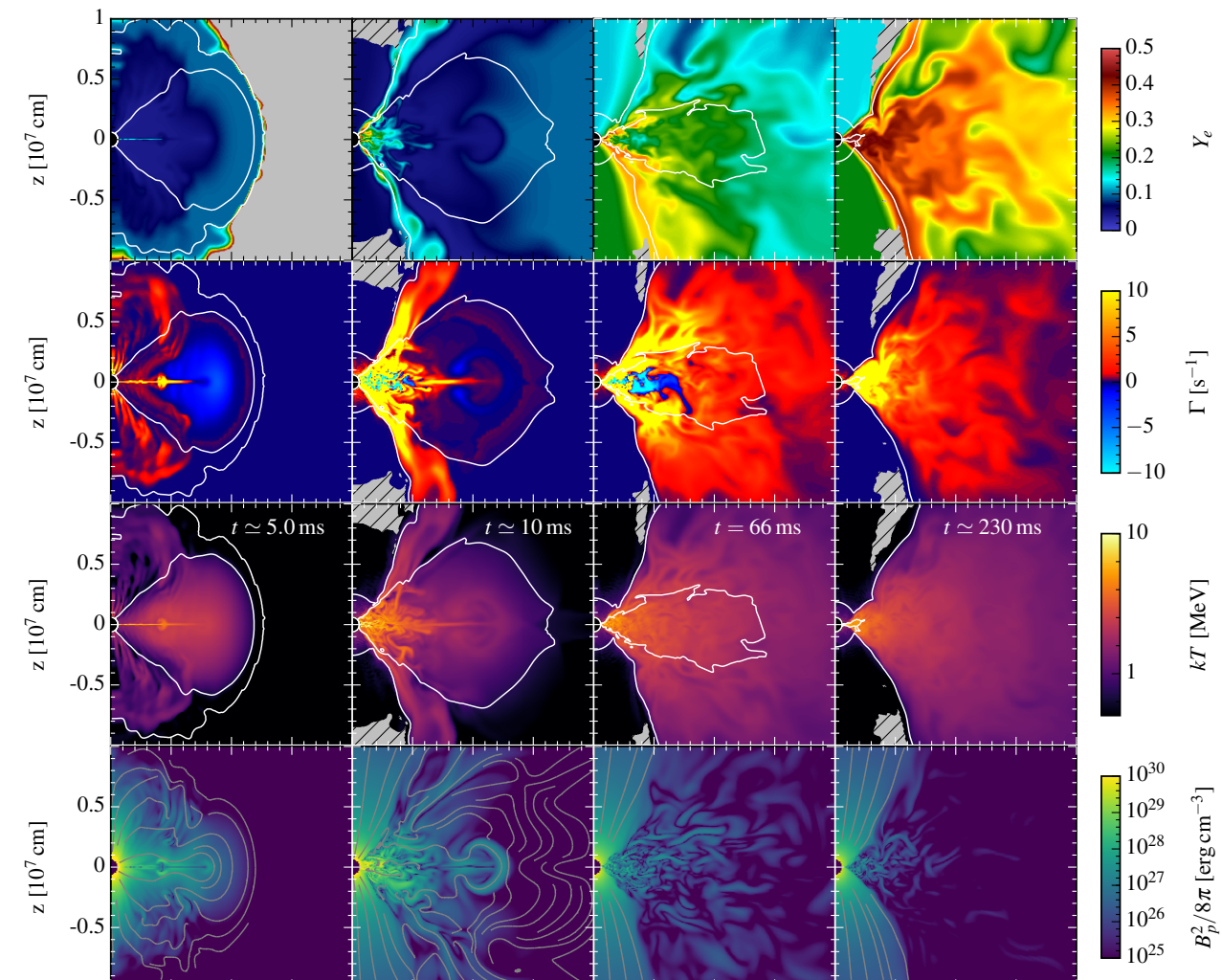
# Relativistic jets

Ref: K. Kiuchi et al. 2015

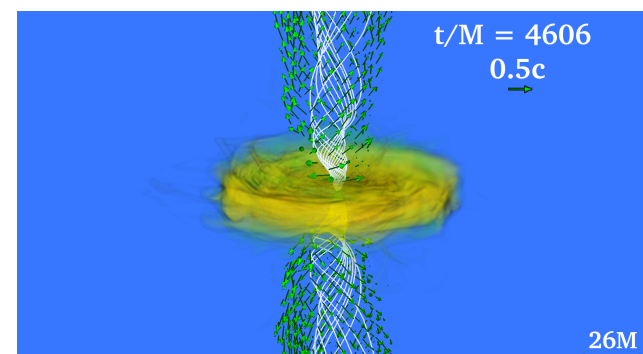
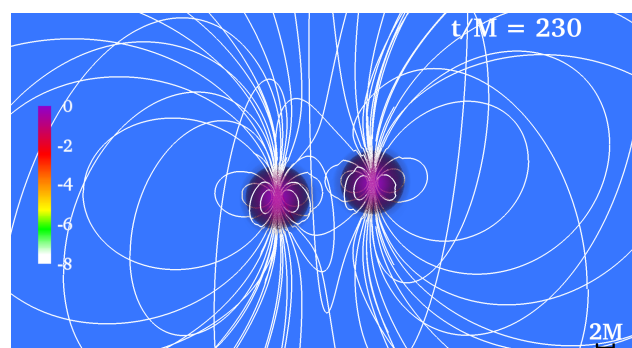
- Relativistic jets could be launched from the BH accretion torus system formed after the merger
- global structure of the magnetic fields would play an important role
- contribution from neutrino pair annihilation seems to be sub-dominant



Ref: R. Fernandez et al. 2018



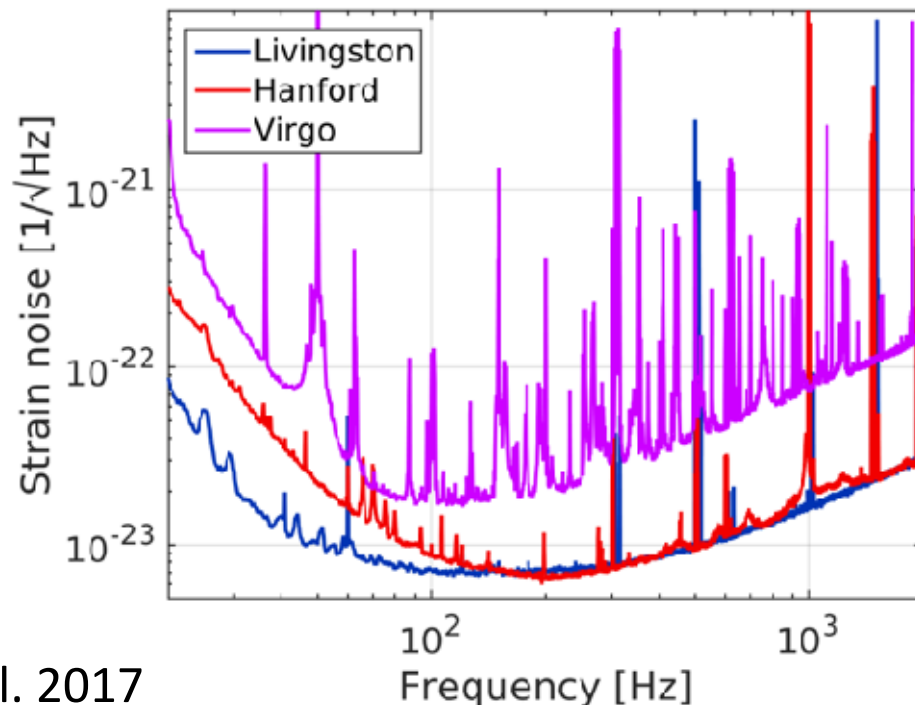
Ref: M. Ruiz et al. 2016



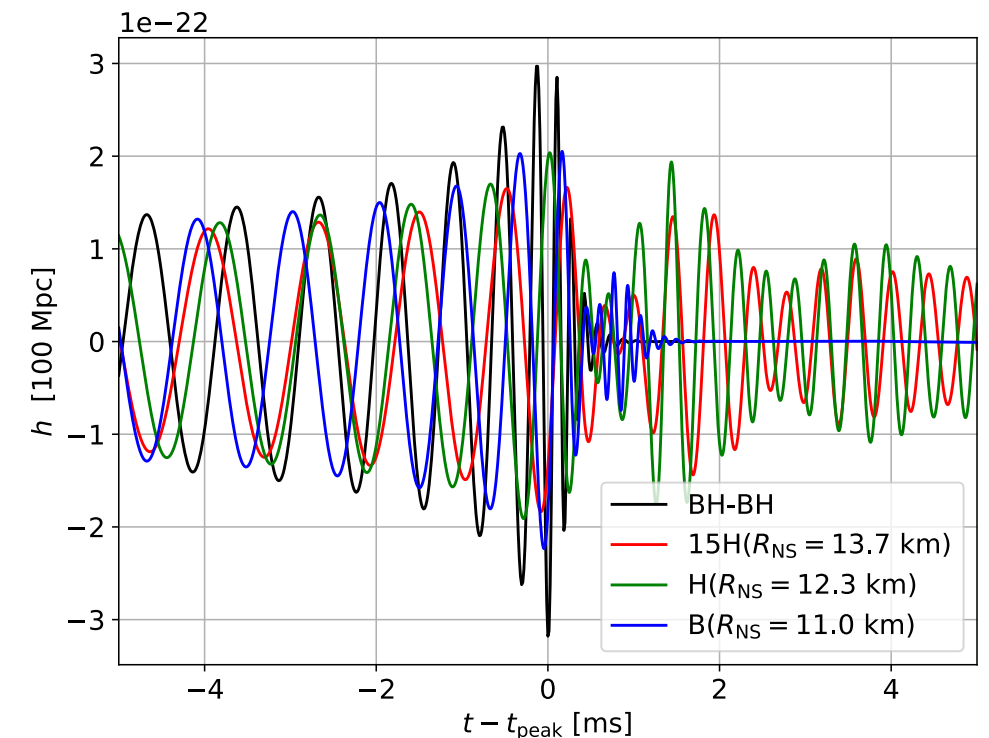
# Post-merger waveforms (NS-NS)

- Post-merger waveforms would contain rich physical information, such as **the evolution of the merger remnant** and **information of high density part of NS EoS**
- Challenging for both detection and waveform modeling
- Complicated physical effects, such as MHD, thermal effect, and  $\nu$  radiation, should be taken into account in the numerical simulations

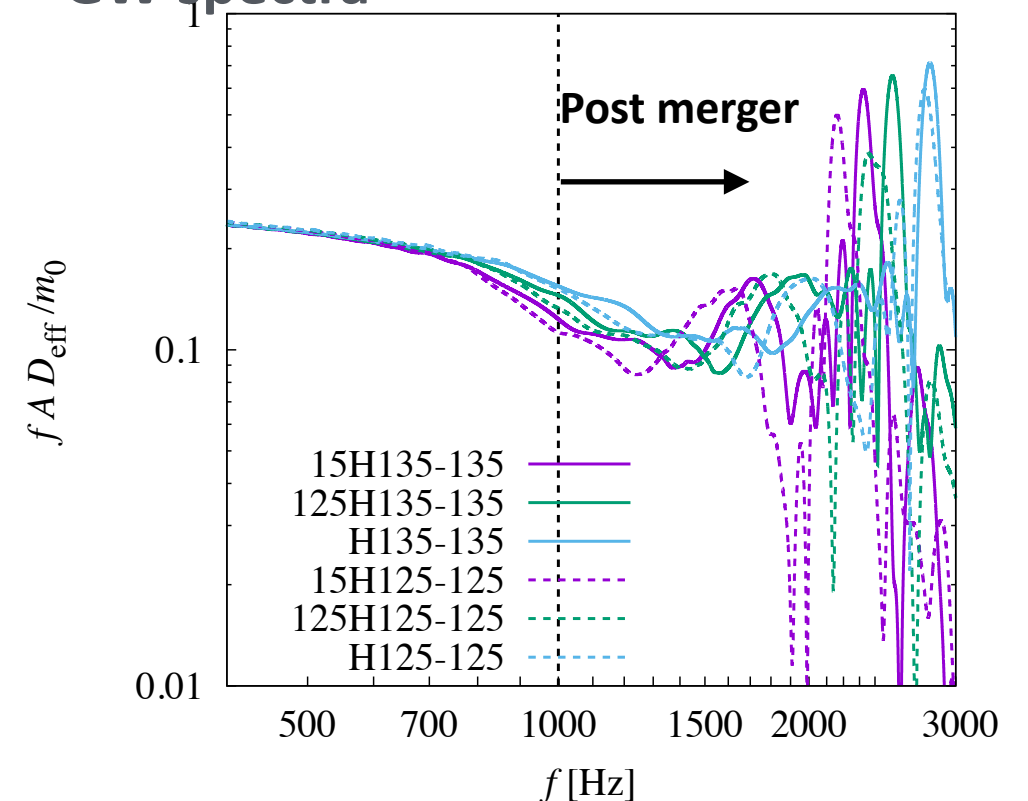
## Detector sensitivity



Ref: B.P. Abbot et al. 2017



## GW spectra

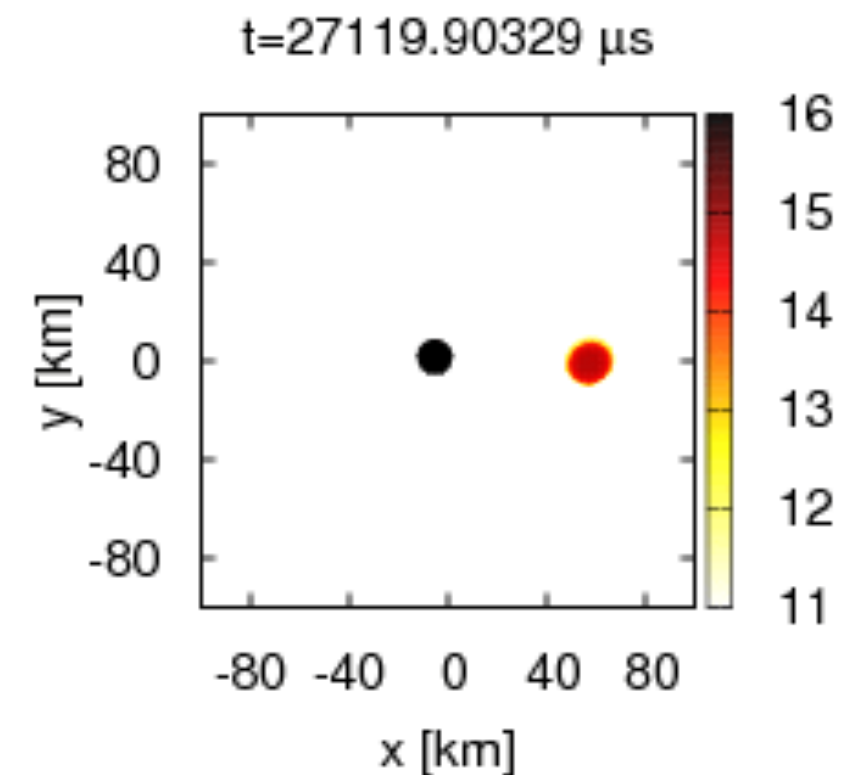
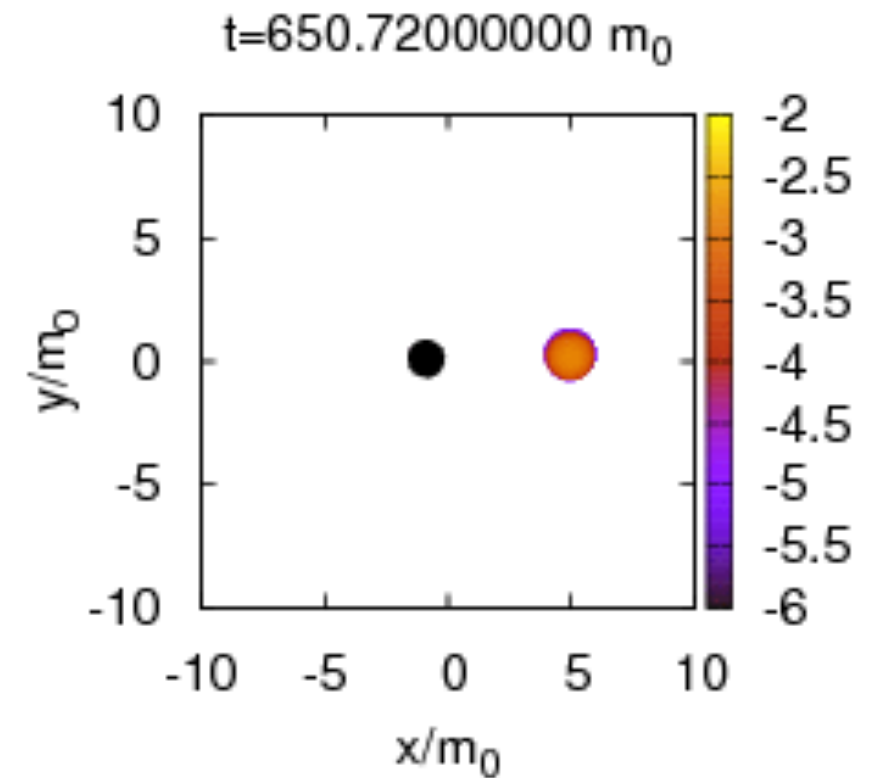
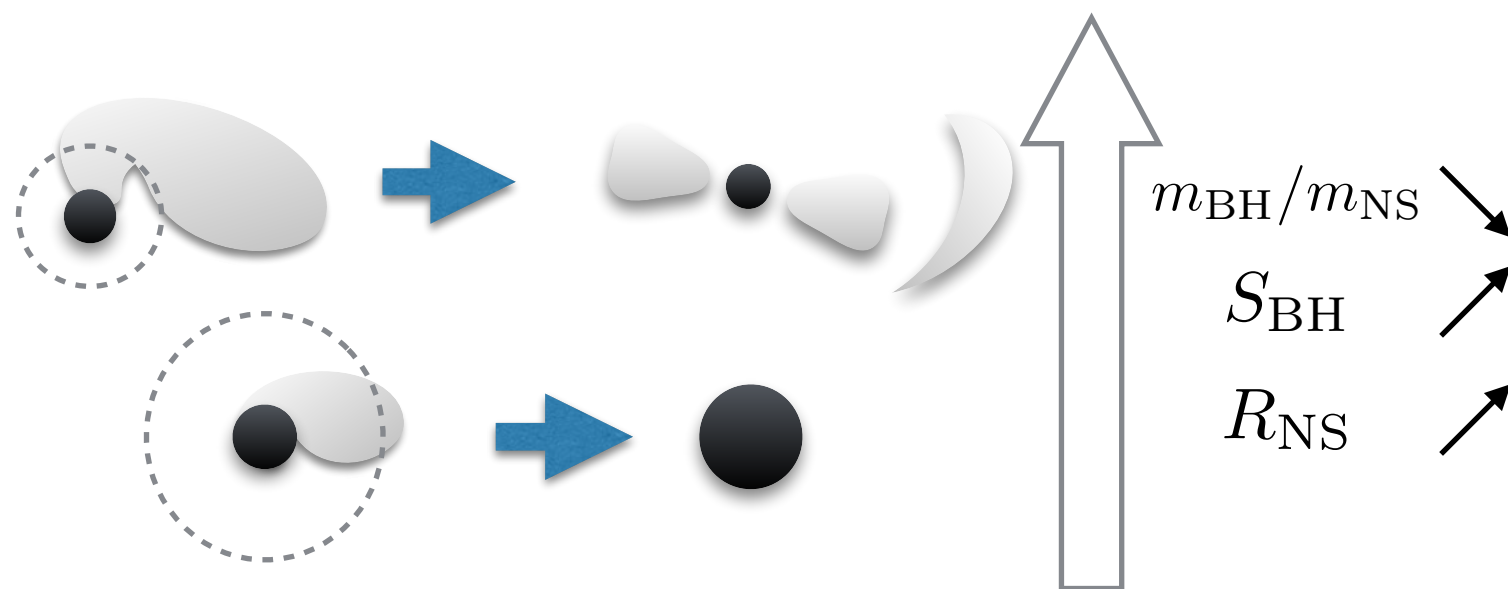


Ref: K. Kiuchi et al. 2017, KK et al. 2018

Black hole-Neutron star

# Tidal disruption of NS (BH-NS)

- If the tidal force of the BH exceeds the self-gravity of the NS, the NS is **tidally disrupted**.
- The NS should be tidally disrupted outside **the ISCO of the BH** to form a **ejecta or remnant torus**, otherwise entire NS material would be swallowed by the BH.
- Whether tidal disruption occurs or not depend on the binary parameters.





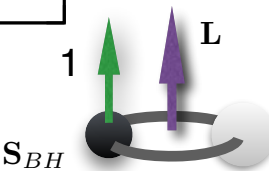
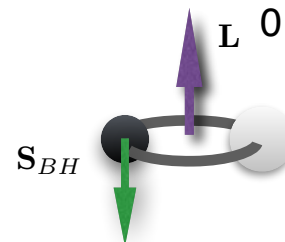
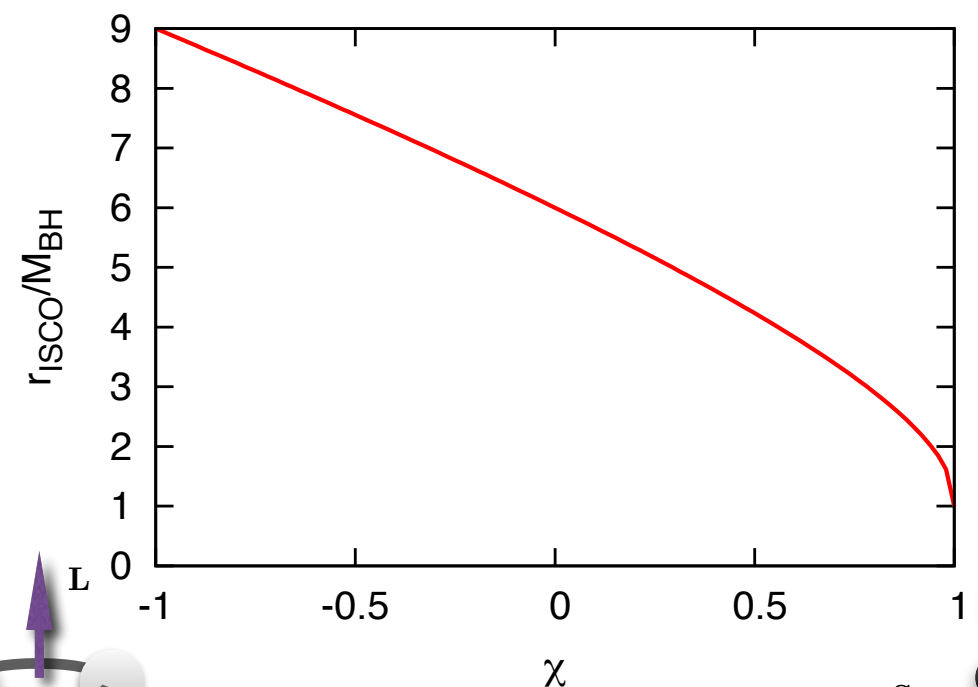
# Parameter dependence: Tidal disruption

$$\frac{M_{NS}}{R_{NS}^2} \leq \frac{M_{BH} R_{NS}}{r_{ISCO}^3} \iff \frac{M_{BH}}{r_{ISCO}} \geq C Q^{2/3}$$

$$M = M_{NS} + M_{BH} \quad Q = M_{BH}/M_{NS} \quad C \equiv M_{NS}/R_{NS} \quad \chi = S_{BH}/M_{BH}^2$$

**Tidal disruption** is likely to occur **outside the ISCO** for the case,

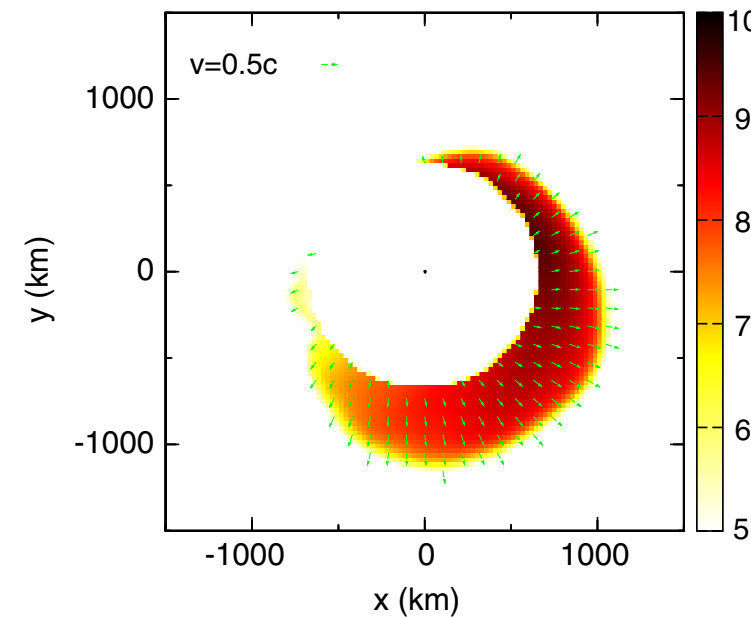
$$Q \searrow \quad C \searrow \quad \chi \nearrow$$



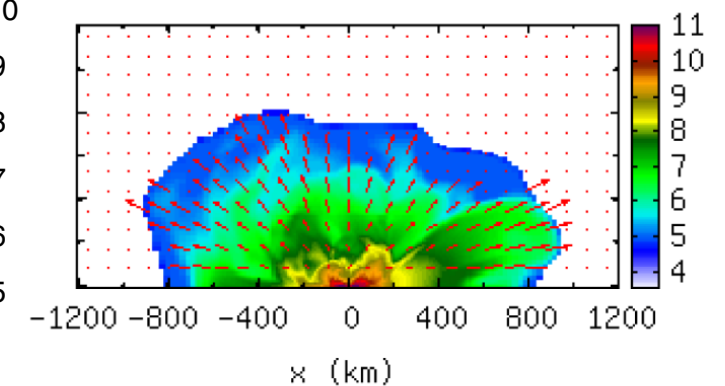
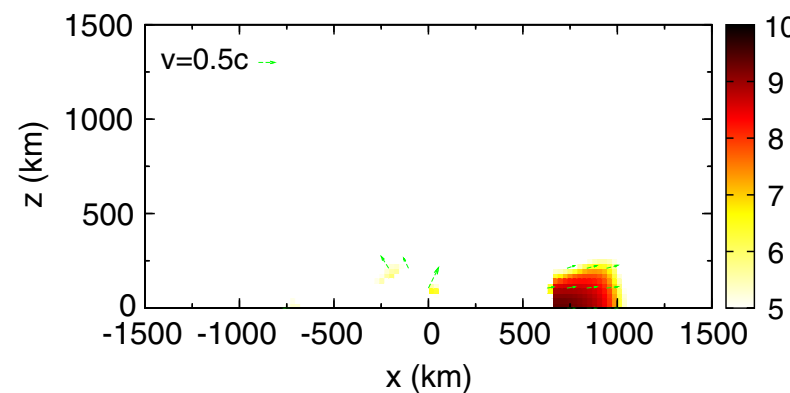
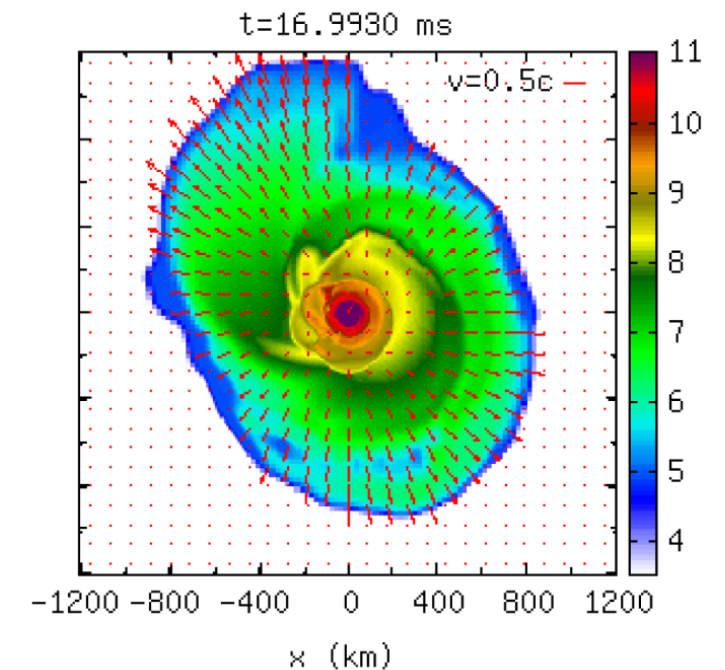
# Ejecta Morphology

- For most cases with  $M_{\text{ej}} \gtrsim 0.01 M_{\odot}$ , the dynamical ejecta from a BH-NS mergers exhibits a **crescent-like shape confined in the equatorial plane.** (c.f. quasi-spherical for NS-NS)
- The ejecta expands **homologously** with **a flat velocity distribution.** (K.Kyutoku et. al 2015)

BH-NS



NS-NS

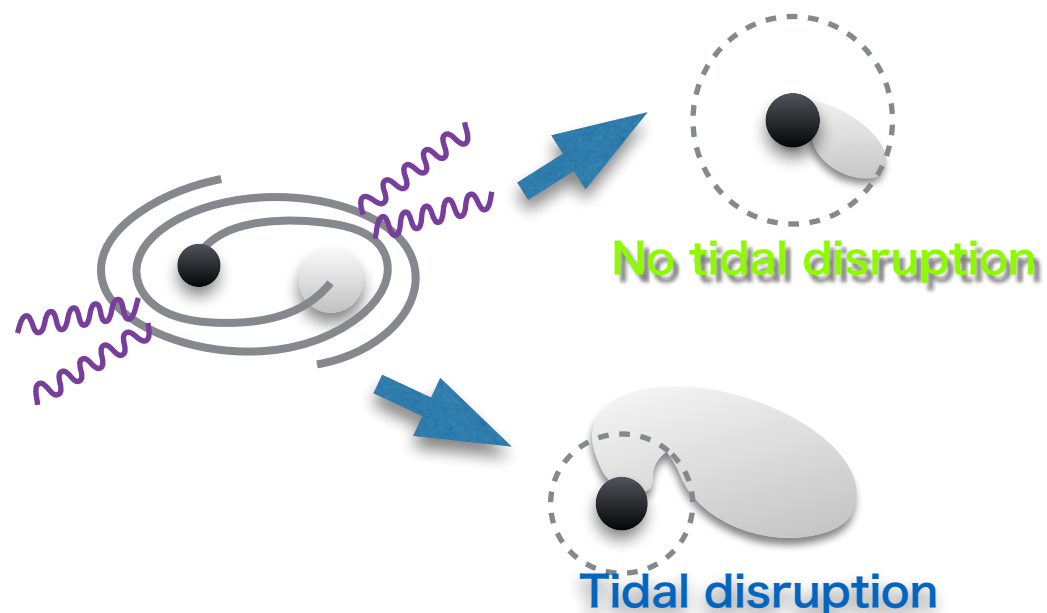


ref) Kyutoku et al. 2013

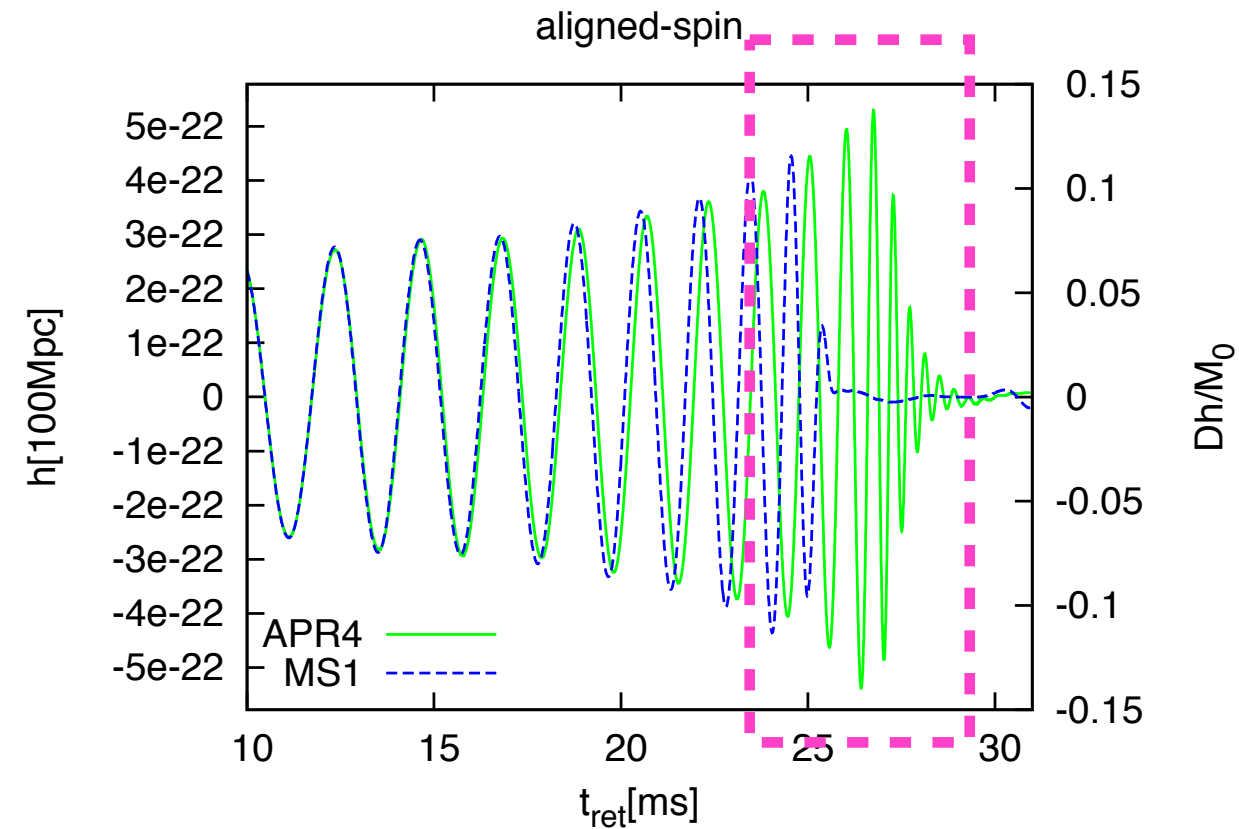
ref) Hotokezaka et al. 2013

# Post-merger waveforms (BH-NS)

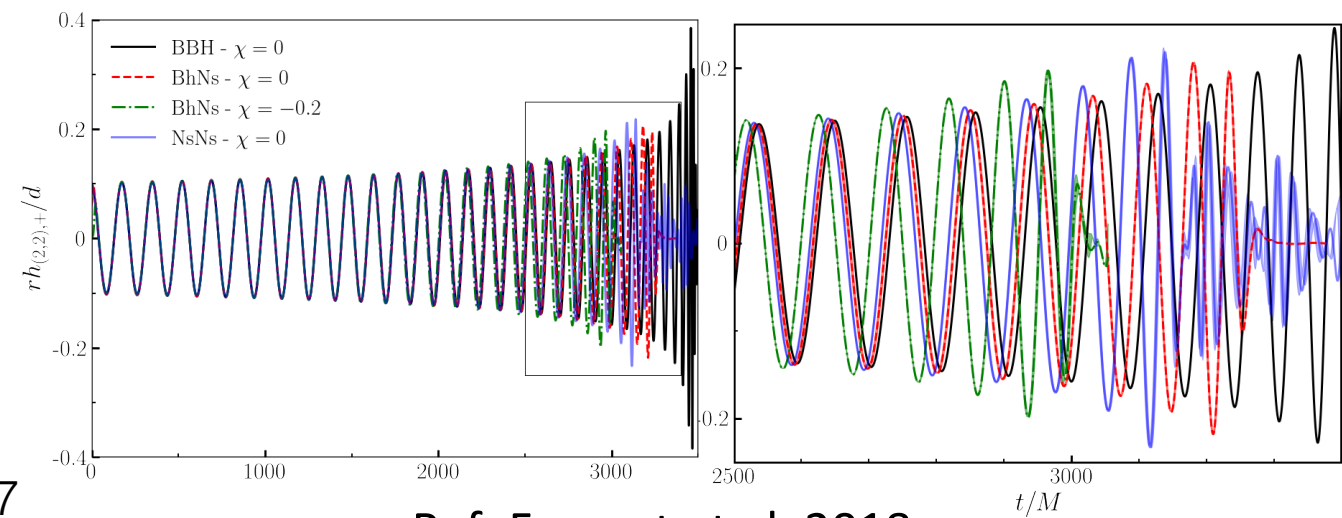
- Waveforms in the inspiral phase would have almost the same behavior as BNS or BBH.  
**→ it is important to distinguish it from BNS or BBH**
- The merger~post merger part of the BHNS waveform could be different if the NS is **tidally disrupted**  
**→ The high frequency part (>1kHz) of GW is important**  
 (see also e.g. Shibata et al. 2009, Lackey et al. 2014, Pannarale et al. 2015)



ref) Kyutoku et al. 2015



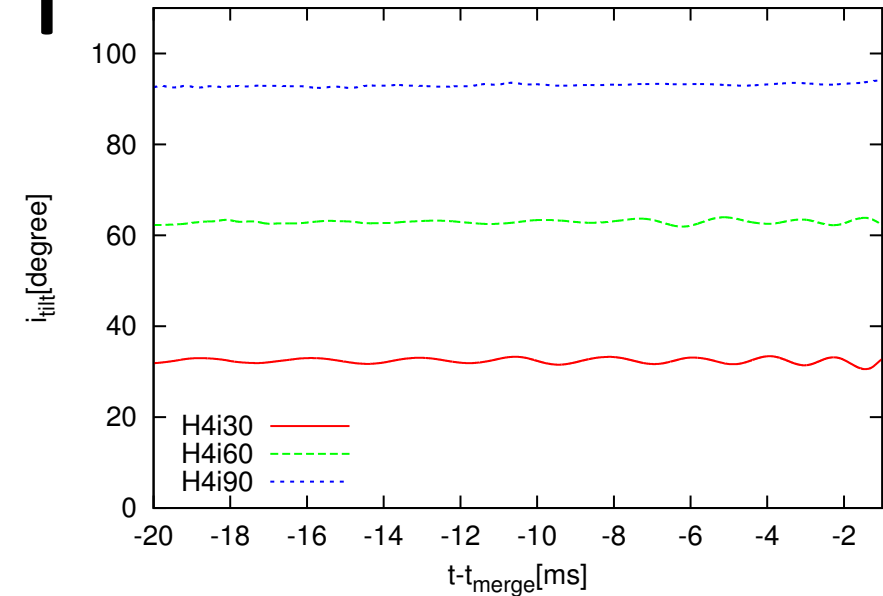
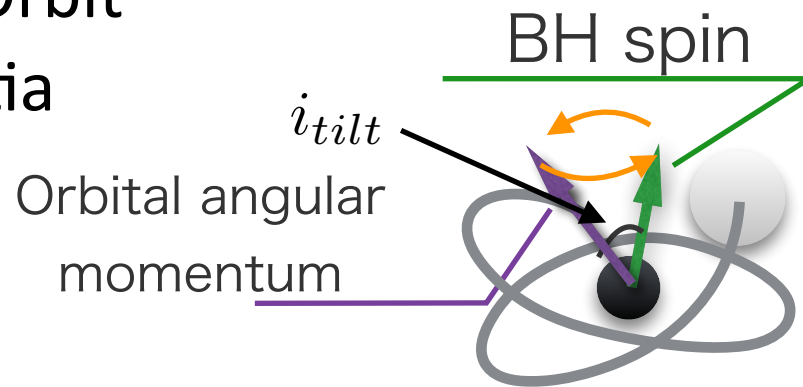
GW comparison between different binary components (Q=1)



Ref: Foucart et al. 2018

# Effect of the BH spin orientation

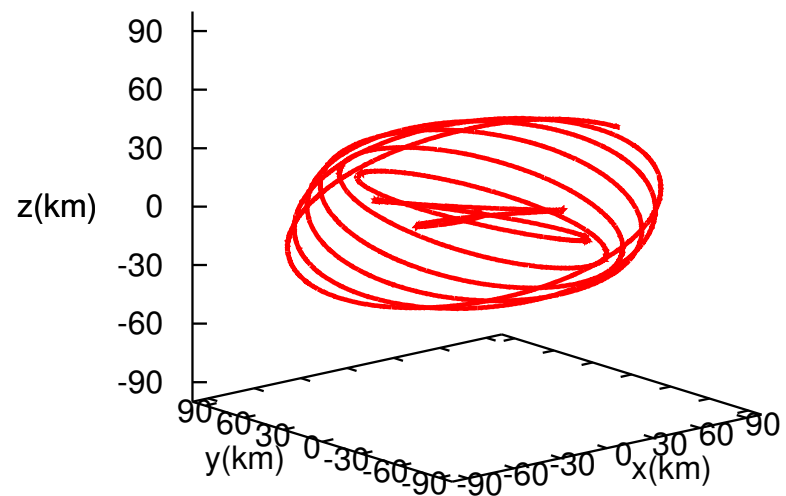
- If the orbital angular momentum and BH spin are **misaligned**, the orbit **precesses** due to Spin-Orbit coupling (or dragging of inertia frames).



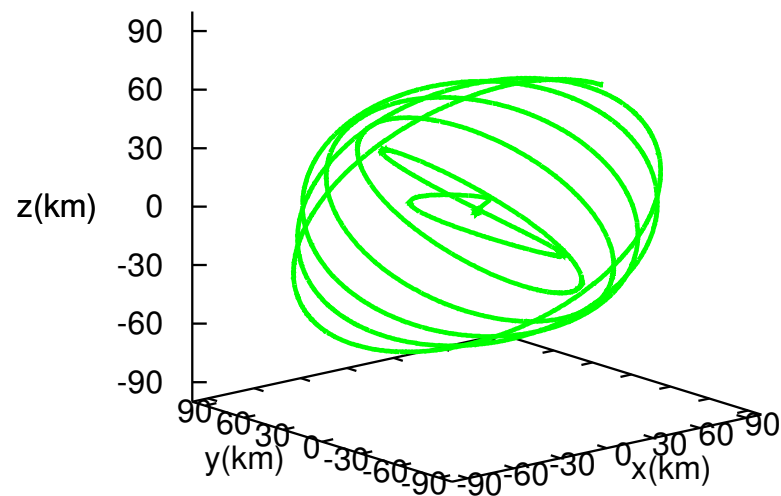
H4i30

H4i60

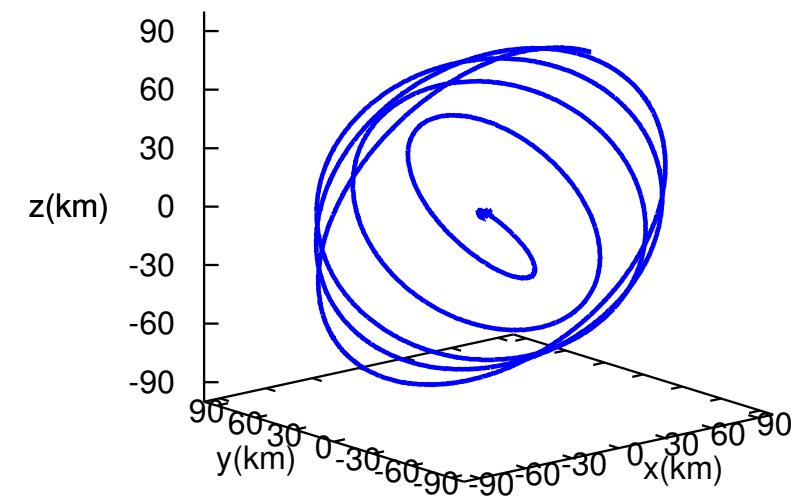
H4i90



$N_{\text{orb}} \approx 8.5$



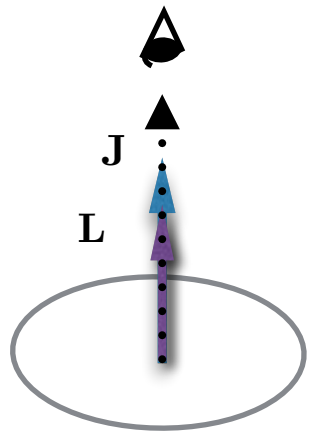
$N_{\text{orb}} \approx 7.5$



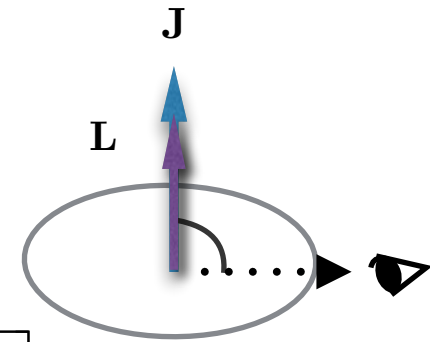
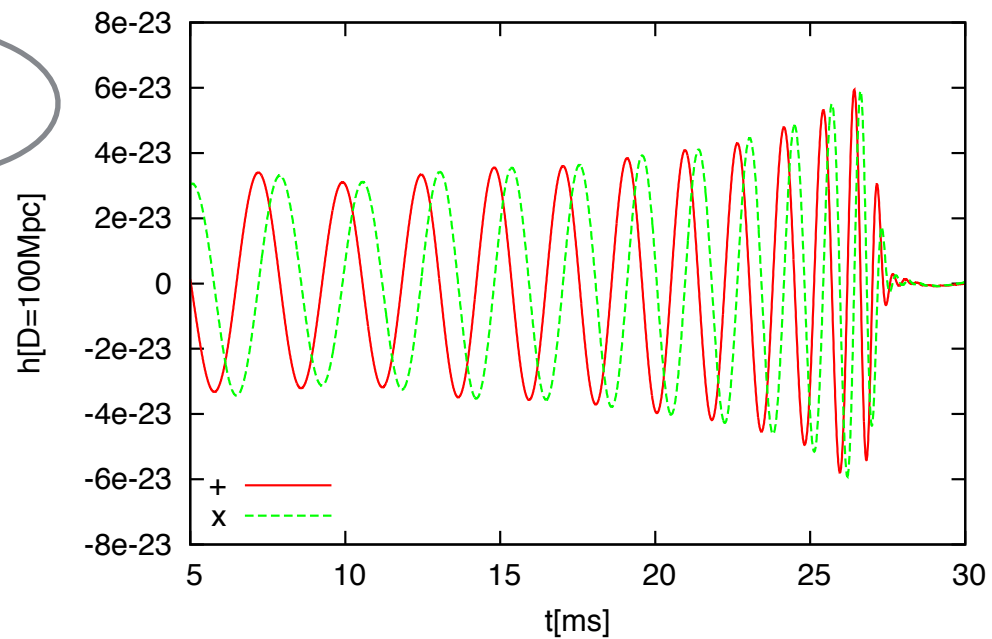
$N_{\text{orb}} \approx 5.5$

$i_{\text{tilt}} \approx \text{const.}$  for inspiral phase (c.f. L. Kidder et al. 1995)

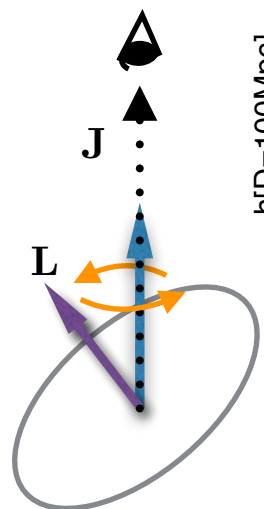
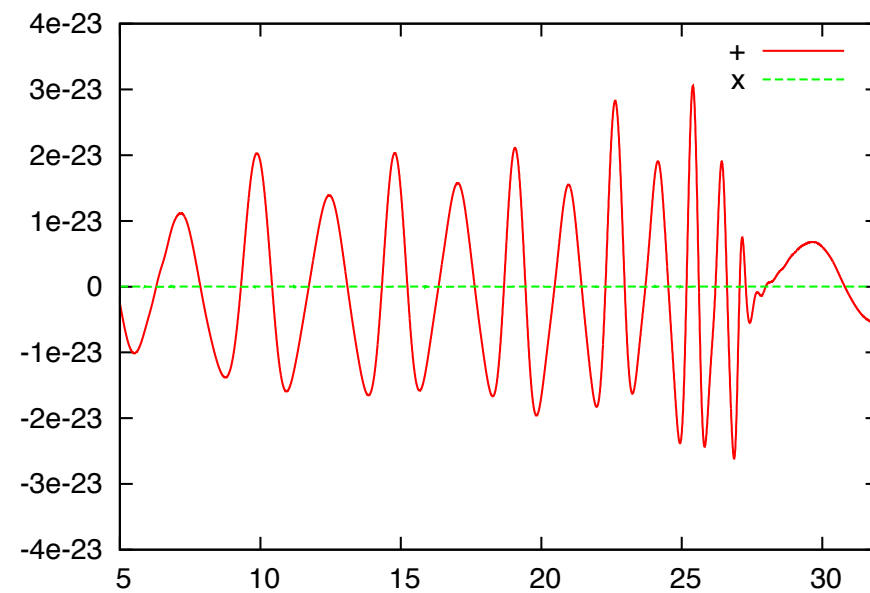
# Gravitational waves



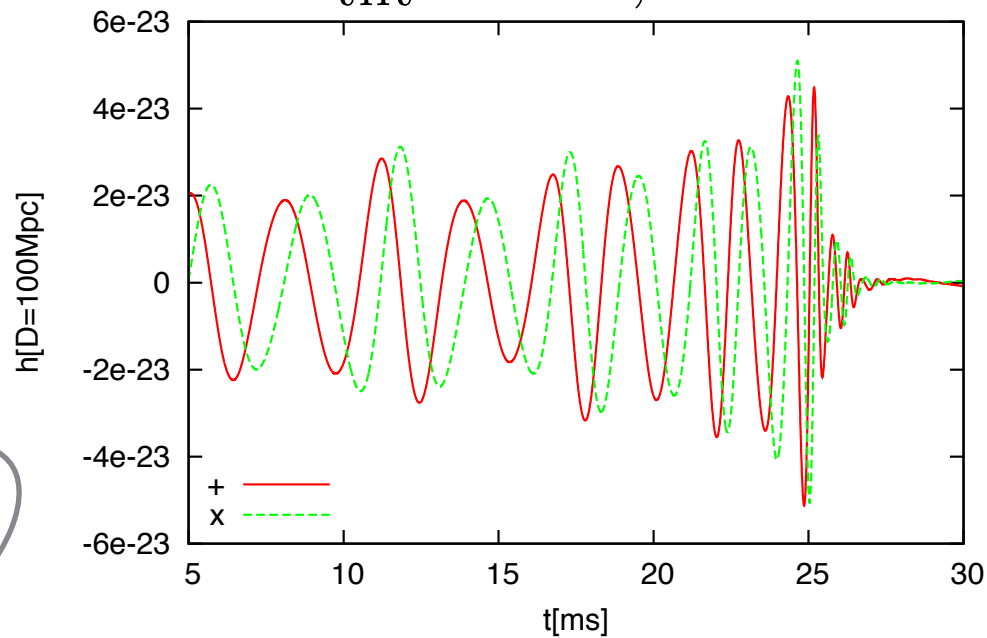
$$i_{\text{tilt}} = 0^\circ, \theta = 0^\circ$$



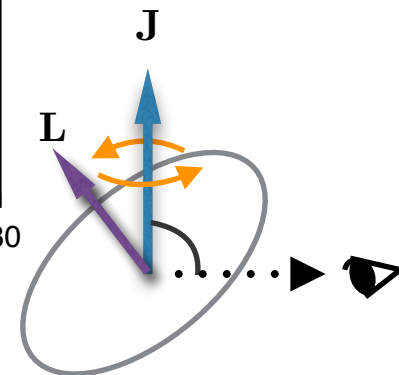
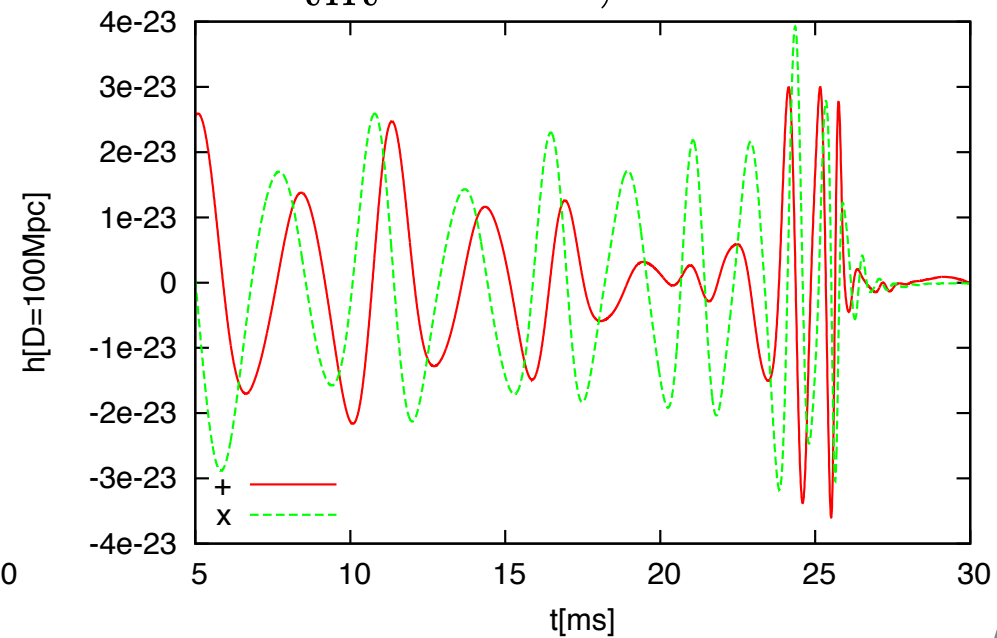
$$i_{\text{tilt}} = 0^\circ, \theta = 90^\circ$$



$$i_{\text{tilt}} = 90^\circ, \theta = 0^\circ$$



$$i_{\text{tilt}} = 90^\circ, \theta = 90^\circ$$

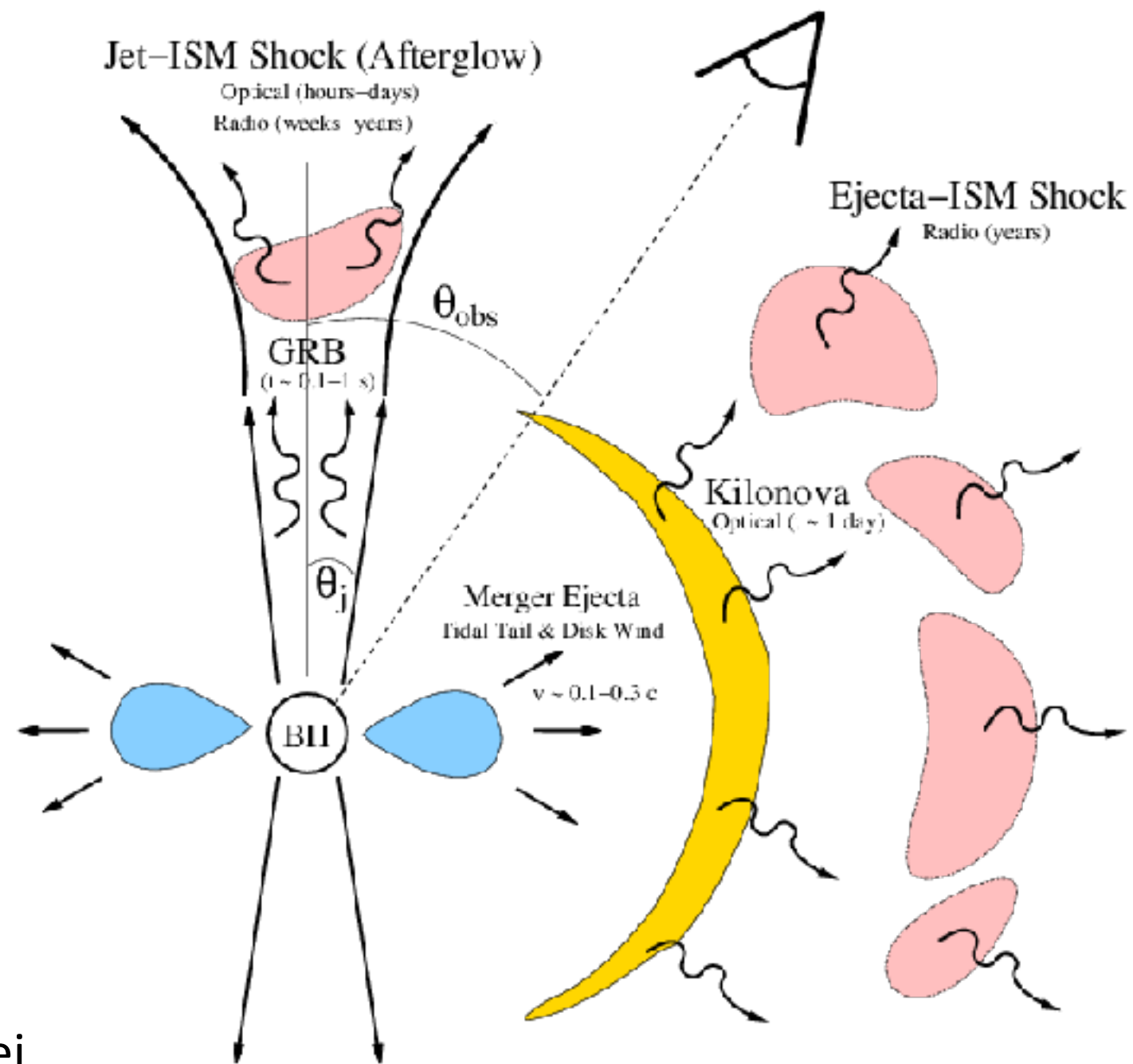




# Kilonova lightcurve prediction

# Electromagnetic Counterparts to NS binary mergers

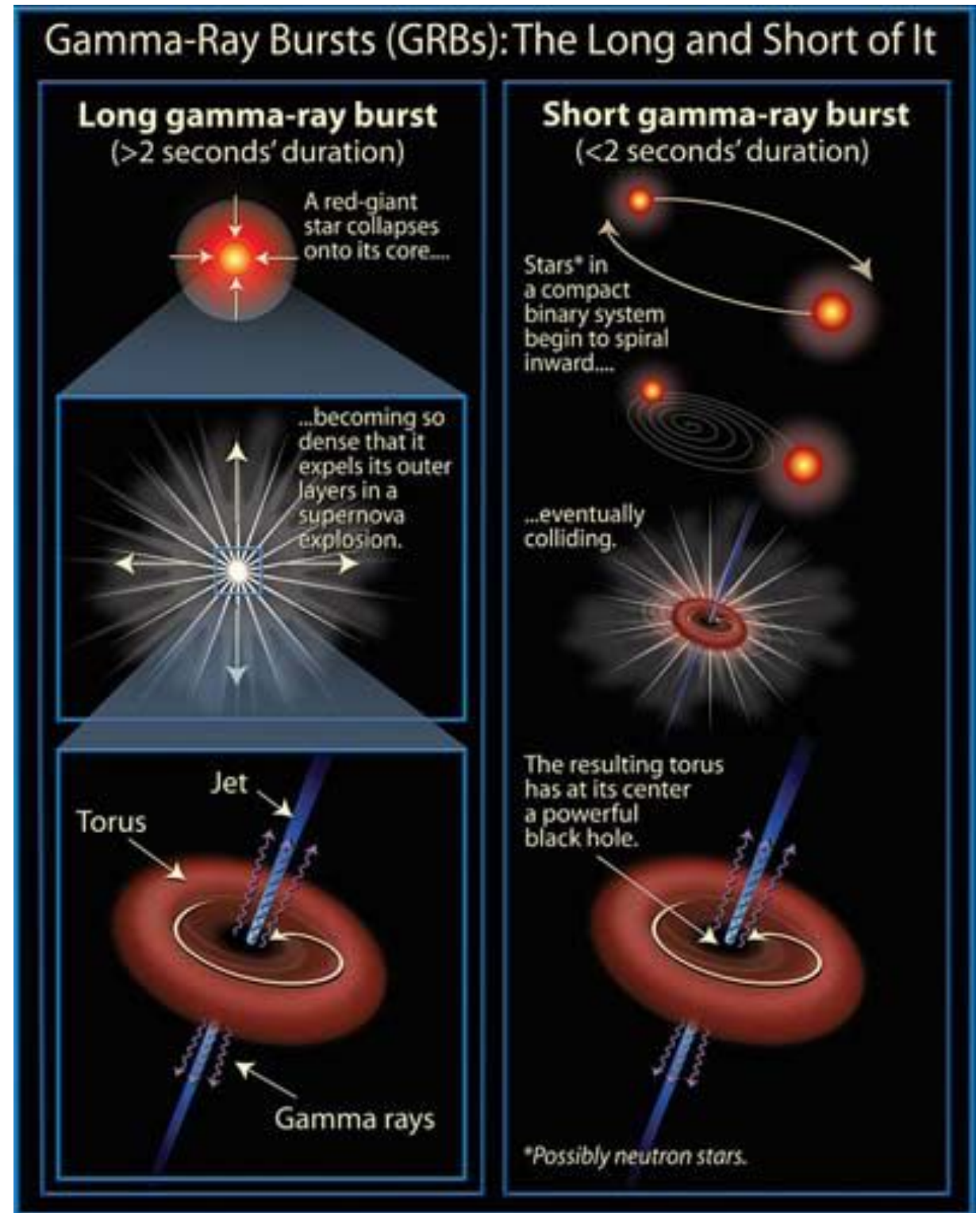
- Various transient EM counterparts are proposed for NS binary mergers
- for example,
  - short-hard gamma-ray-burst
  - Afterglow
  - cocoon emission
  - kilonovae/macronovae
  - radio flare, etc.
- Host galaxy identification, remnant properties, environment
- Possible synthesis site of r-process nuclei



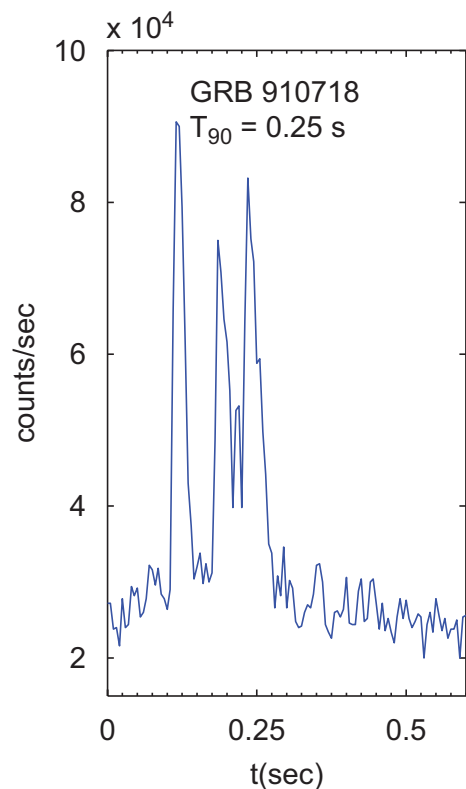
Ref: B. Metzger and E. Berger 2012

# short-hard gamma-ray burst

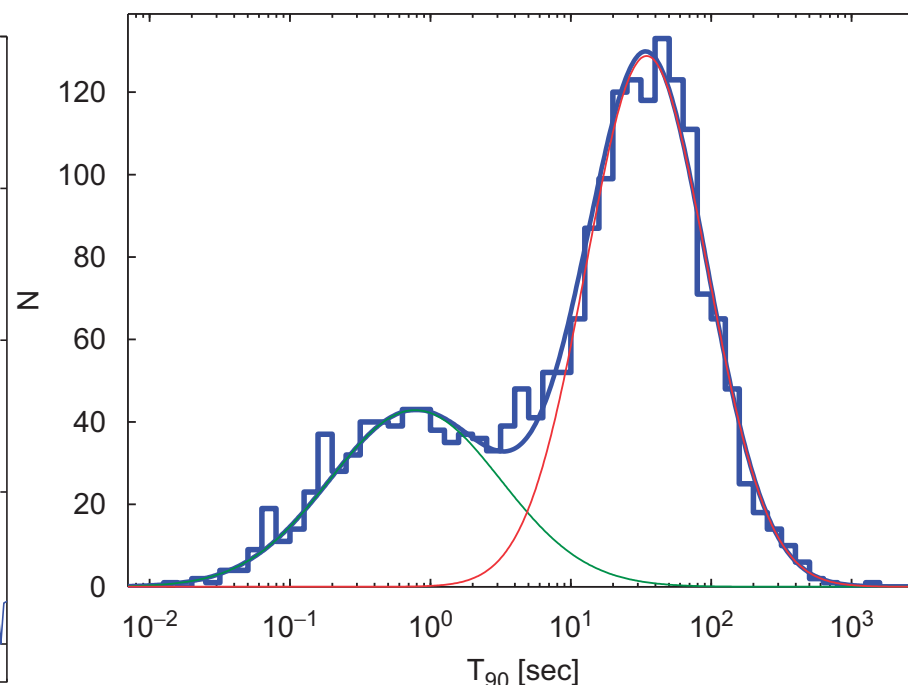
- $L \sim 10^{51} \text{ erg/s}$ ,  $\Delta t = 0.01\text{-}1000 \text{ s}$
- launched by highly relativistic jet ( $\Gamma \sim 100\text{-}1000$ )
- Long-soft GRB:  $\geq 2\text{ s}$   
deaths of massive stars
- Short-hard GRB:  $\leq 2\text{ s}$   
neutron star binary merger?



sGRB light curve



Duration distribution of GRBs

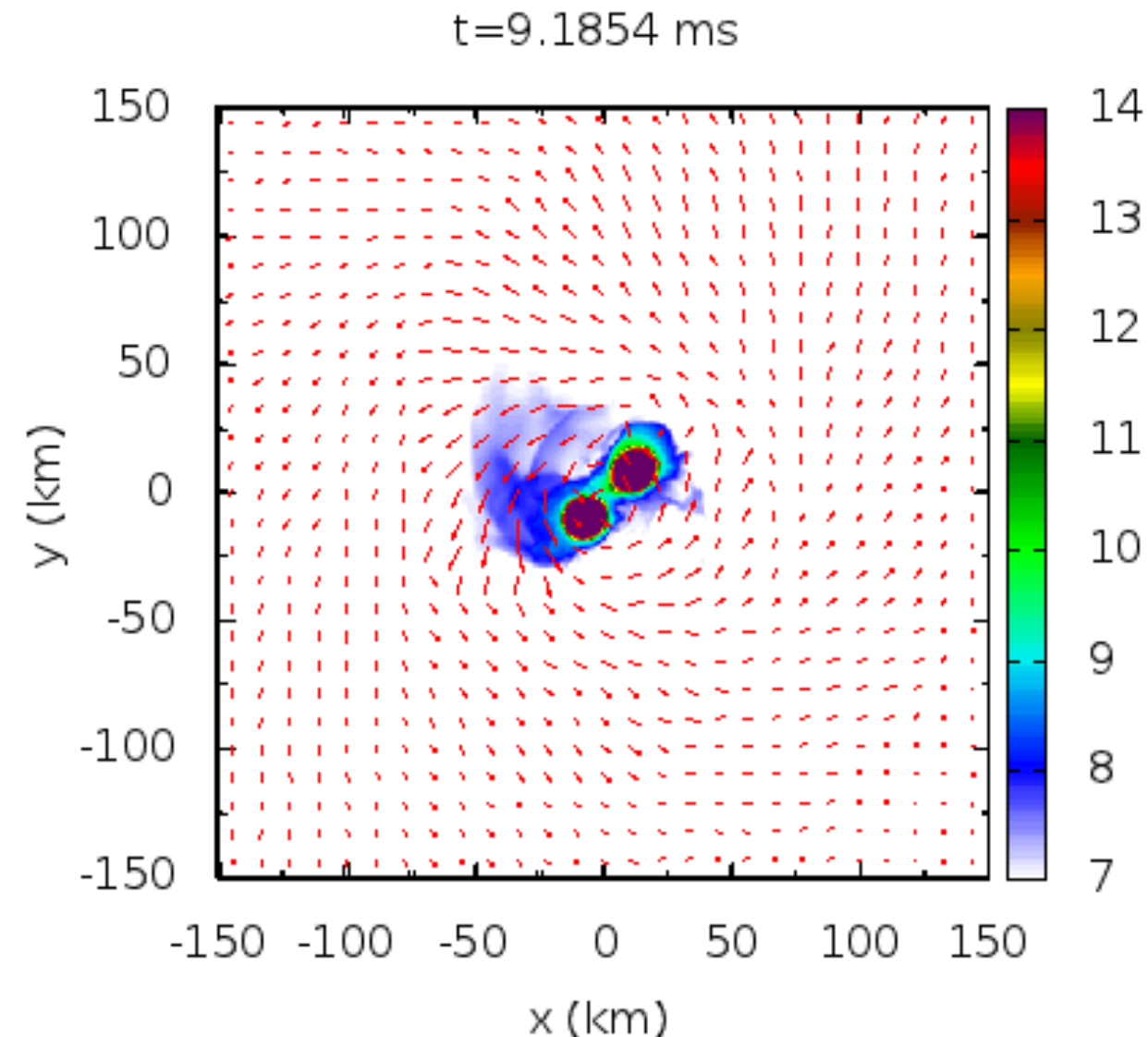


ref) Nakar 2007

# Kilonova/Macronova

- A **Kilonova/macronova** is an electromagnetic (EM) emission which is expected to be associated with a NS binary merger.
- Ejected material is neutron-rich  
→ heavy radioactive nuclei would be synthesized in the ejecta by the so-called **r-process nucleosynthesis**  
→ EM emission in optical and infrared wavelengths could occur by radioactive decays of heavy elements  
: **kilonova/macronova**

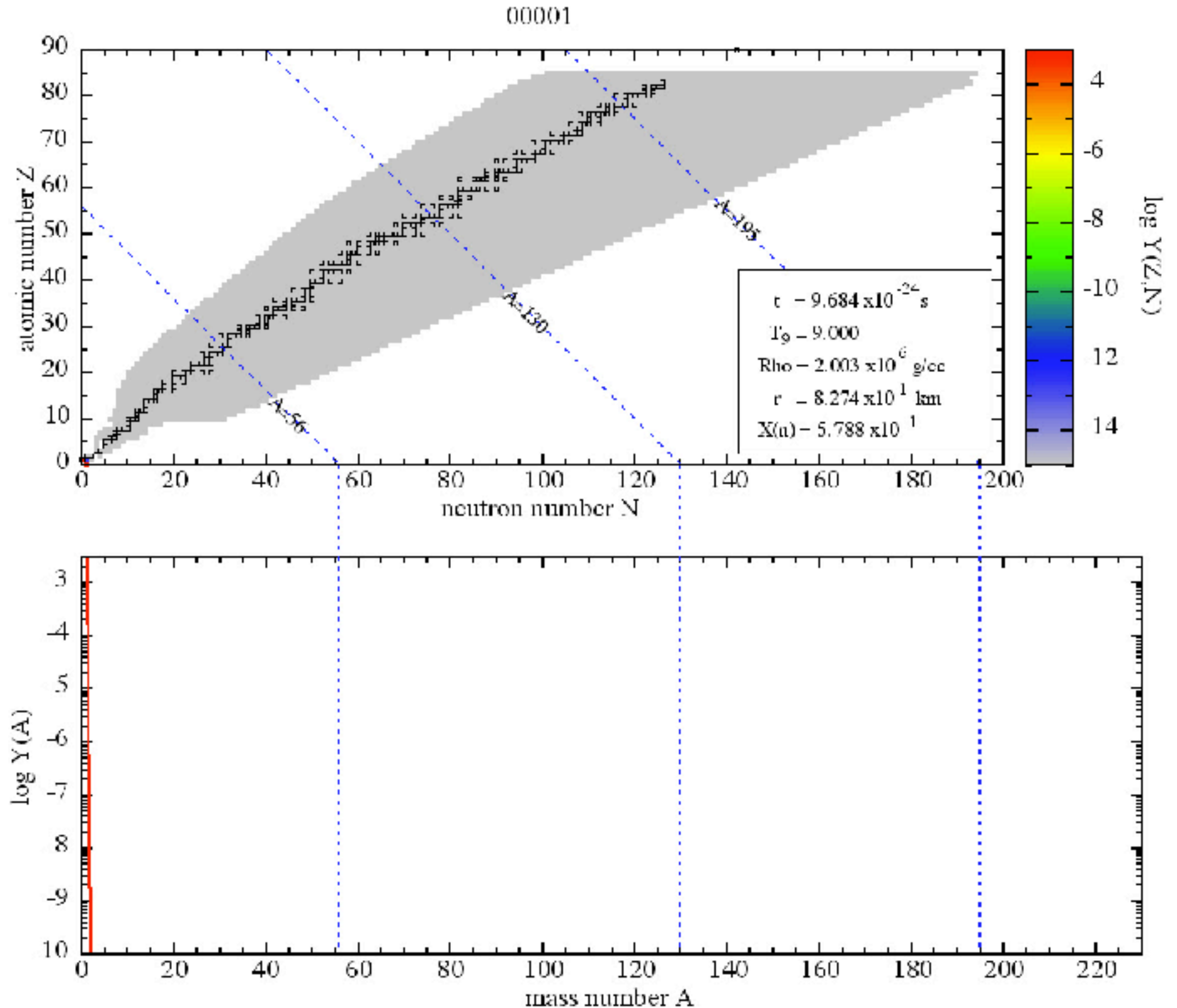
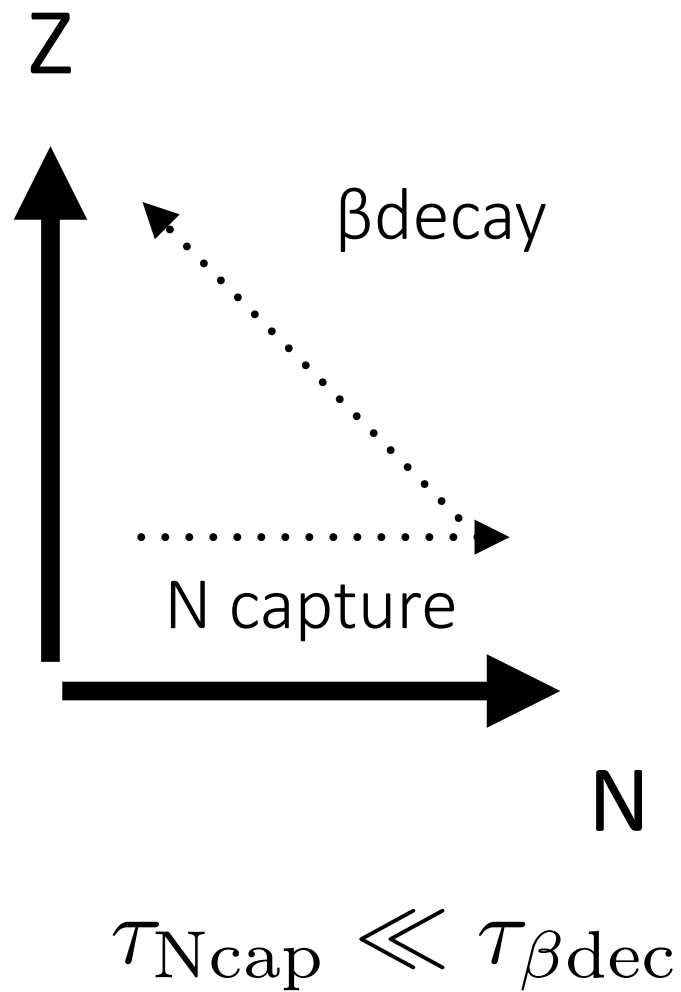
Li & Paczyński 1998, Kulkarni 2005,  
Metzger et al. 2010 ...



Ref: K. Hotokezaka et al. 2013

# R-process nucleosynthesis

Credit) Sho Fujibayashi





# Properties of kilonovae / macronovae

## Order Estimation

ref) Li & Paczyński 1998

$$t_{\text{peak}} \approx 3.3 \text{ days}$$

$$\times \left( \frac{M}{0.03M_{\odot}} \right)^{1/2} \left( \frac{v}{0.2c} \right)^{-1/2} \left( \frac{\kappa}{1 \text{ cm}^2/\text{g}} \right)^{1/2}$$

$M_{\text{eje}}$  :ejecta mass

$v_{\text{eje}}$  :expanding velocity

$$L_{\text{peak}} \approx 2.0 \times 10^{41} \text{ ergs/s}$$

$$\times \left( \frac{f}{10^{-6}} \right) \left( \frac{M}{0.03M_{\odot}} \right)^{1/2} \left( \frac{v}{0.2c} \right)^{1/2} \left( \frac{\kappa}{1 \text{ cm}^2/\text{g}} \right)^{-1/2}$$

$\kappa$  :opacity

$f$  : energy conversion rate

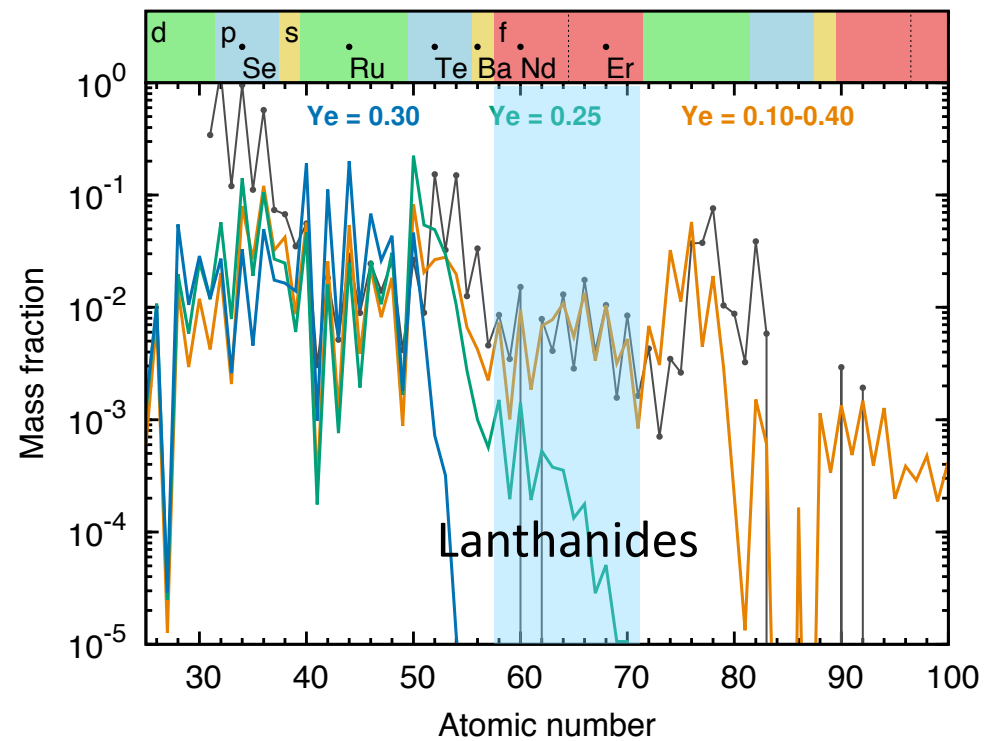
$$T_{\text{peak}} \approx 3.1 \times 10^3 \text{ K}$$

$$\times \left( \frac{f}{10^{-6}} \right)^{1/4} \left( \frac{M}{0.03M_{\odot}} \right)^{-1/8} \left( \frac{v}{0.2c} \right)^{-1/8} \left( \frac{\kappa}{1 \text{ cm}^2/\text{g}} \right)^{-3/8}$$

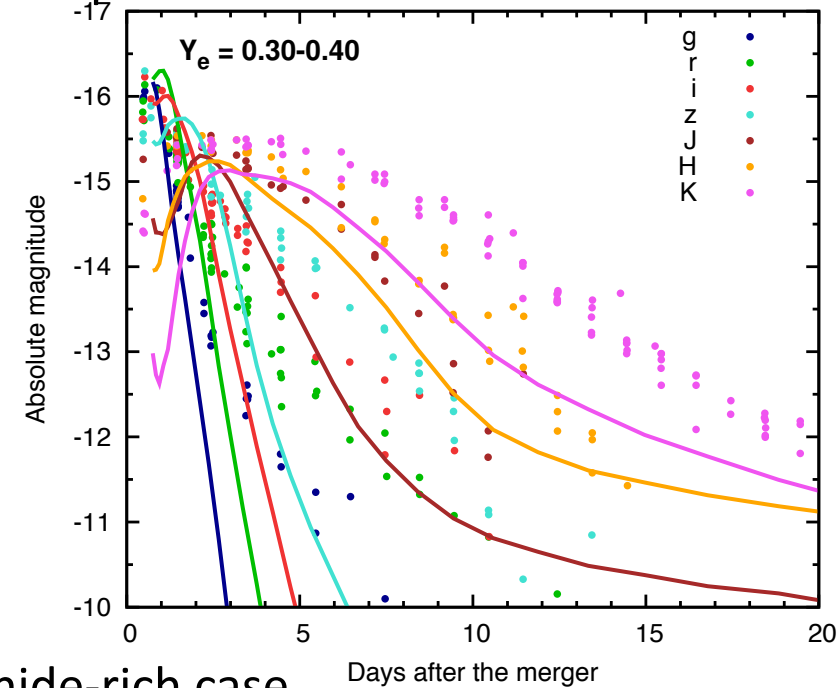
- The emission is expected to be bright in **the optical and infrared wavelength**.
- **The mass, velocity, morphology, and the composition(electron fraction)** of the ejecta characterize the lightcurve of the kilonova/macronova.

# Ejecta opacity

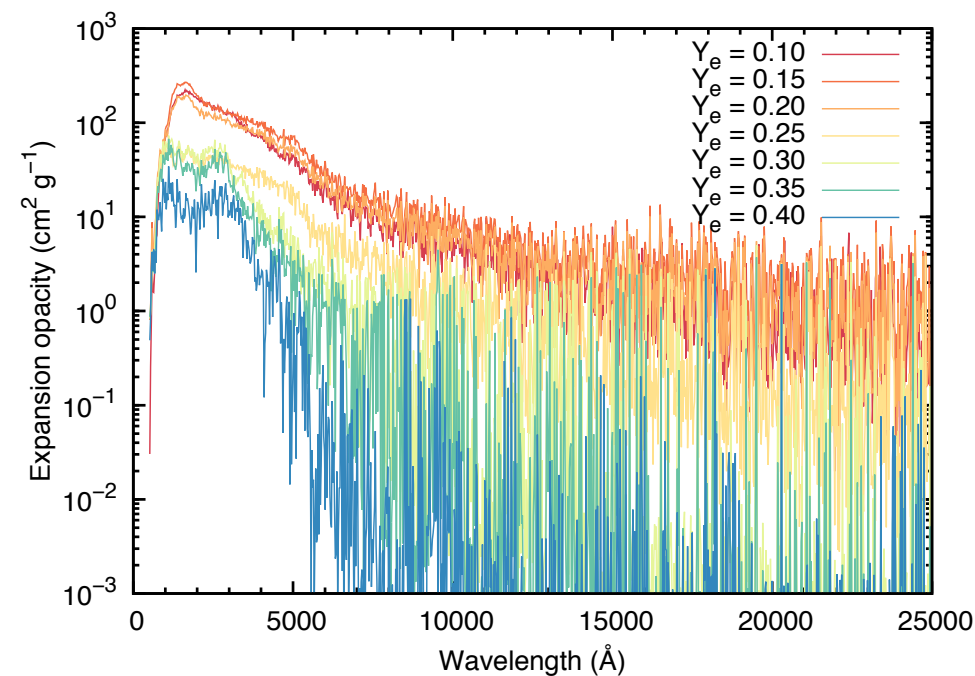
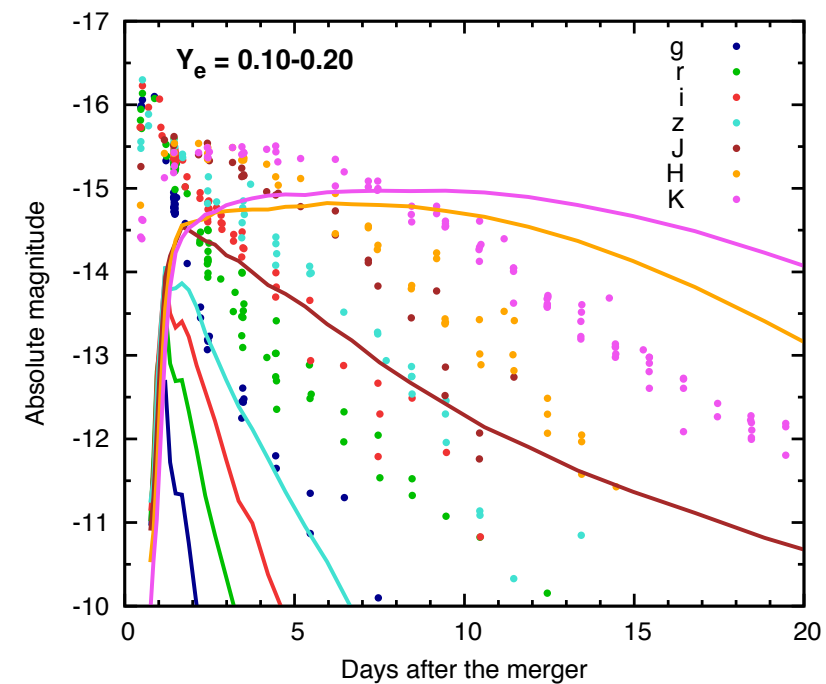
ref) Tanaka et al. 2018,2019



Lanthanide-poor case



Lanthanide-rich case



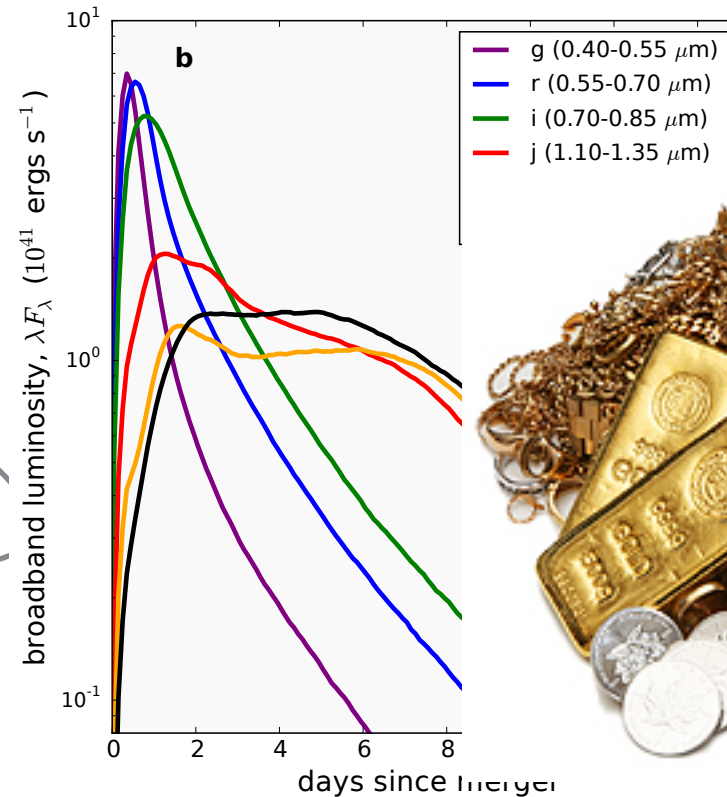
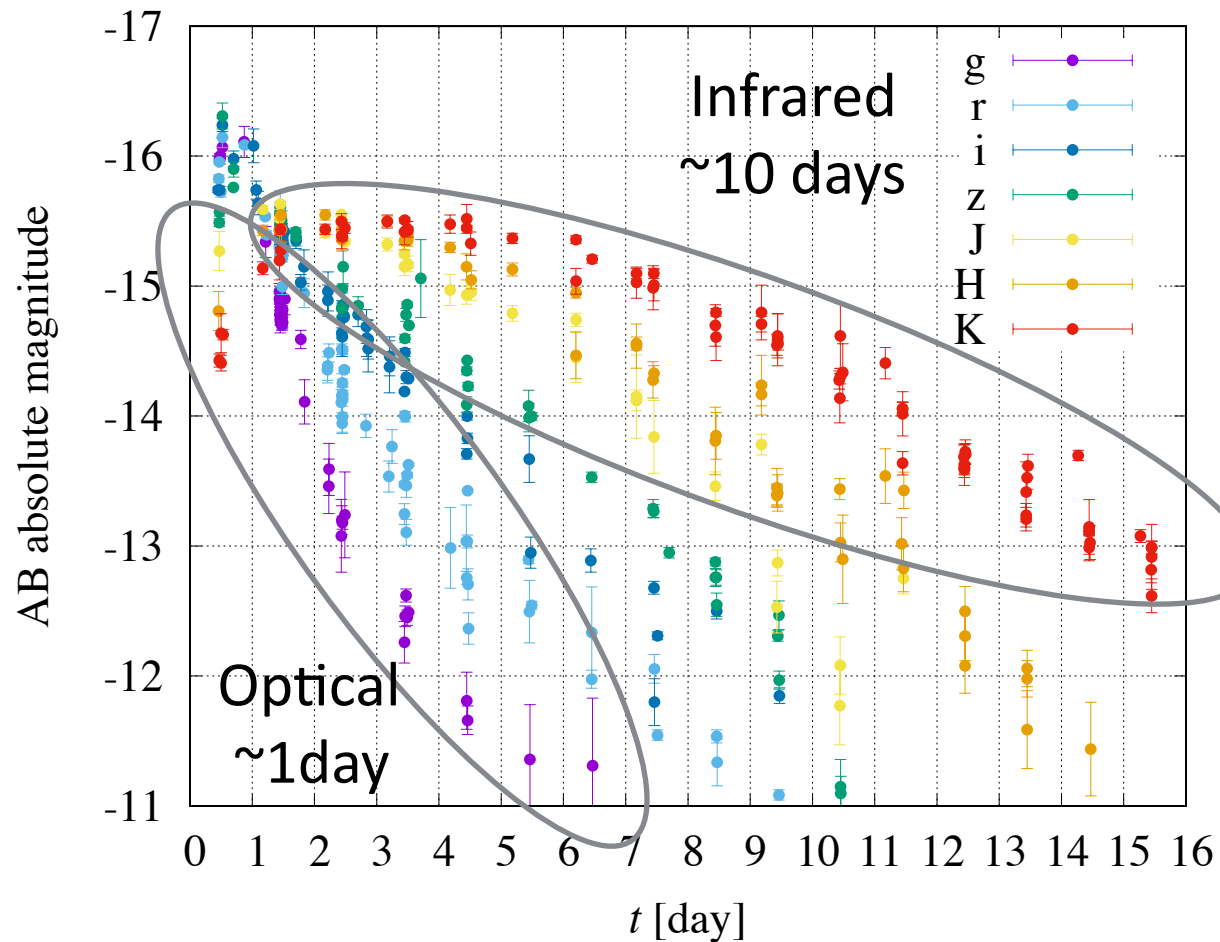
$$Y_e = \frac{[p]}{[p] + [n]}$$

The ejecta opacity varies significantly ( $0.1-10 \text{ cm}^2/\text{g}$ ) depending on whether **lanthanide elements** are synthesized or not, which reflects the electron fraction,  $Y_e$ , of ejecta. (Kasen et al. 2013, Barnes et al. 2013, Tanaka et al. 2013)

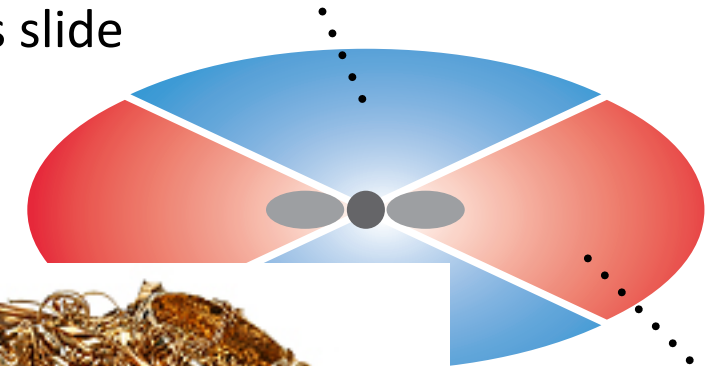
# GW170817:

## Kilonova/macronova with multiple components

Data: Summarized in Villar et al. 2017  
D=40 Mpc



Blue (lanthanide-free)  
ref) Masaomi's slide



lanthanide-rich



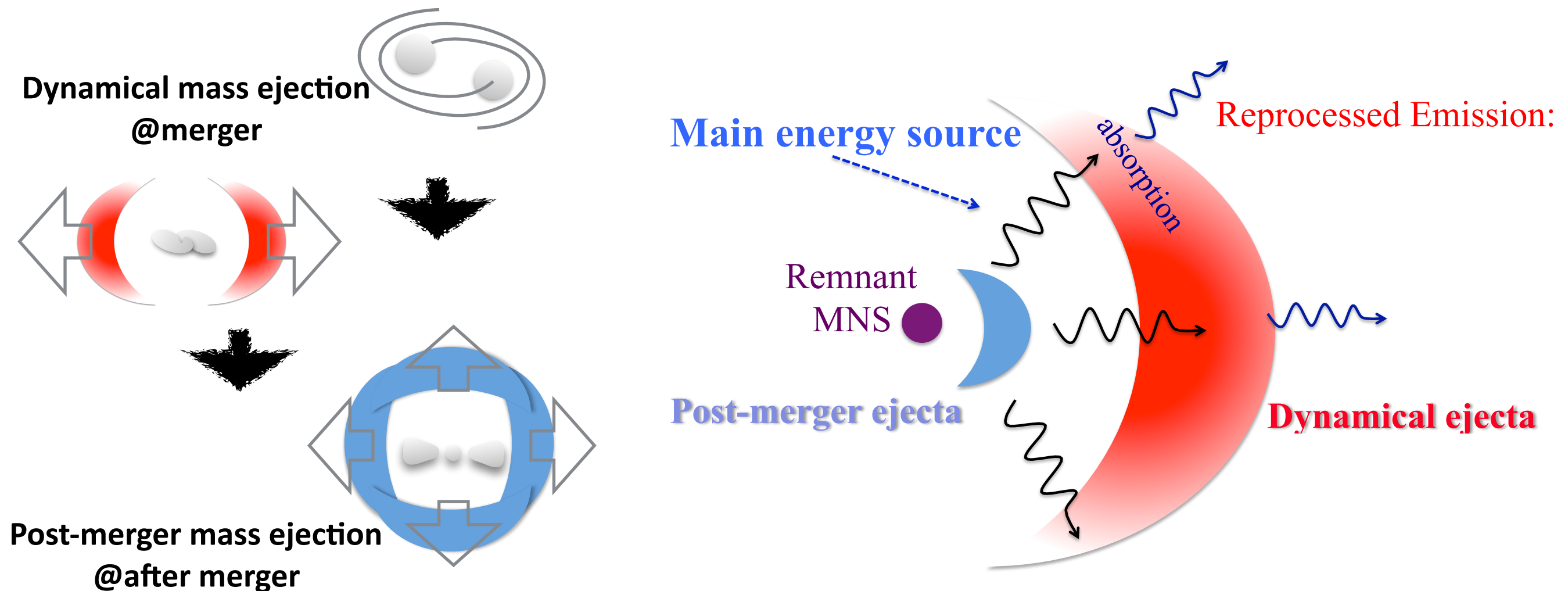
ref) D. Kasen et al. 2017

• **A Kilonova/macronova model with multiple components well interprets the optical-Infrared observation** (see e.g., Kasliwal et al. 2017, Cowperthwaite et al. 2017, Kasen et al. 2017, Villar et al. 2017)

- early-blue component ( $\sim 1$ day) from **lanthanide-free ejecta ( $\sim 0.01 M_{\text{sun}}$ , opacity  $\sim 0.1-1 \text{ cm}^2/\text{g}$ )**  
+ long-lasting red component ( $\sim 10$ days) from **lanthanide-rich ejecta ( $\sim 0.04 M_{\text{sun}}$ , opacity  $\sim 10 \text{ cm}^2/\text{g}$ )**

✳radiation transfer effect among the multiple ejecta components would change the ejecta mass estimation

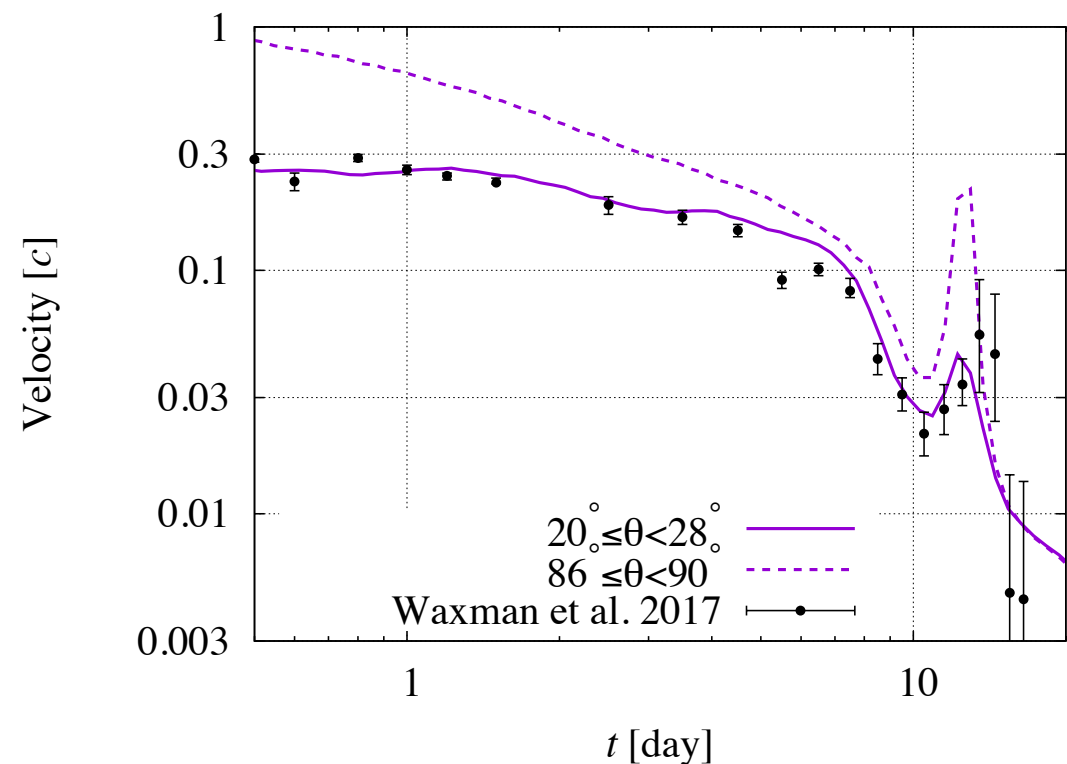
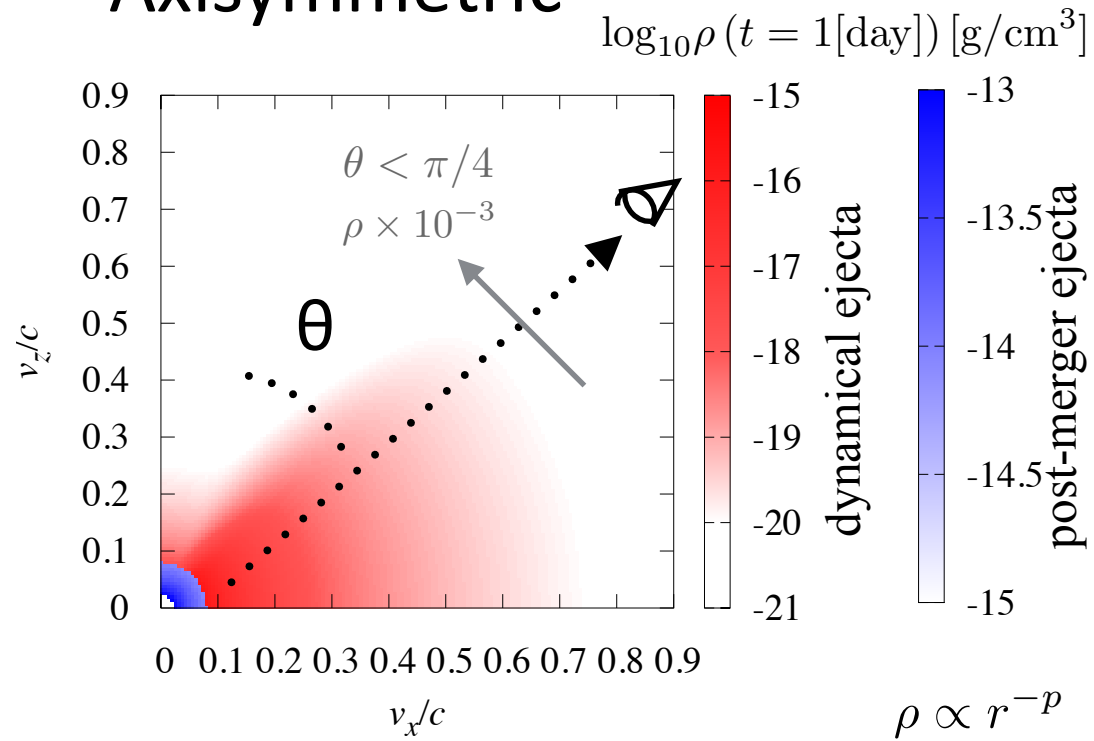
# Photon interaction among different ejecta components



Radiative transfer of photons among the multiple ejecta components has a large impact on the lightcurve predictions (see Perego et al. 2017, Wollaeger et al. 2017 for studies with similar setups and also Matsumoto et al. 2018 for reprocessing models in different context)

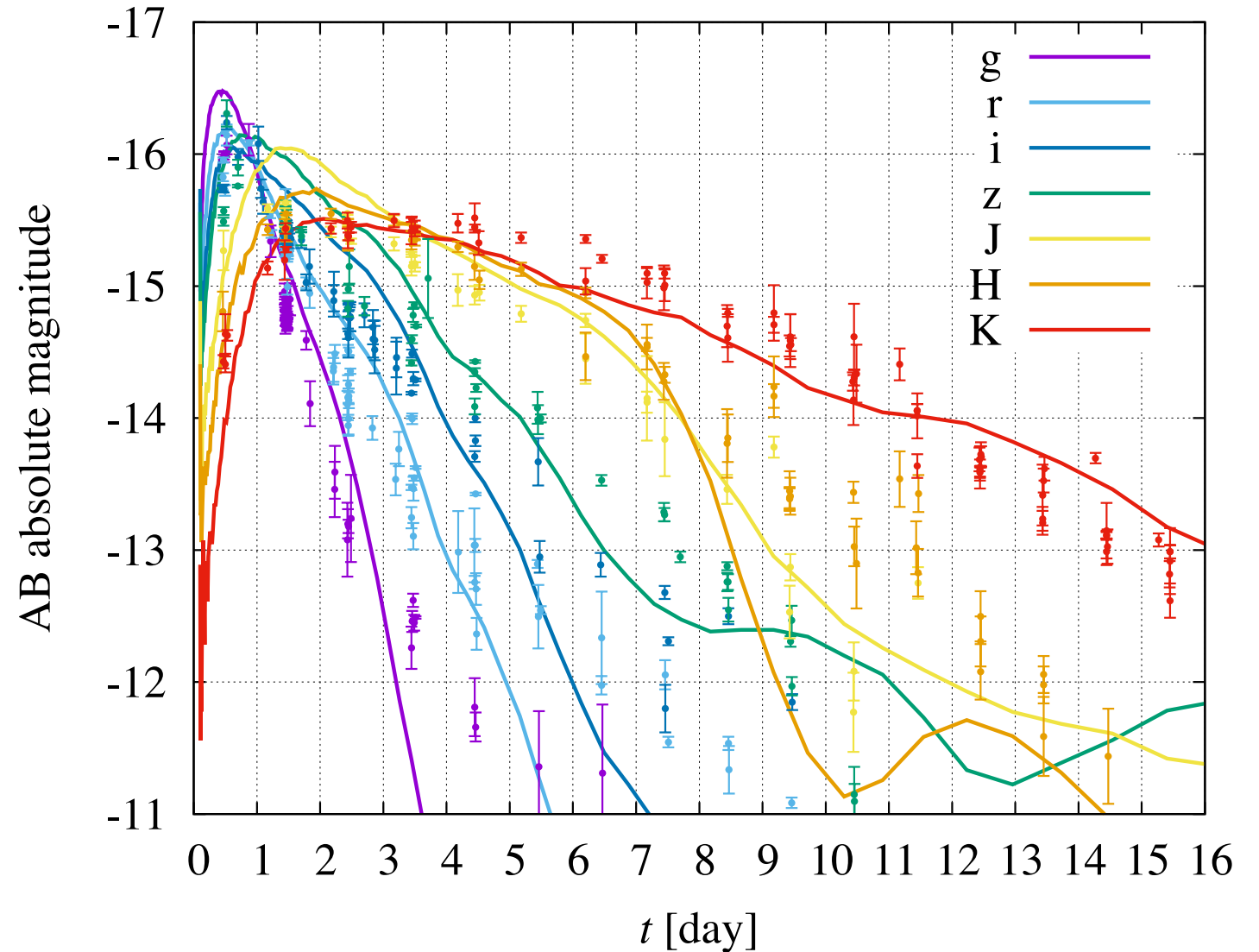
# GW170817

## Axisymmetric



GW data analysis constraint :  $\theta < \sim 30^\circ$

$D=40$  Mpc,  $20^\circ \leq \theta < 28^\circ$

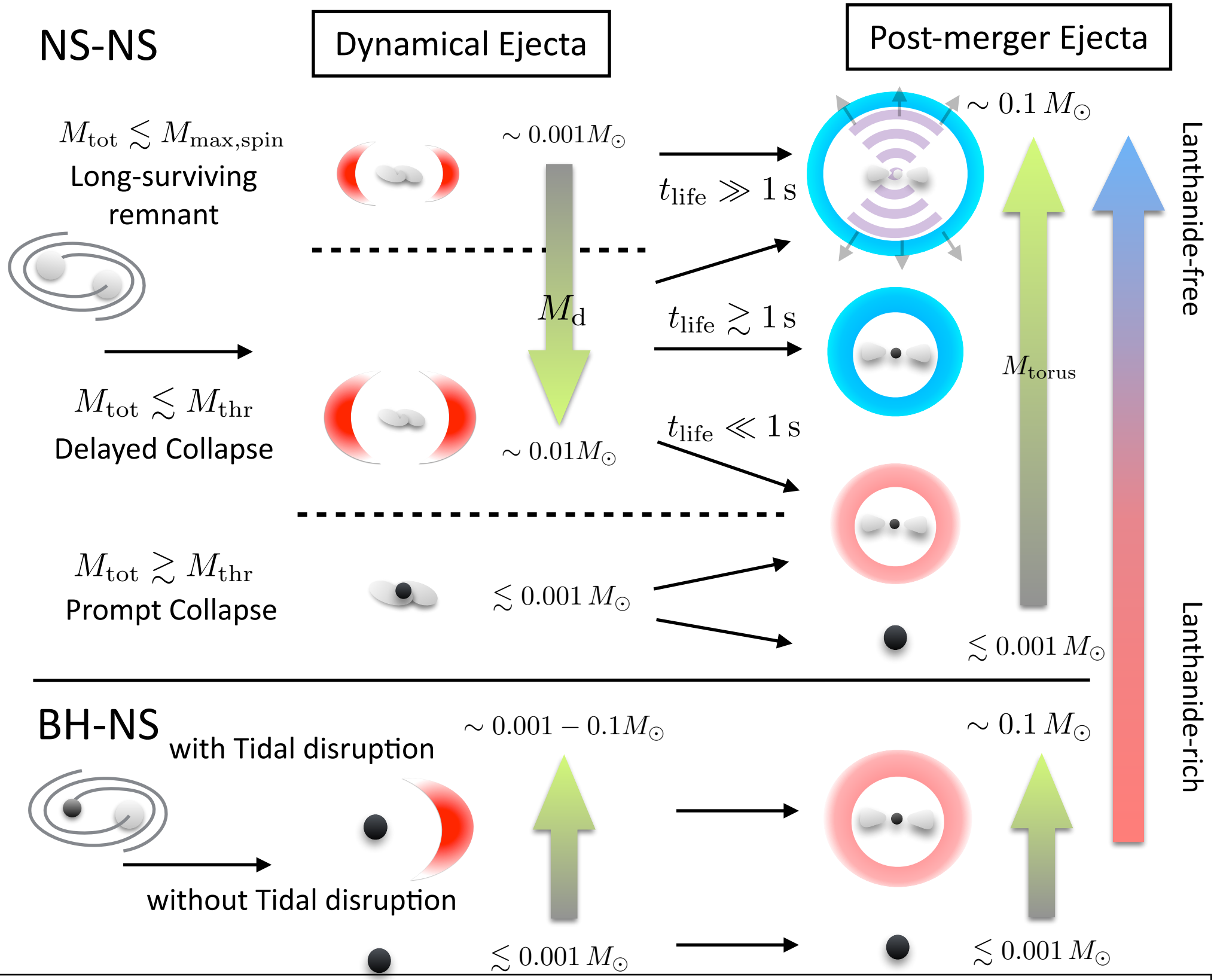


Ref: KK, Shibata, Tanaka 2018

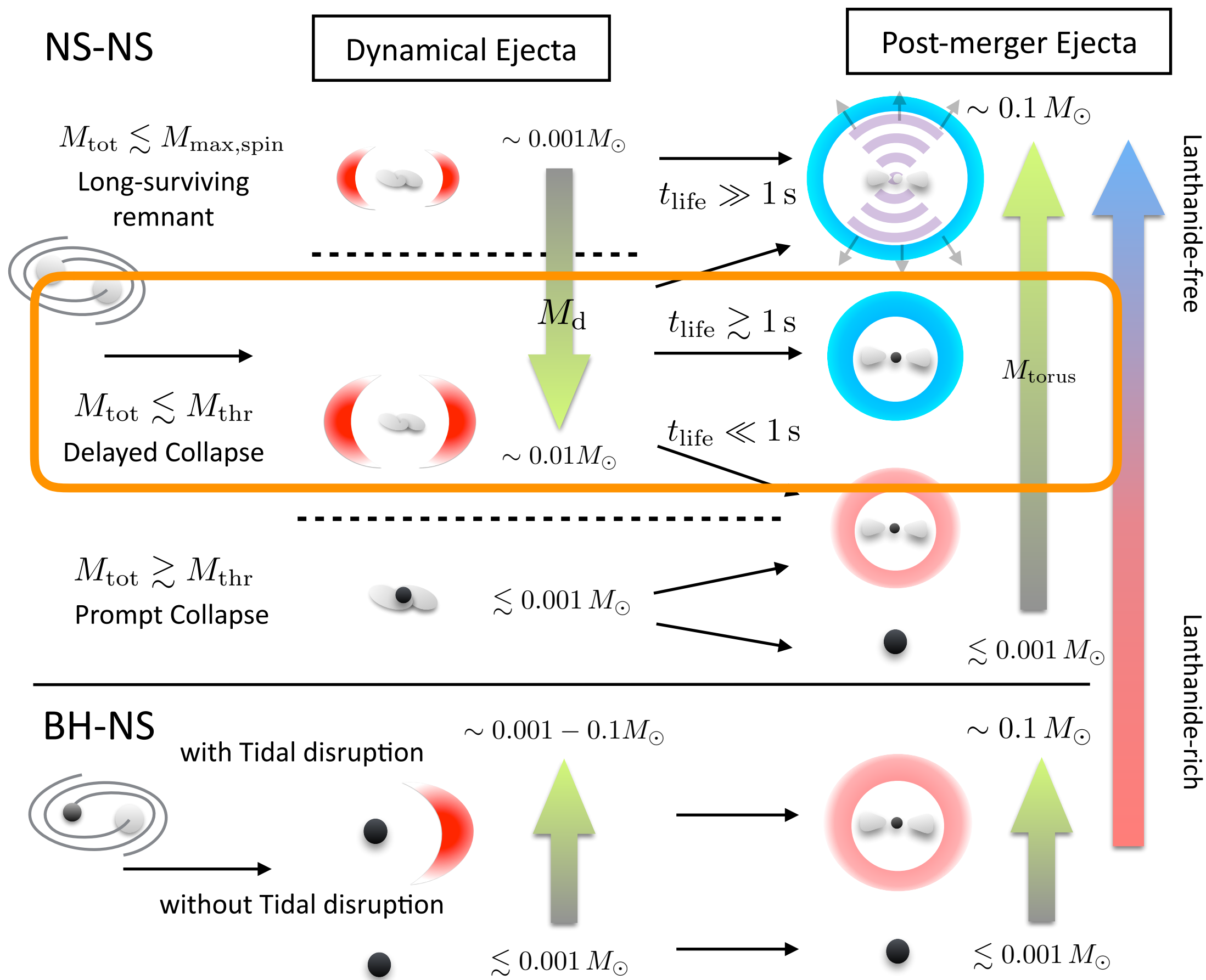
Dynamical ejecta: **0.01 M\_sun**, 0.08—0.9 c,  $Y_e=0.1-0.4$ ,  $p=-6$

Post-merger ejecta: 0.02 M\_sun, **0.025—0.08 c**,  $Y_e=0.3-0.4$ ,  $p=-3$

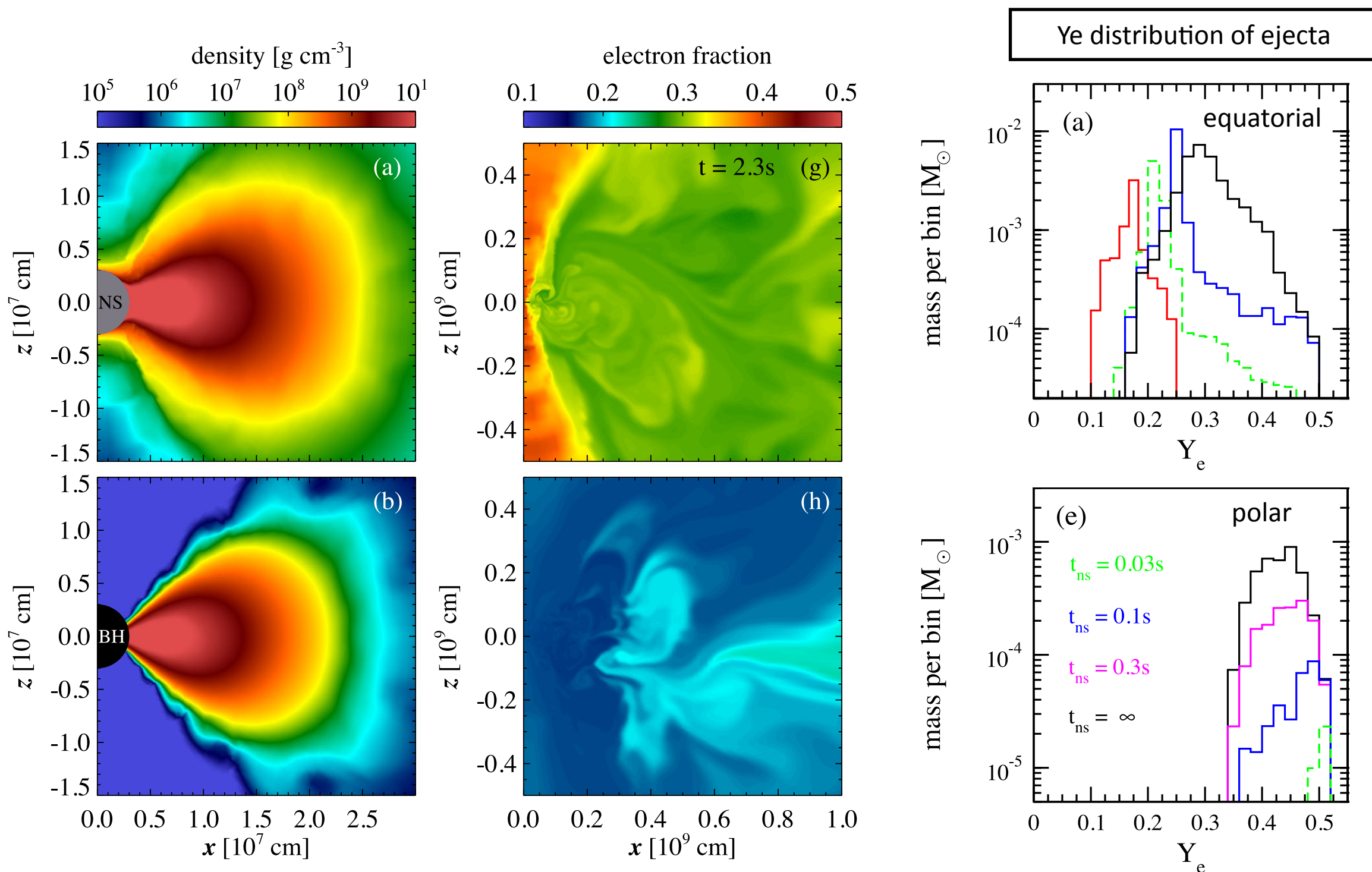




Kilonova lightcurves could show large diversity reflecting the variety in the binary parameters or the binary composition (see also e.g. Gompertz et al. 2018, Rossi et al. 2019)



# Remnant NS Lifetime



Ref: Metzger & Fernández et al. 2014

- Life time of the remnant NS has a large impact on the  $Y_e$  distribution of the post merger ejecta: low (high)  $Y_e \rightarrow$  large (small) lanthanide fraction (See also Lippuner et al. 2017)

# Ye dependence

Optical/infrared EM data points observed in  
GW170817 summarized by Villar et al. 2017 (D=40Mpc)

$$M_{\text{pm}} = 0.03 M_{\odot},$$

$$M_{\text{d}} = 0.01 M_{\odot}$$

Solid:

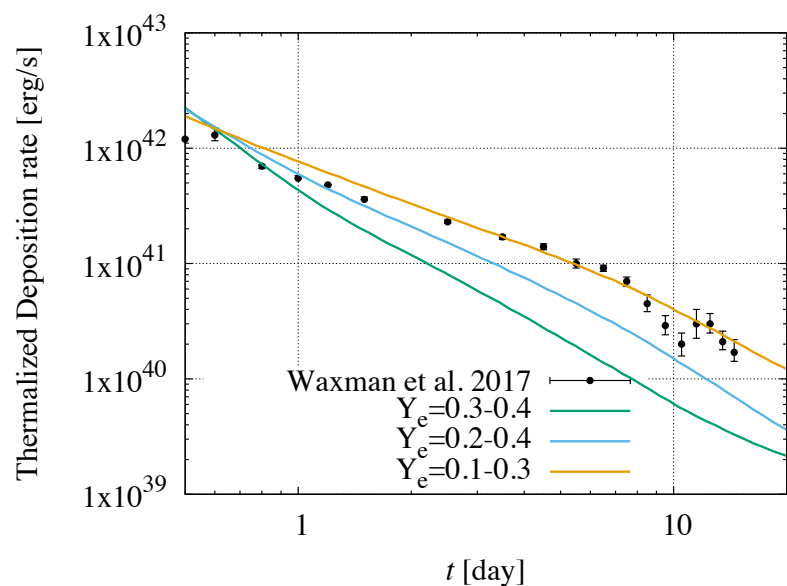
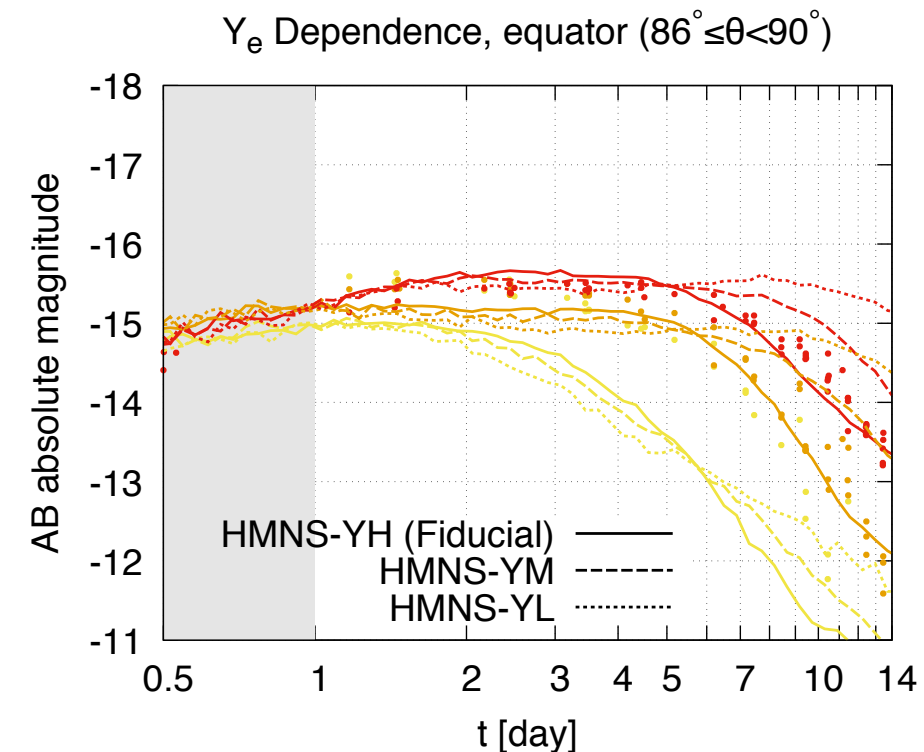
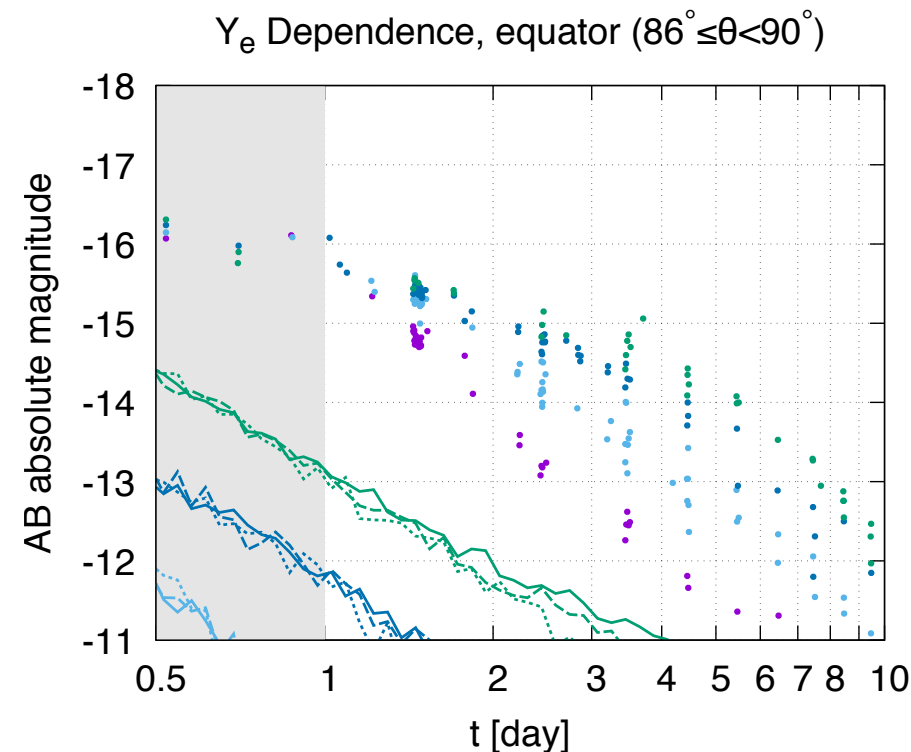
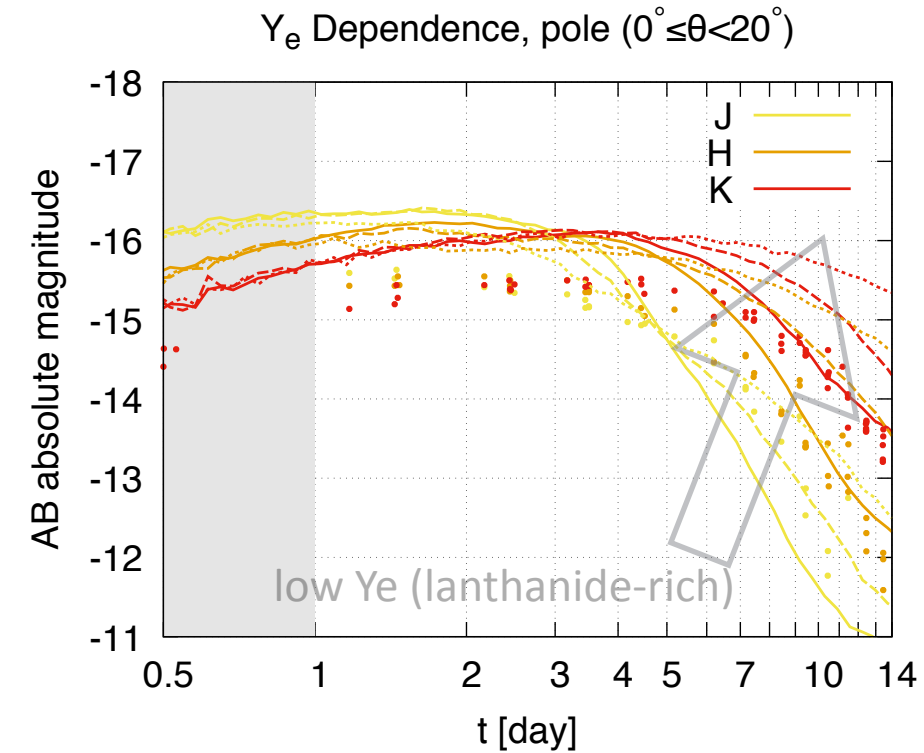
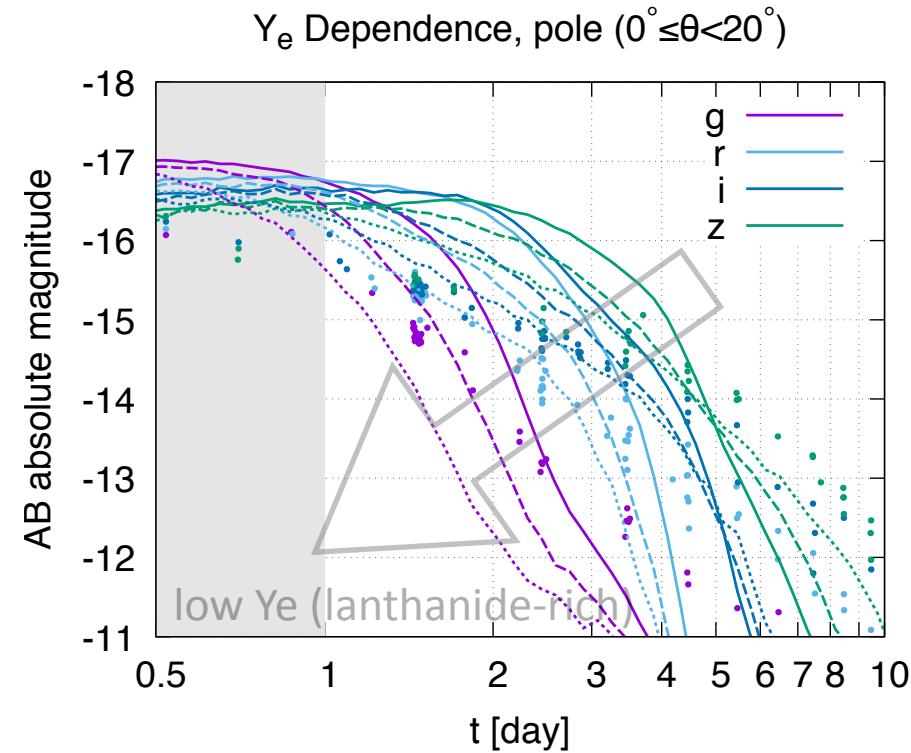
$$Y_{e,\text{pm}} : 0.3 - 0.4 (X_{\text{lan}} \ll 1)$$

Dashed:

$$Y_{e,\text{pm}} : 0.2 - 0.4 (X_{\text{lan}} \approx 0.025)$$

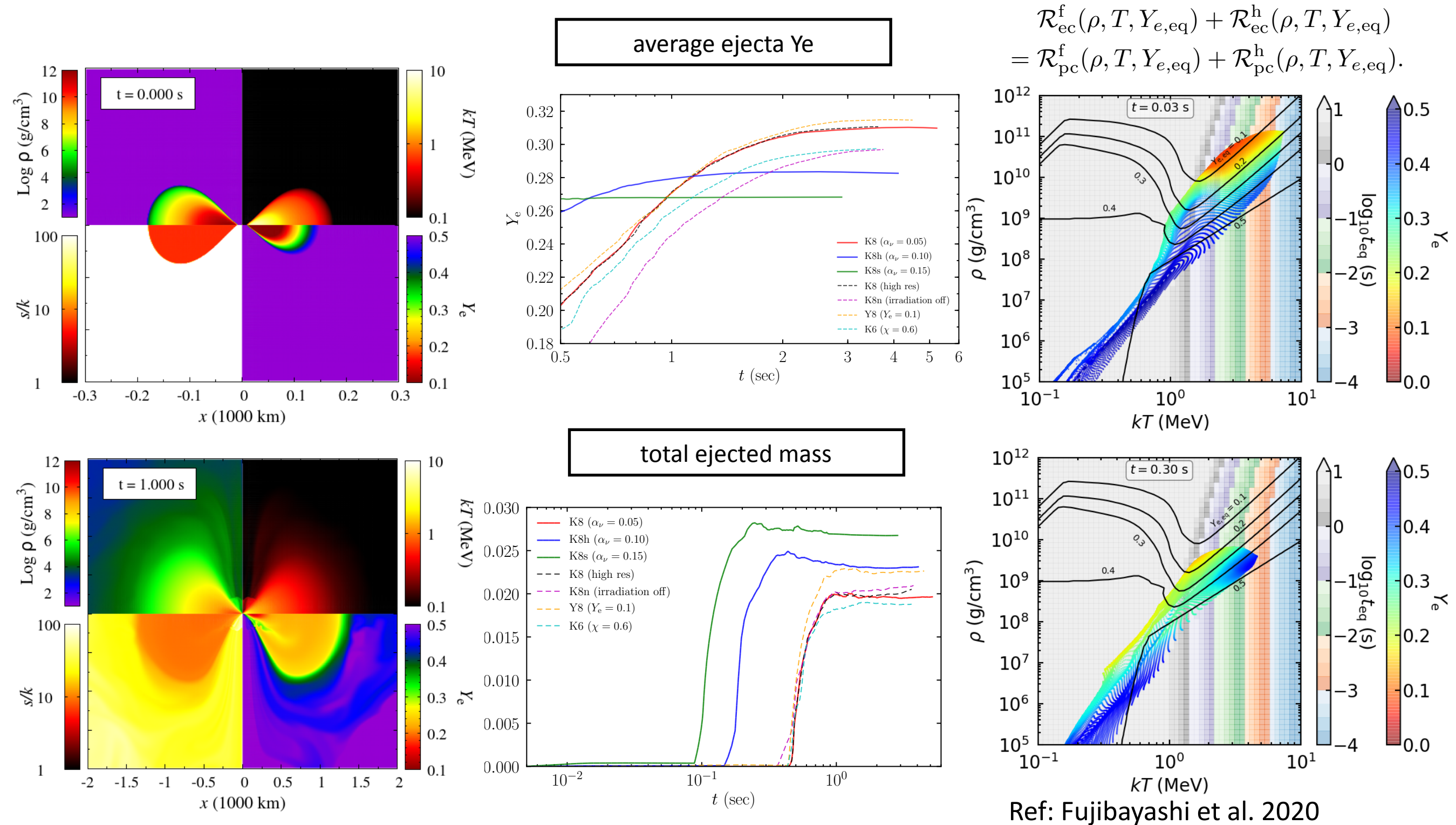
Dotted:

$$Y_{e,\text{pm}} : 0.1 - 0.3 (X_{\text{lan}} \approx 0.15)$$



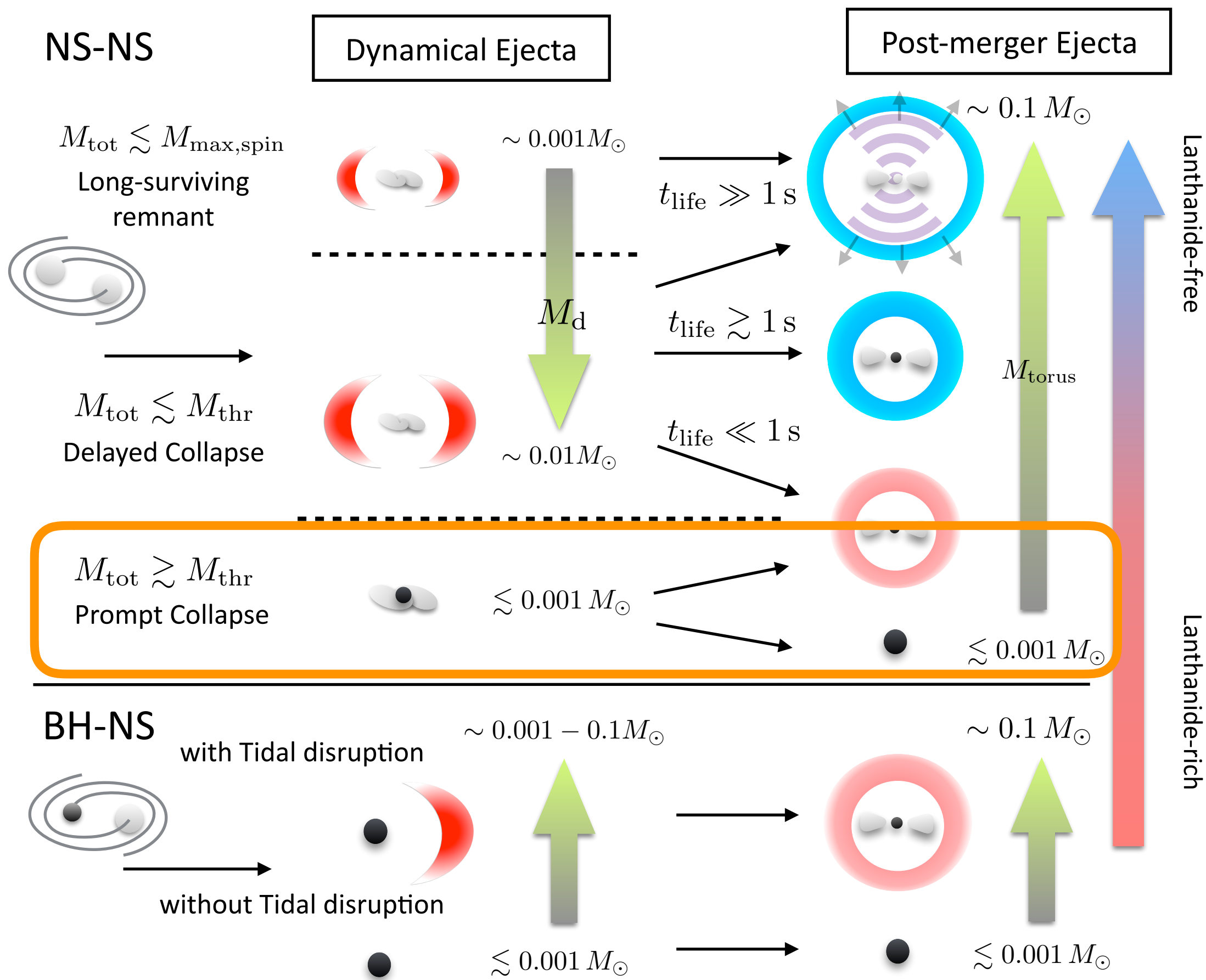


# Hi- $Y_e$ ejecta from BH accretion torus?



- Recent GR viscous RHD simulation suggests that Hi- $Y_e$  ejecta ( $Y_e > 0.3$ ) may also be formed in the absence of remnant MNS if the ejection times scale is long ( $\sim > 0.3$  s) (See also Fujibayashi et al. 2020)

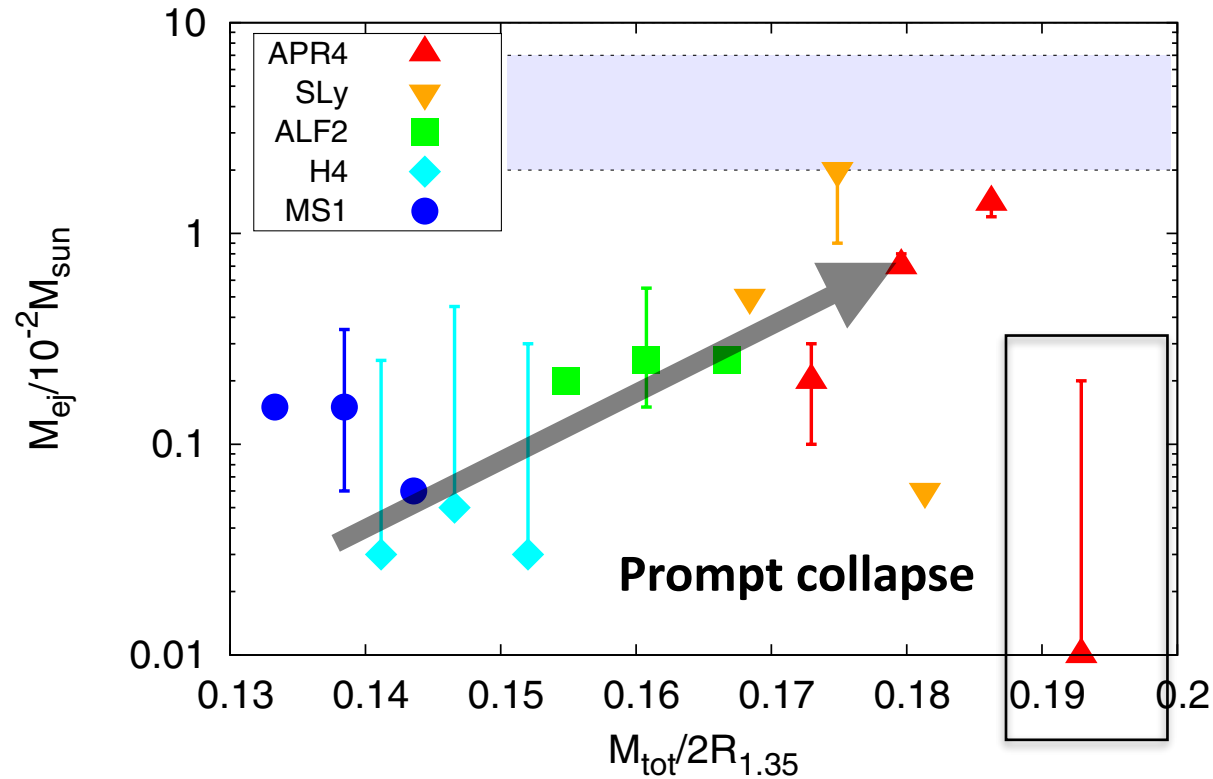




# Prompt collapse case

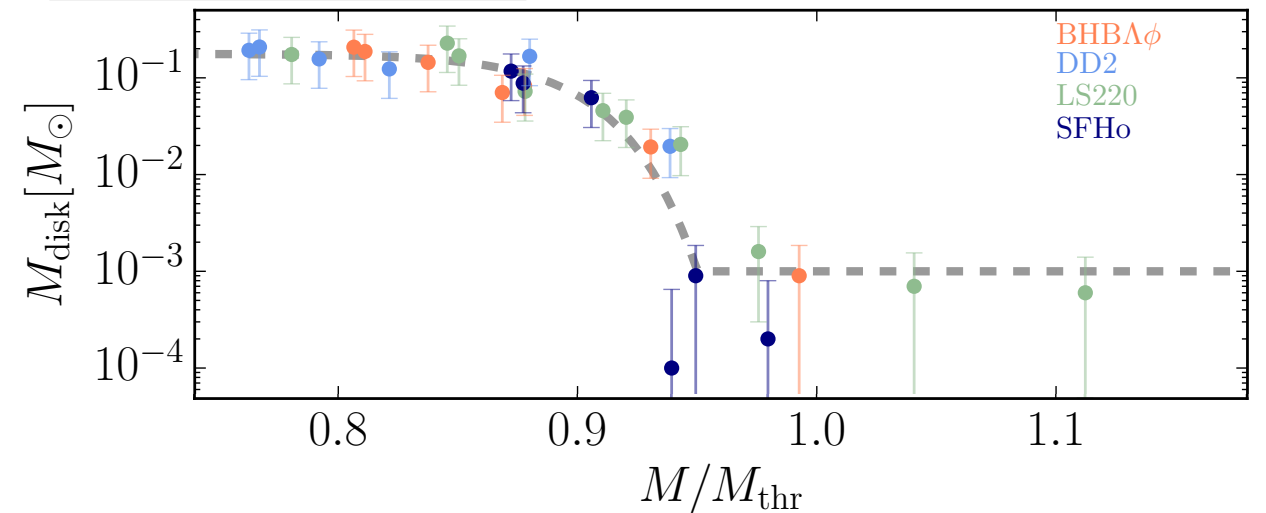
Dynamical ejecta mass

Ref: K. Hotokezaka et al. 2013  
NS-NS models



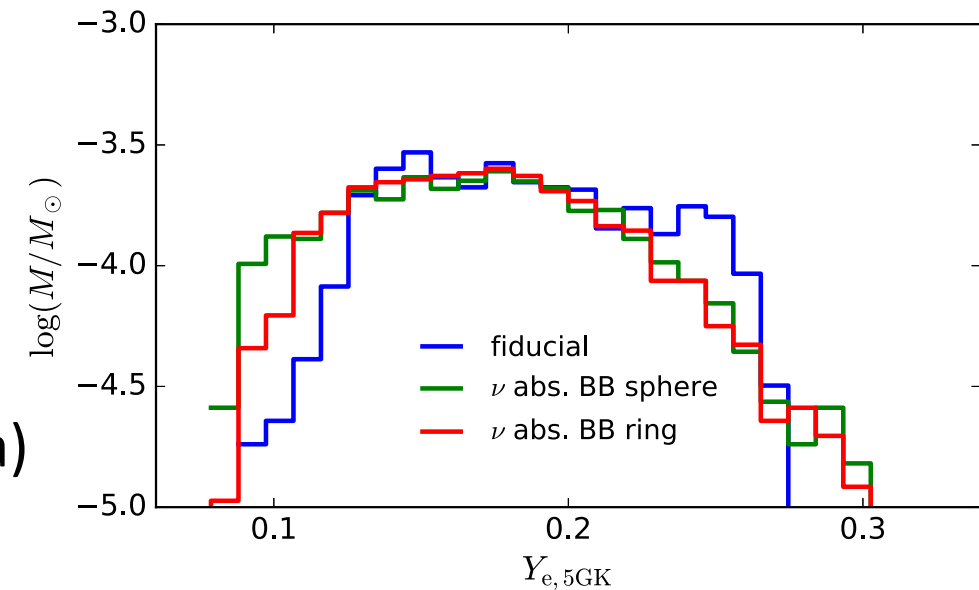
Remnant torus mass

Ref: Radice et al. 2018,  
Coughlin et al. 2019



Ye distribution of post merger ejecta  
in the absence of remnant NS

Ref: Siegel et al. 2018



- Both dynamical ejecta and remnant torus mass are significantly suppressed for most of the prompt collapse cases. (\*however, it depends on the mass ratio; see Kiuchi et al. 2019a)
- In addition, post-merger ejecta would be lanthanide-rich in the absence of  $\nu$  irradiation from the remnant NS (see e.g., Just et al. 2015, Wu et al. 2016, Siegel et al. 2018, Fernandez et al. 2018)

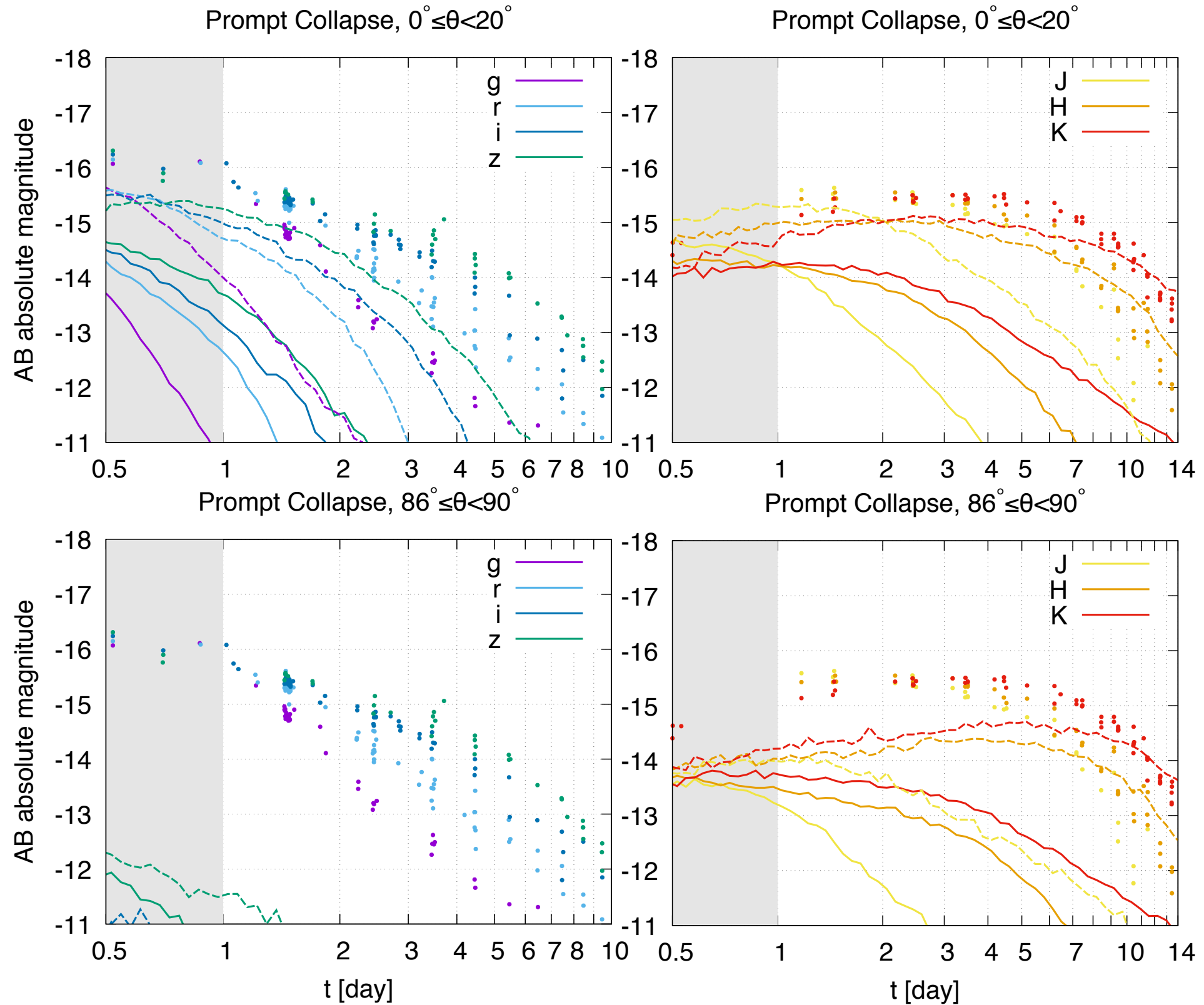
# Prompt collapse

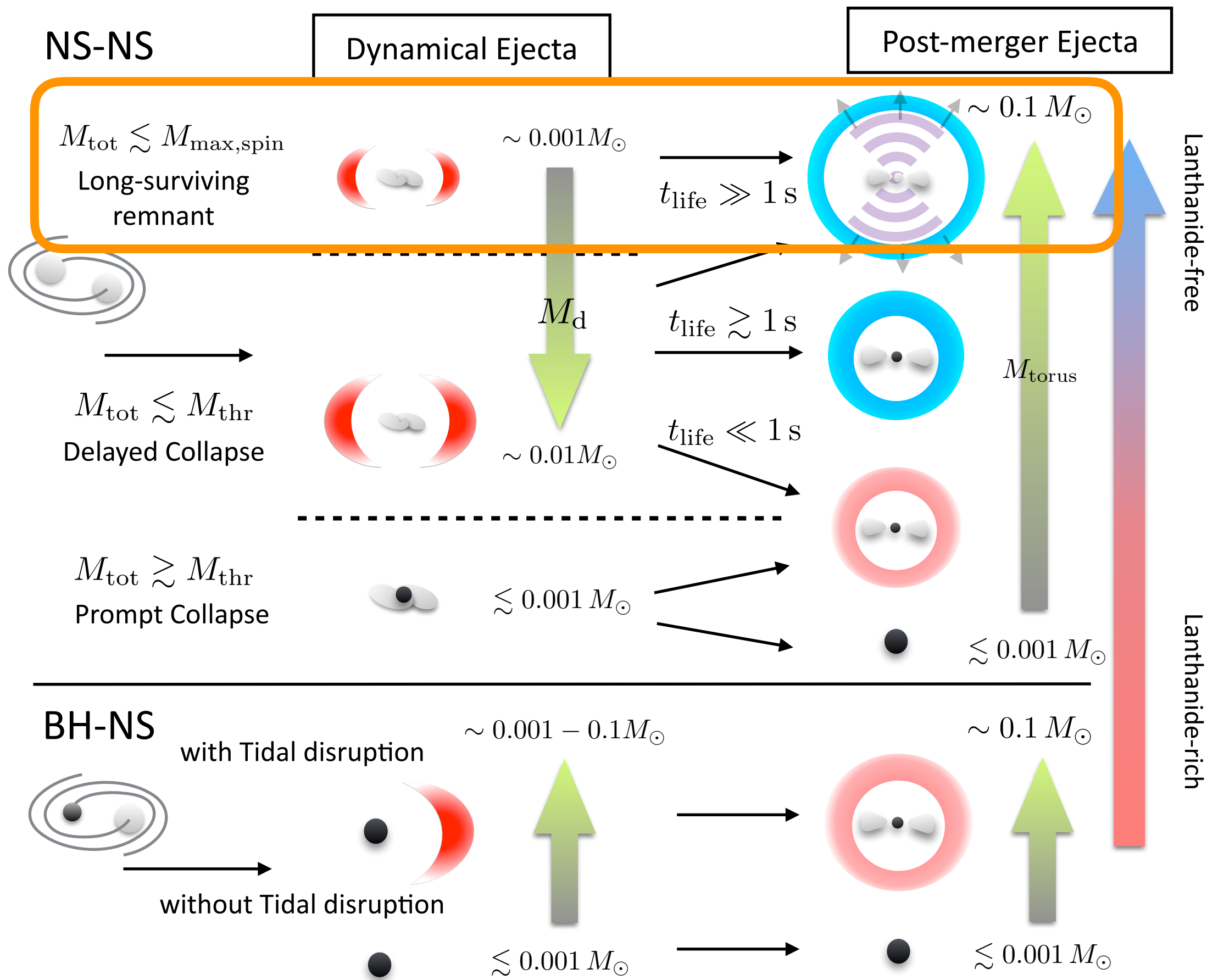
$$M_d = 0.001 M_\odot$$

$$\text{Solid: } M_{\text{pm}} = 0.001 M_\odot$$

$$\text{Dashed: } M_{\text{pm}} = 0.01 M_\odot$$

$$Y_{e,\text{pm}} = 0.1 - 0.3$$

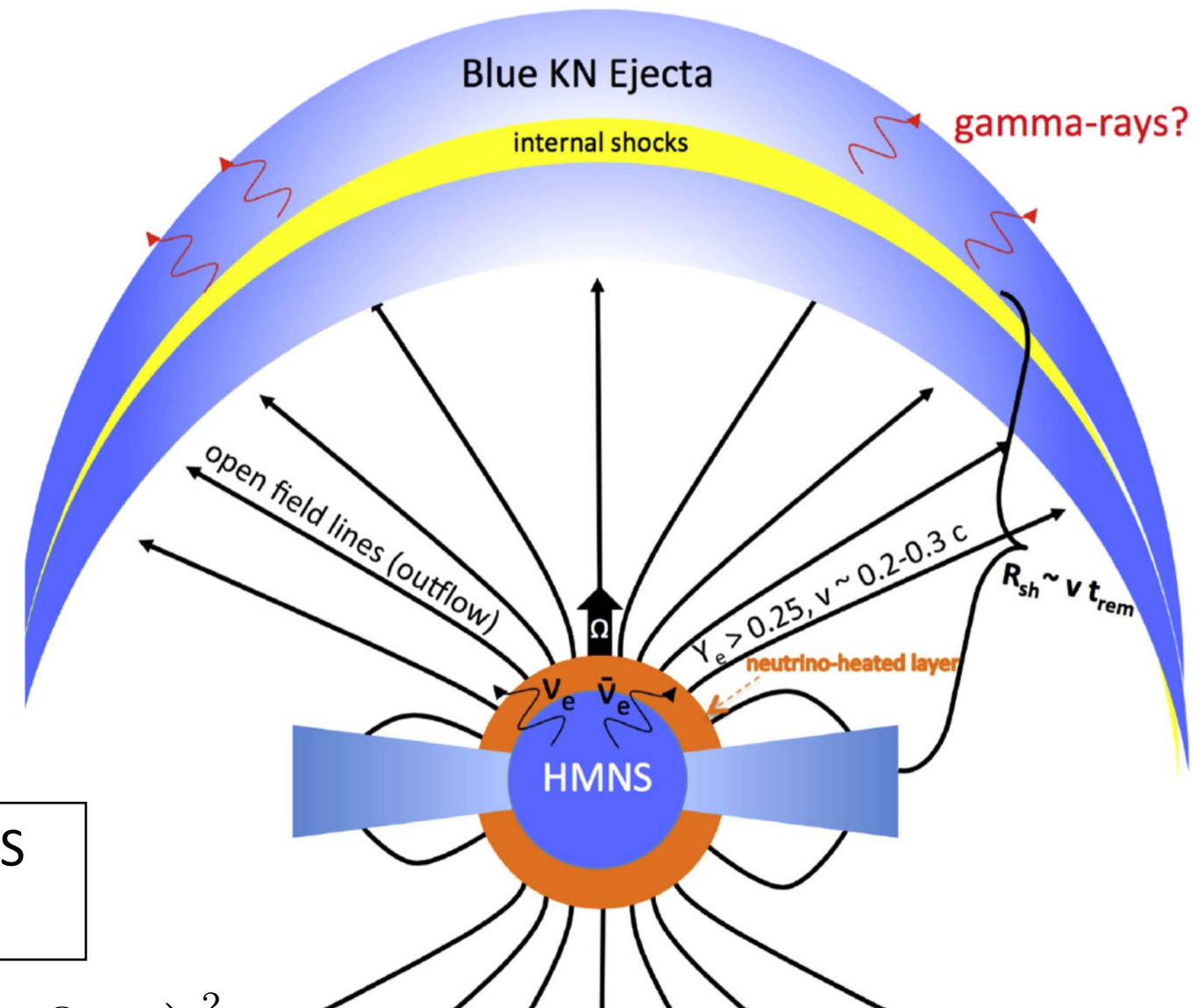




# Long-surviving NS/Magnetar

Ref: Martínez-Pinedo et al 2012,  
Metzger et al. 2018

- If the remnant NS survives for sufficiently long time, the rotational energy of the remnant NS could be an additional energy source to the ejecta by releasing it via magnetic fields
- Even if the energy injected into the ejecta is lost due to adiabatic cooling and does not directly reflected to the lightcurves, the velocity profile of the ejecta would be modified



Rotational kinetic energy of a rigidly rotating NS at maximum mass (ref: Shibata et al. 2019)

$$E_{rot} \approx 2 \times 10^{53} \text{ erg} \left( \frac{M_{MNS}}{2.6 M_{\odot}} \right) \left( \frac{R_{MNS}}{15 \text{ km}} \right)^2 \left( \frac{\Omega}{10^4 \text{ rad/s}} \right)^2$$

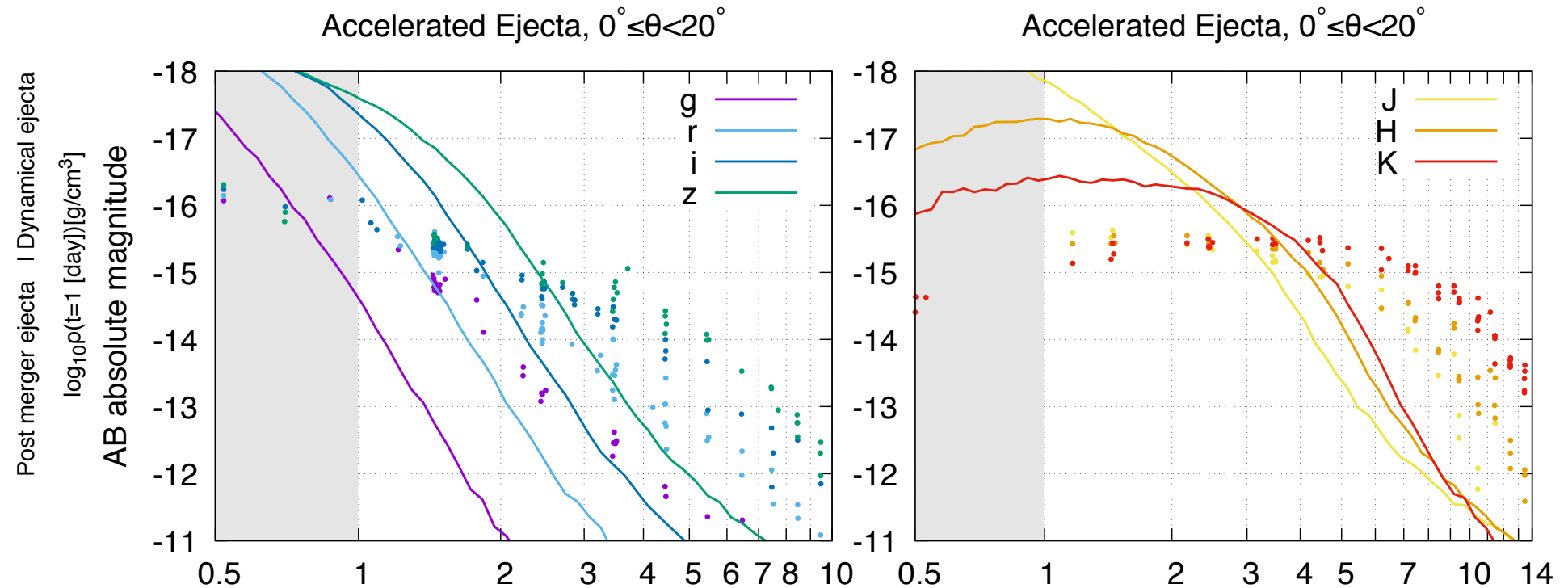
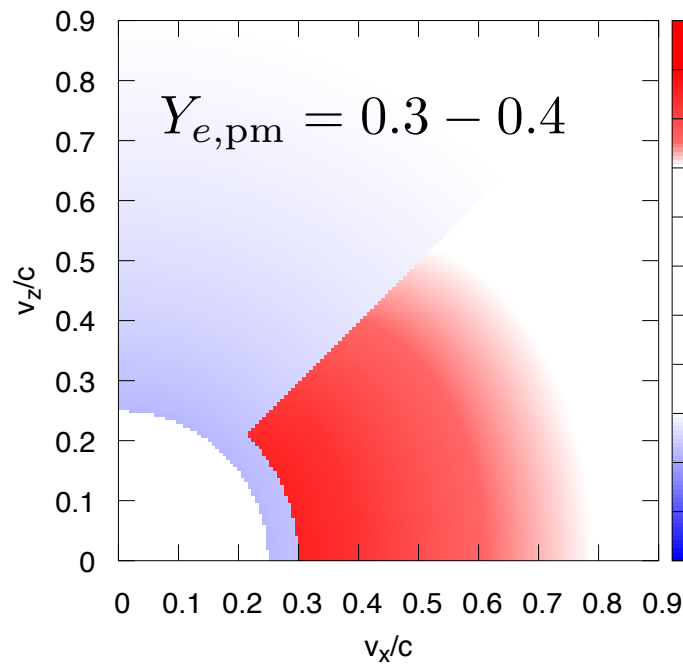
c.f. typical total kinetic energy of ejecta

$$E_{k,eje} \sim 10^{49} - 10^{51} \text{ erg}$$

\*relativistic jets would also be the cause of energy injection/ejecta acceleration (e.g. Gottlieb et al. 2017)



# Accelerated ejecta



Post-merger ejecta:

$$v = 0.25c - 0.9c$$

$$\langle v \rangle \approx 0.5c$$

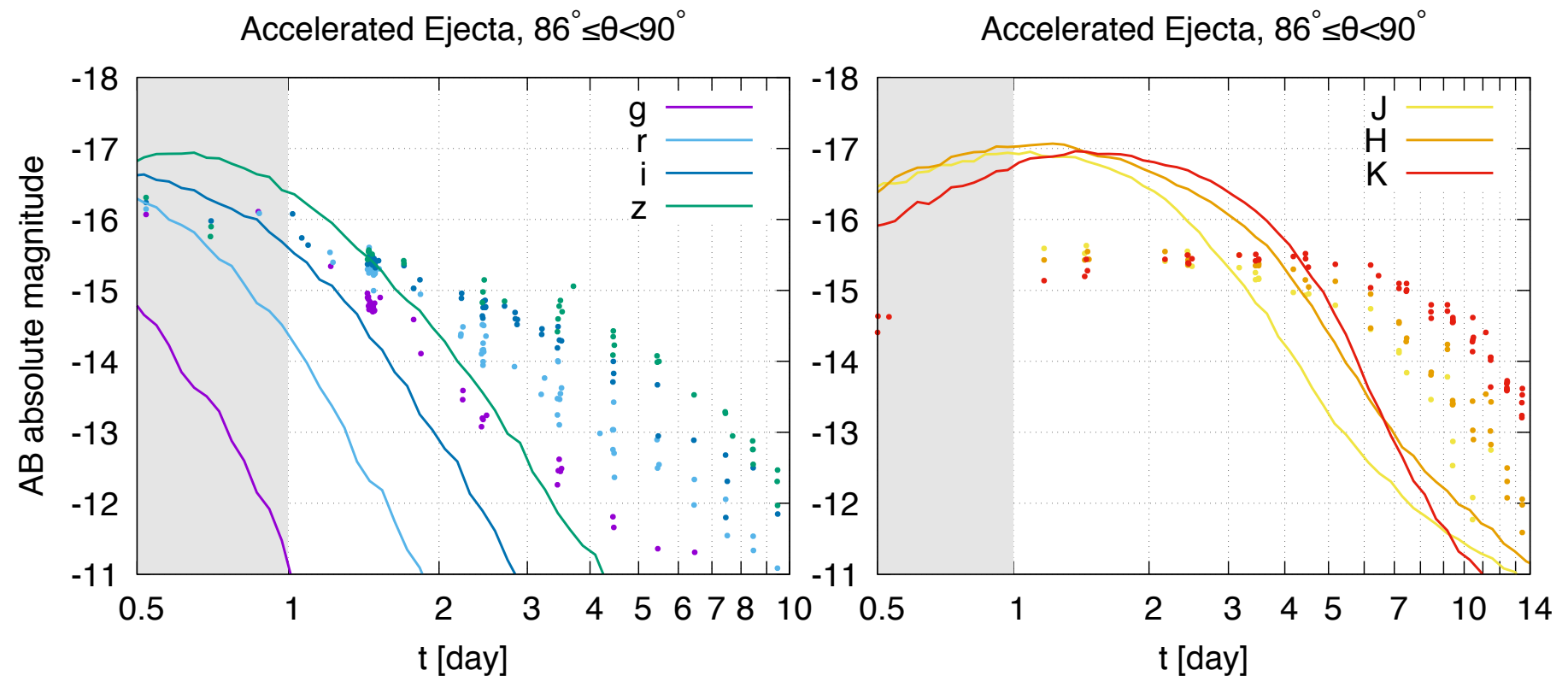
Dynamical ejecta:

$$v = 0.3c - 0.9c$$

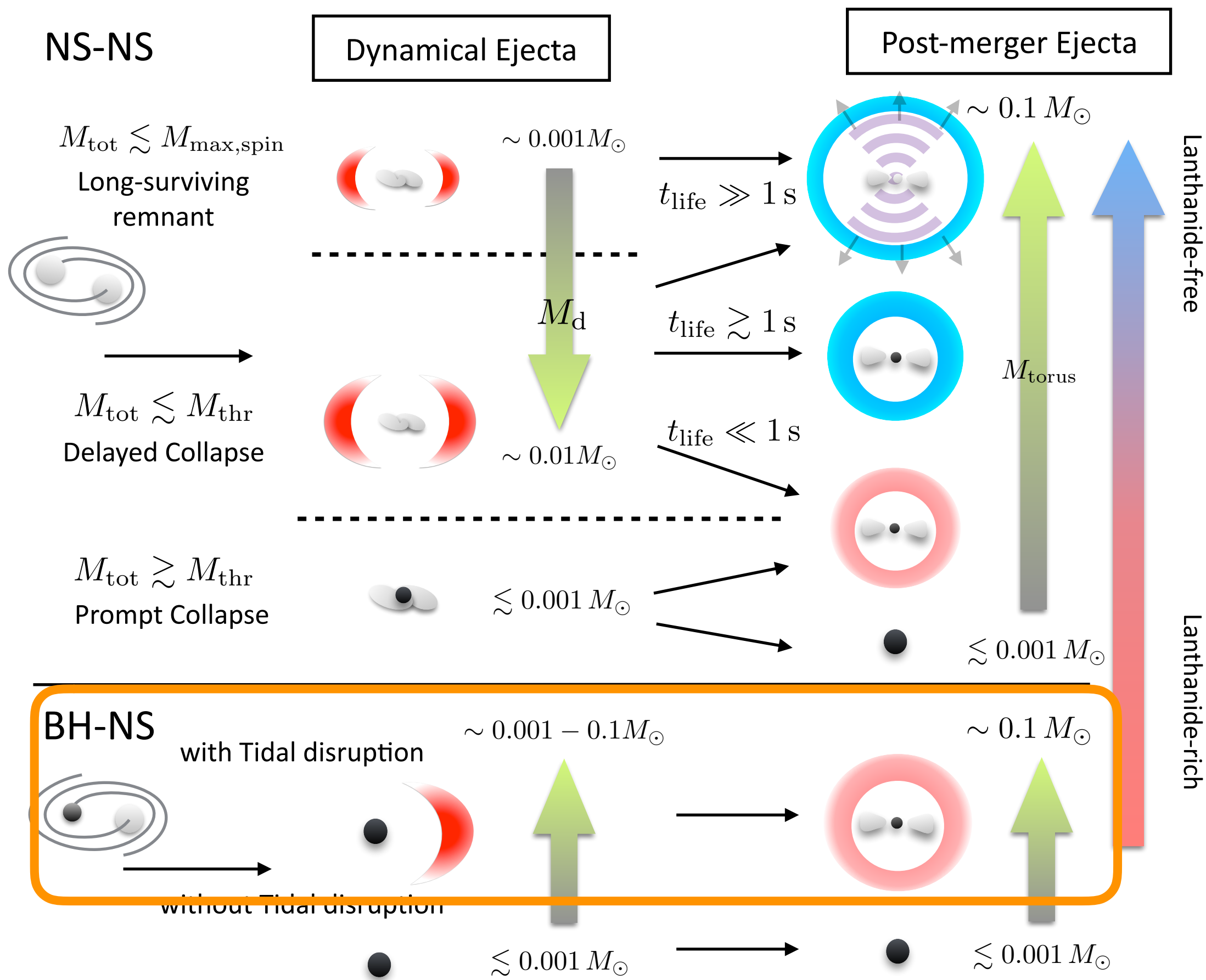
$$\langle v \rangle \approx 0.4c$$

$$M_{pm} = 0.05 M_\odot,$$

$$M_d = 0.003 M_\odot$$



\*correspond to the case for which  $\sim 10\%$  of the rotational kinetic energy of remnant NS,  $\sim 10^{52}$  erg, is converted to the ejecta kinetic energy



# Black hole-Neutron star (BH-NS) merger

Ref: Kyutoku et al. 2018

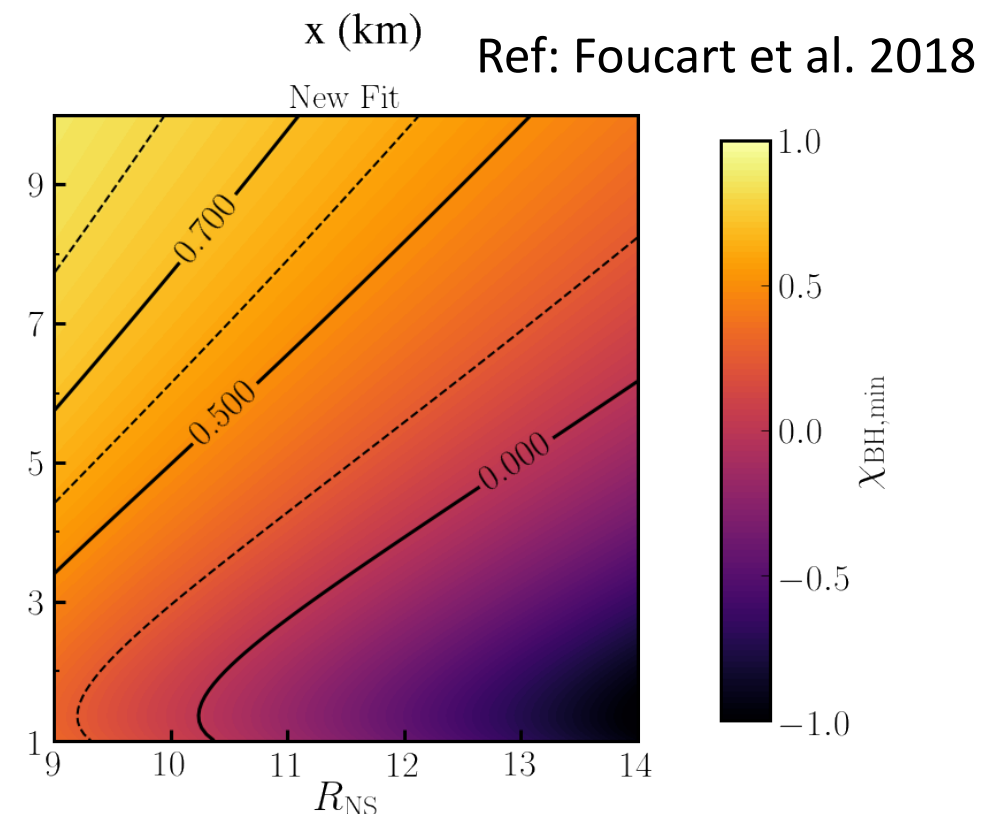
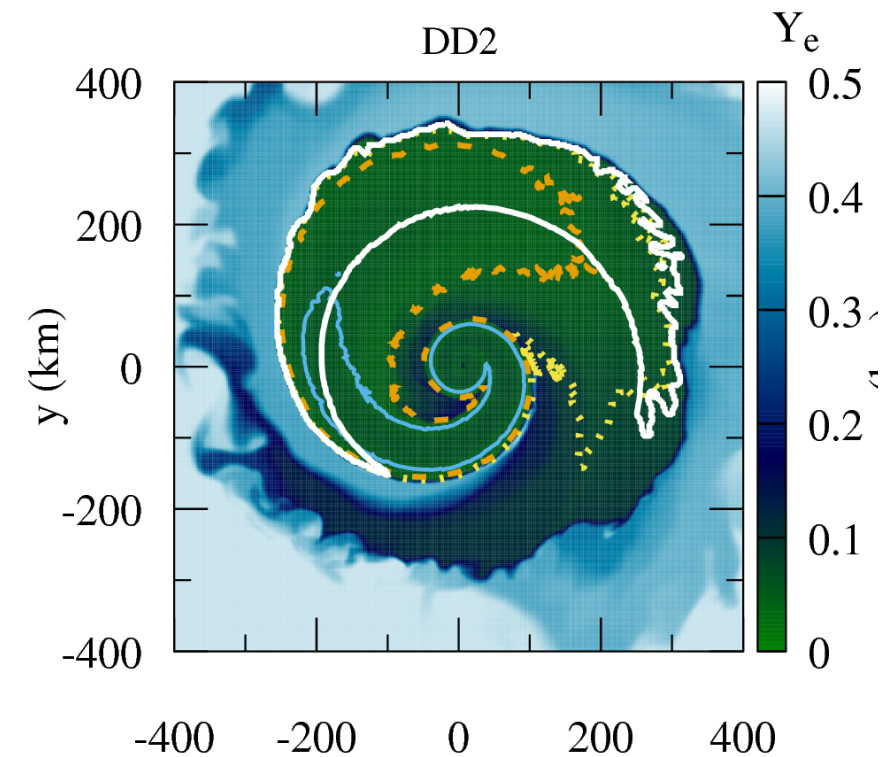
- If the NS is **tidally disrupted** substantial amount of material would remain/ejected after the merger



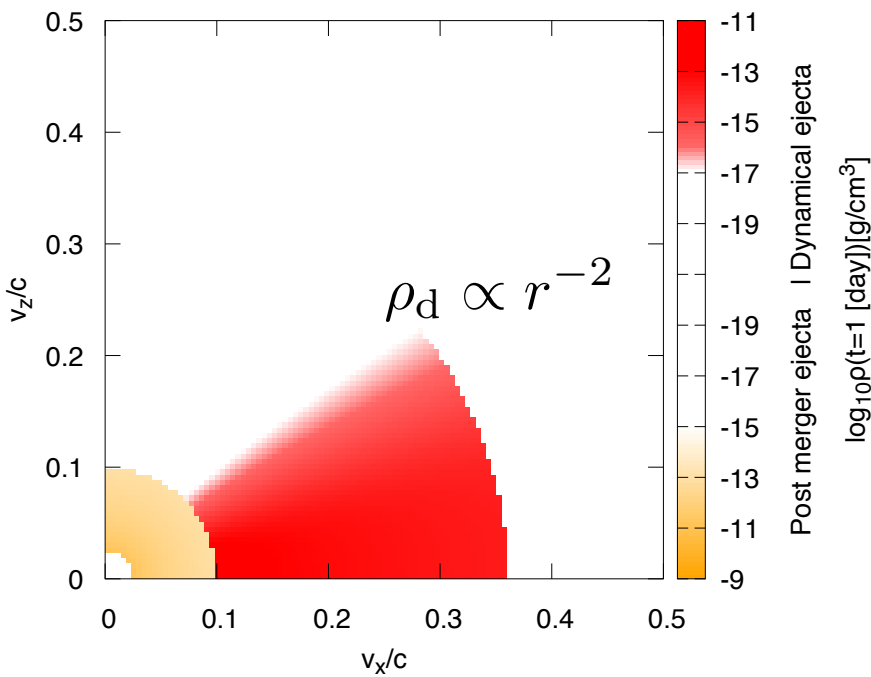
For BHNS merger, lanthanide fraction of the ejecta would be higher in the absence of shock heating and neutrino irradiation

(e.g. Just et al. 2015, Foucart et al. 2017, Kyutoku et al. 2018)

- Whether NS is tidally disrupted or not, and the remnant disk/ejecta mass depends strongly on the binary parameters.
- If NS is **not tidally disrupted**, no ejecta or remnant torus are formed after the merger, and we would expect **no EM counterparts** for such a case.



# Black hole-Neutron star



$$Y_{e,\text{pm}} = 0.1 - 0.3$$

$$Y_{e,\text{d}} \approx 0.1$$

Solid: (BHNS-A)

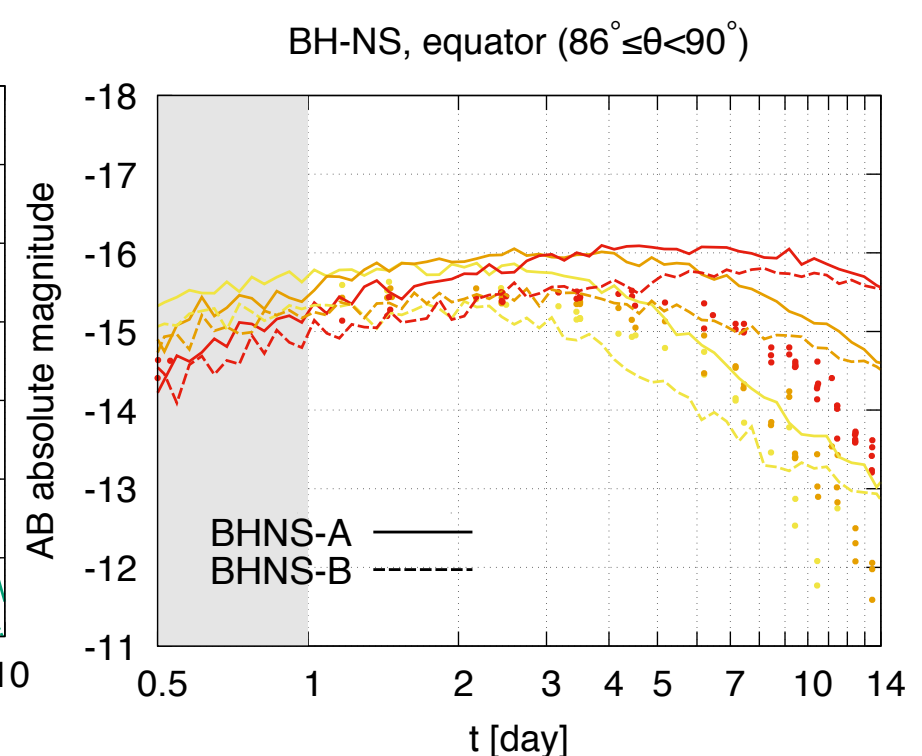
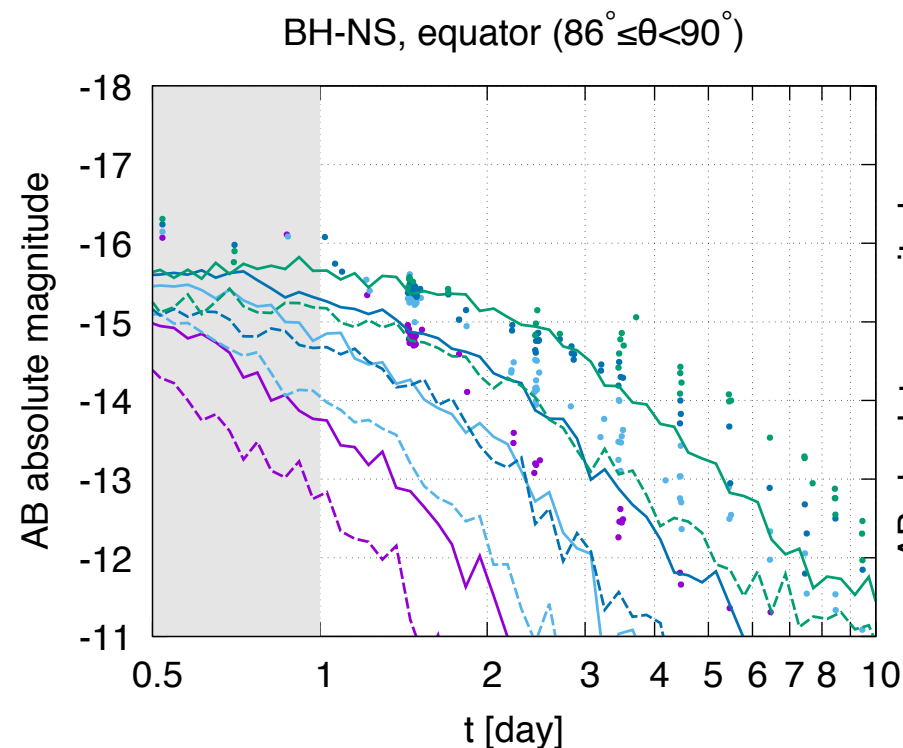
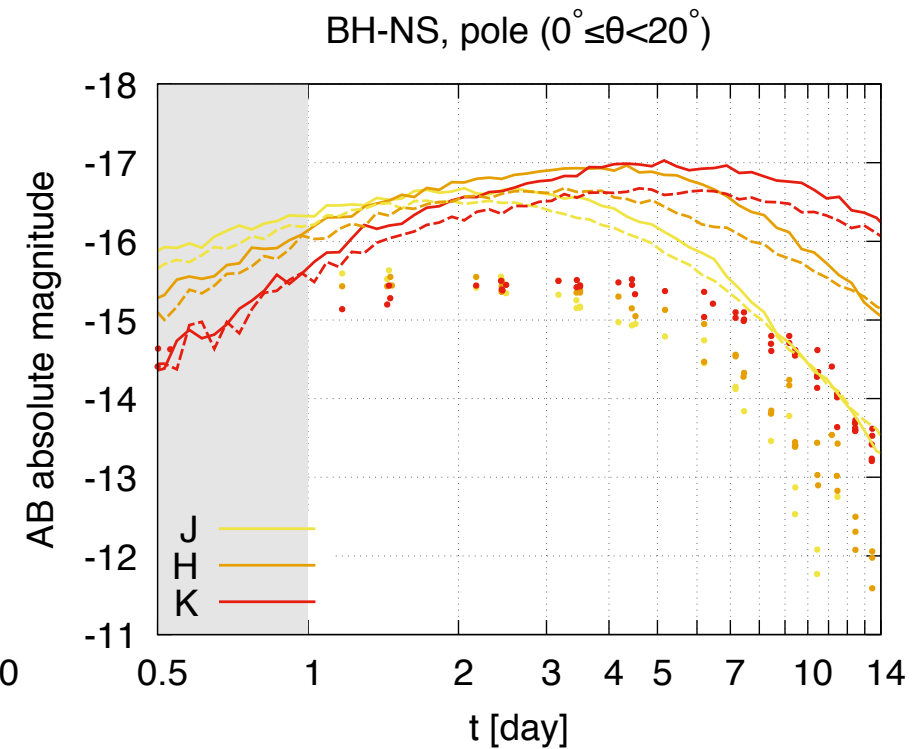
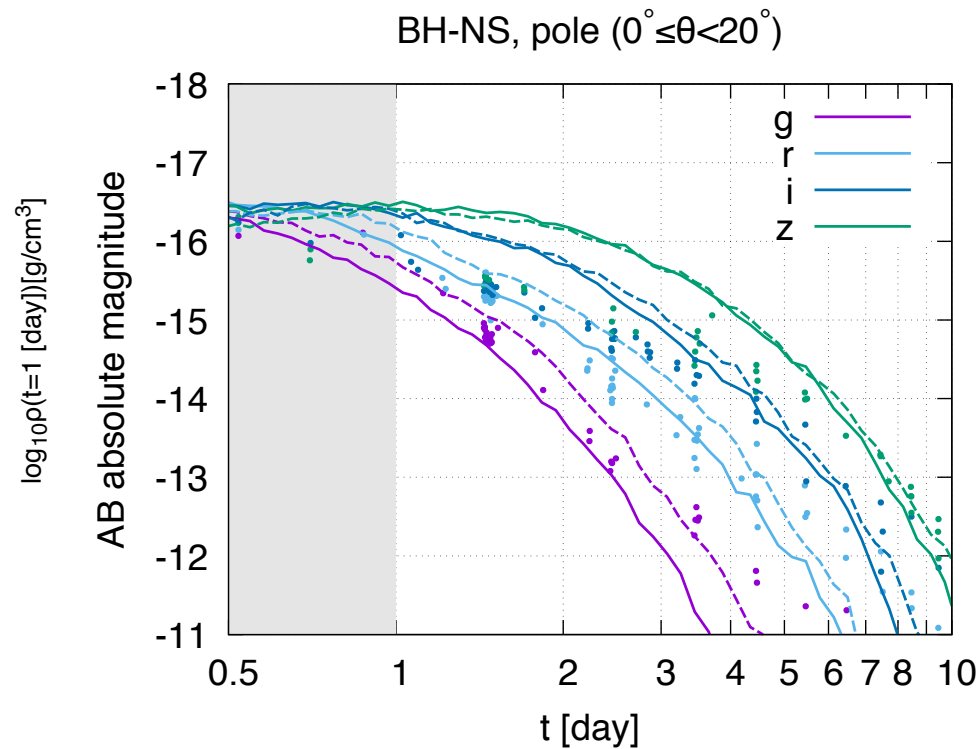
$$M_{\text{pm}} = 0.02 M_{\odot},$$

$$M_{\text{d}} = 0.02 M_{\odot}$$

Dashed: (BHNS-B)

$$M_{\text{pm}} = 0.04 M_{\odot},$$

$$M_{\text{d}} = 0.01 M_{\odot}$$



Ref: KK, Shibata, Tanaka 2019

\*note that the ejecta mass from BH-NS merger could have a large variety depending on the binary parameters



# Black hole-Neutron star (BH-NS) merger

Ref: Kyutoku et al. 2018

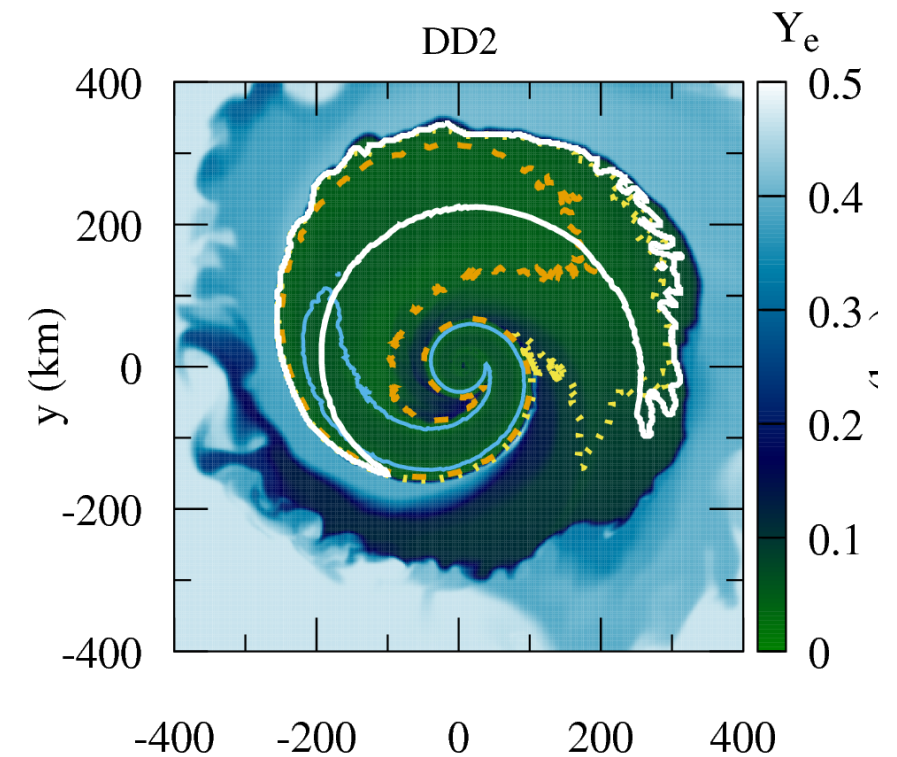
- If the NS is **tidally disrupted** substantial amount of material would remain/ejected after the merger



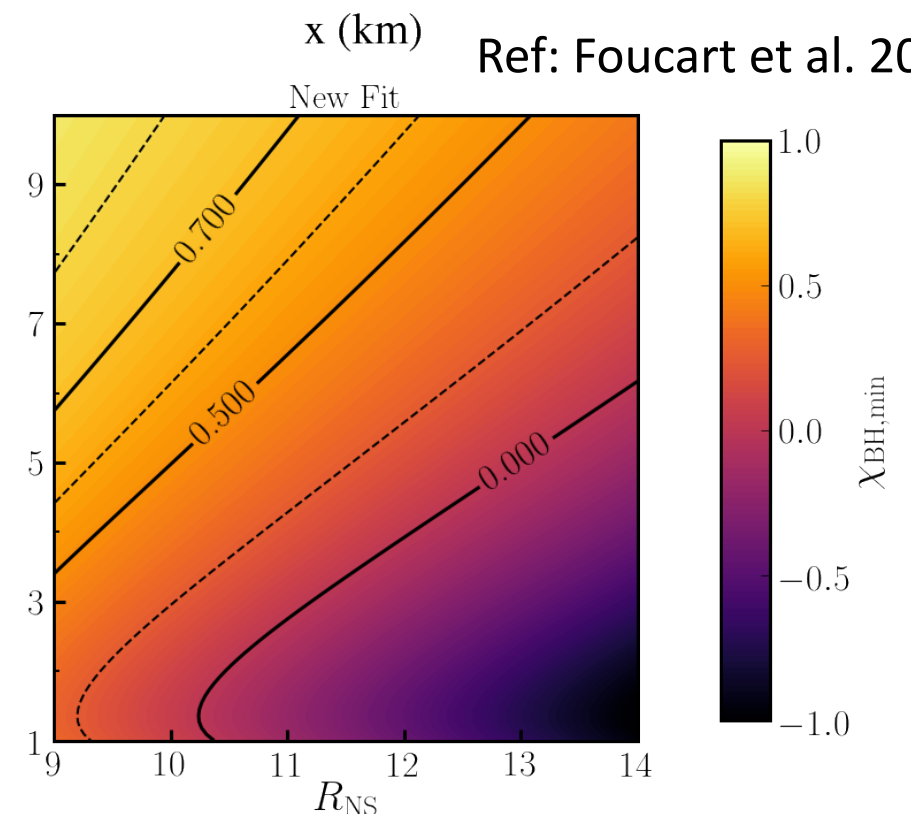
For BHNS merger, lanthanide fraction of the ejecta would be higher in the absence of shock heating and neutrino irradiation

(e.g. Just et al. 2015, Foucart et al. 2017, Kyutoku et al. 2018)

- Whether NS is tidally disrupted or not, and the remnant disk/ejecta mass depends strongly on the binary parameters.
- If NS is **not tidally disrupted**, no ejecta or remnant torus are formed after the merger, and we would expect no EM counterparts for such a case.

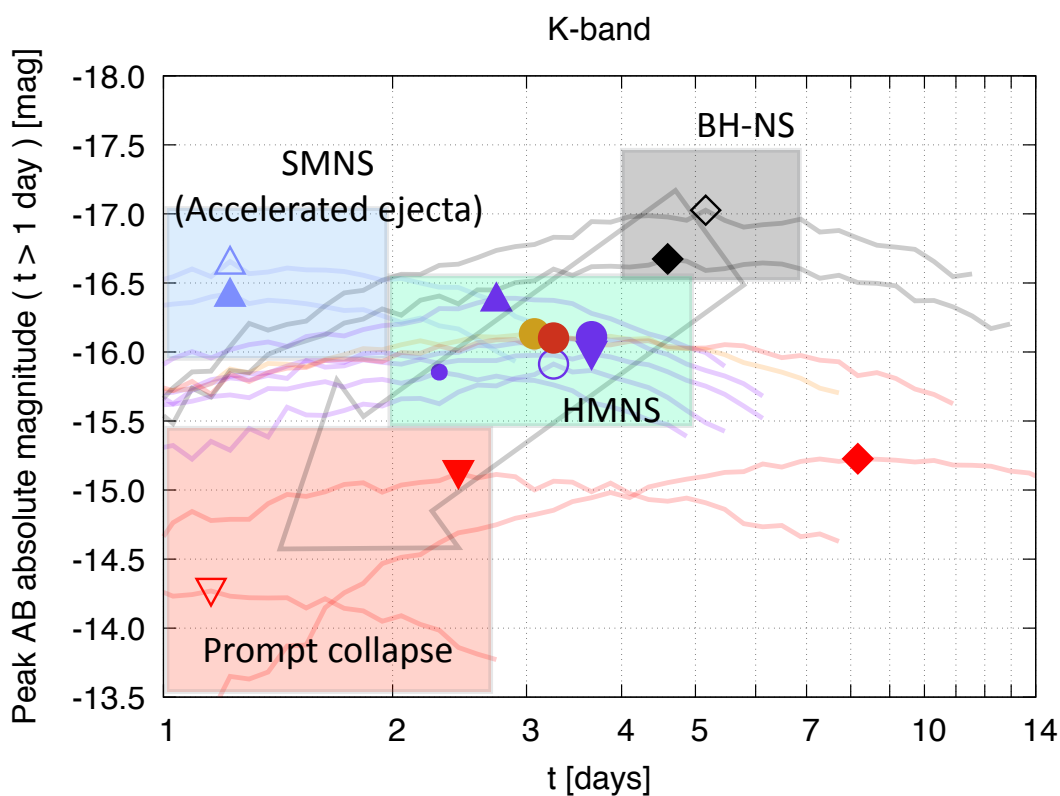
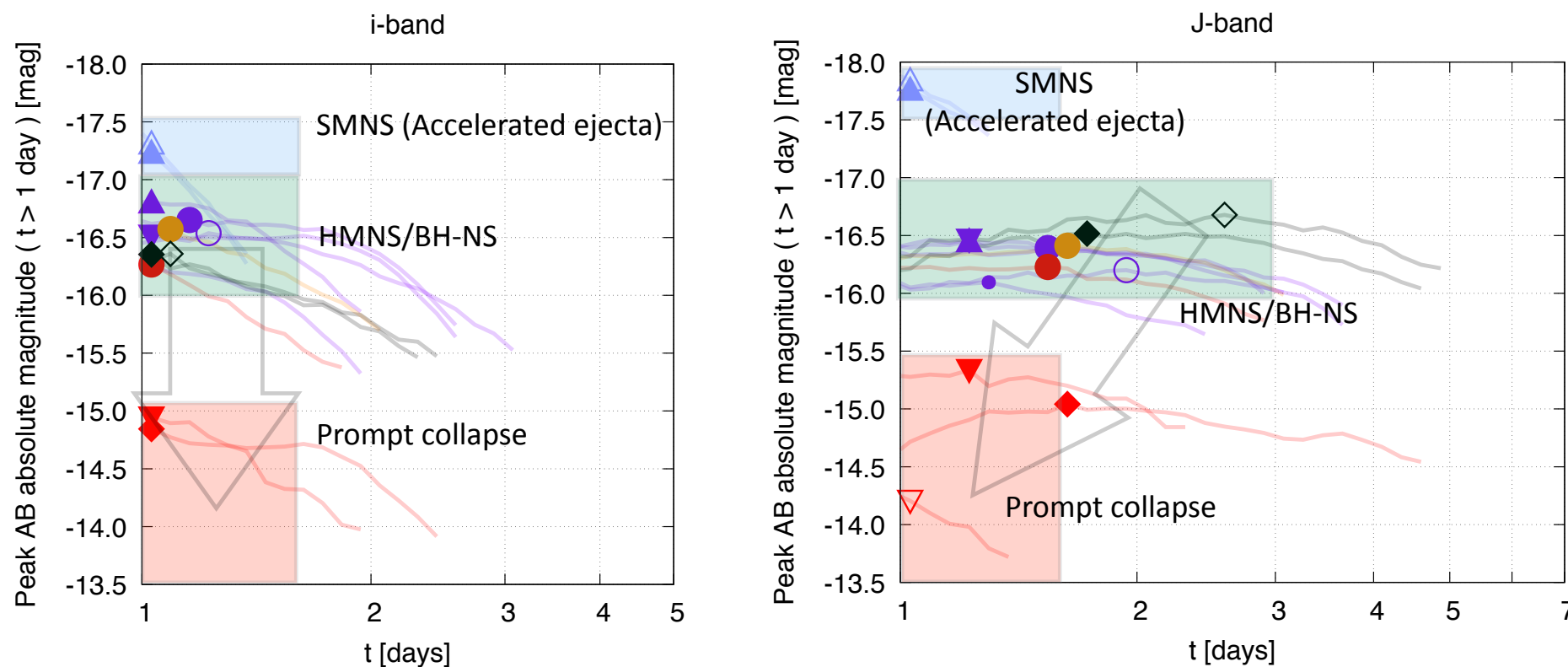


Ref: Foucart et al. 2018





# Comparison among various models (polar)



Pole (  $0^\circ \leq \theta \leq 20^\circ$  )

HMNS-YH ●  
 HMNS-YH-DYN0.003 ○  
 HMNS-YH-PM0.01 ●  
 HMNS-YH-VL ▼  
 HMNS-YH-VH ▲  
 HMNS-YM ●  
 HMNS-YL ●  
 BH-PM0.001 ▼  
 BH-PM0.01 ▼  
 SMNS-DYN0.01 ▲  
 SMNS-DYN0.003 ▲  
 BHNS-A ◇  
 BHNS-B ◆  
 PM-YL ◆

**SMNS:**

cases that the remnant NS survives for a long time scale ( $\gg 1$  s)

**HMNS:**

cases that the remnant NS survives temporarily and eventually collapses to a BH

**Prompt collapse:**

cases that the NSs collapses to a BH immediately after the merger

- Comparison of peak time vs. peak magnitude\* among various models

\*since the lightcurves for  $t < 1$  day are not reliable for our calculation, we define the peak magnitude as the brightest point after  $t = 1$  day.

03 observation

# O3 detection candidates

<https://gracedb.ligo.org/superevents/public/O3/>

- BH-BH: 20 candidates
  - S190915ak, S190828l, S190828j, S190728q, S190727h, S190720a, S190707q, S190706ai, S190701ah, S190630ag, S190602aq, S190521r, S190521g, S190519bj, S190517h, S190513bm, S190512at, S190503bf, S190421ar, S190412m, S190408an
- Mass gap: 2 candidates
  - S190930s, S190924h
- NS-NS: 1 (6) candidates
  - **S190425z** (, S190910h, S190901ap, S190718y, S190510g, S190426c)
- BH-NS: 1 (6) candidates
  - **S190814bv** (, S190930t, S190923y, S190910d, S190901ap, S190426c)

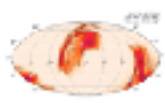
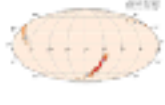



**GraceDB — Gravitational-Wave Candidate Event Database**

HOME PUBLIC ALERTS SEARCH LATEST DOCUMENTATION LOGIN

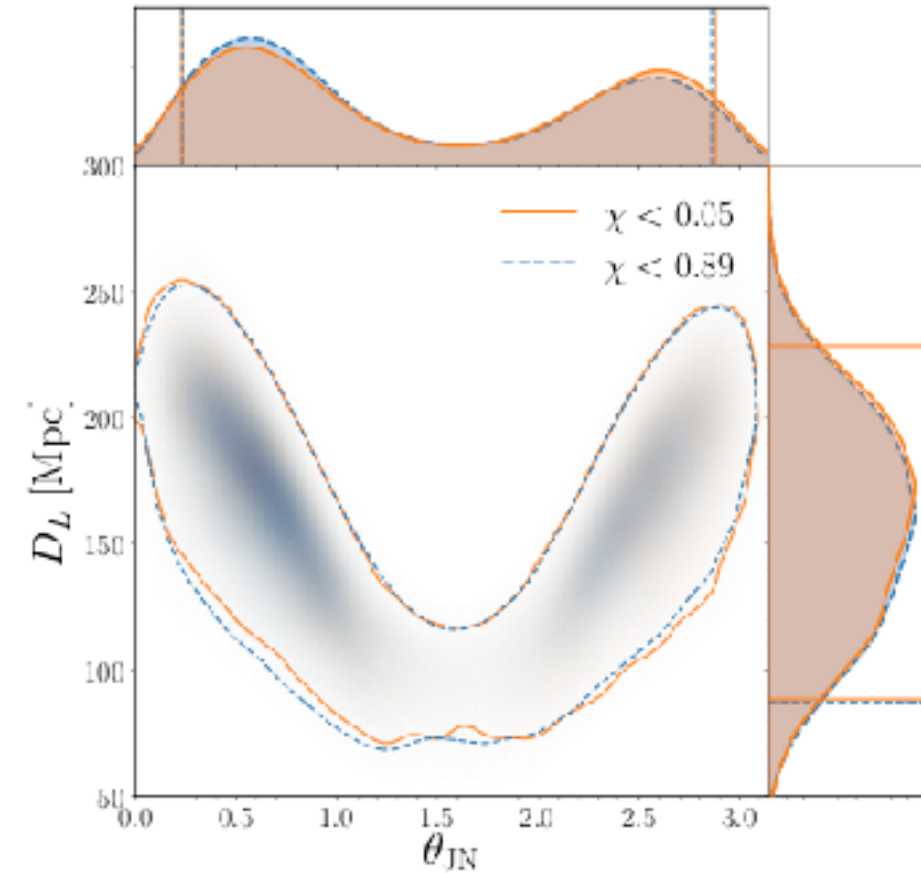
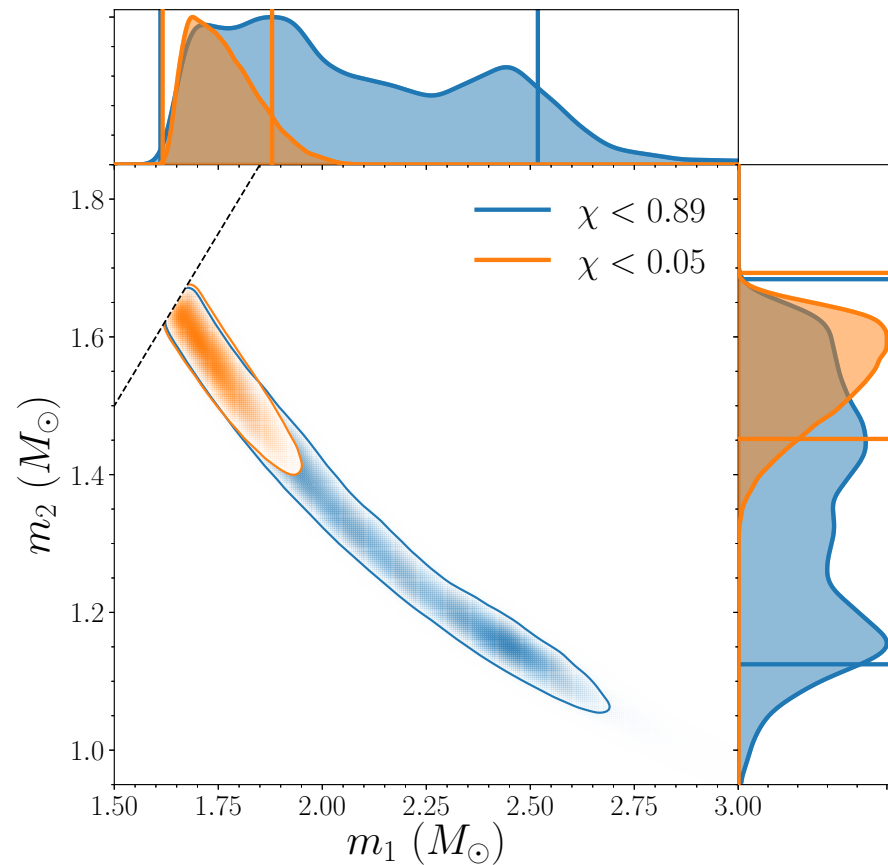
### LIGO/Virgo O3 Public Alerts

Detection candidates: 25

SORT: EVENT ID (A-Z) ▾

Event ID	Possible Source (Probability)	UTC	GCN	Location
<a href="#">S190829u</a>	MassGap (90%), Terrestrial (10%)	Aug. 29, 2019 21:05:56 UTC	<a href="#">GCN Circulars</a> <a href="#">Notices</a>   <a href="#">VOE</a>	
<a href="#">S190828l</a>	BBH (>99%)	Aug. 28, 2019 06:55:09 UTC	<a href="#">GCN Circulars</a> <a href="#">Notices</a>   <a href="#">VOE</a>	
<a href="#">S190828j</a>	BBH (>99%)	Aug. 28, 2019 06:34:05 UTC	<a href="#">GCN Circulars</a> <a href="#">Notices</a>   <a href="#">VOE</a>	
<a href="#">S190822c</a>	BNS (>99%)	Aug. 22, 2019 01:29:59 UTC	<a href="#">GCN Circulars</a> <a href="#">Notices</a>   <a href="#">VOE</a>	
<a href="#">S190816l</a>	NSBH (83%), Terrestrial (17%)	Aug. 16, 2019 17:04:31 UTC	<a href="#">GCN Circulars</a> <a href="#">Notices</a>   <a href="#">VOE</a>	

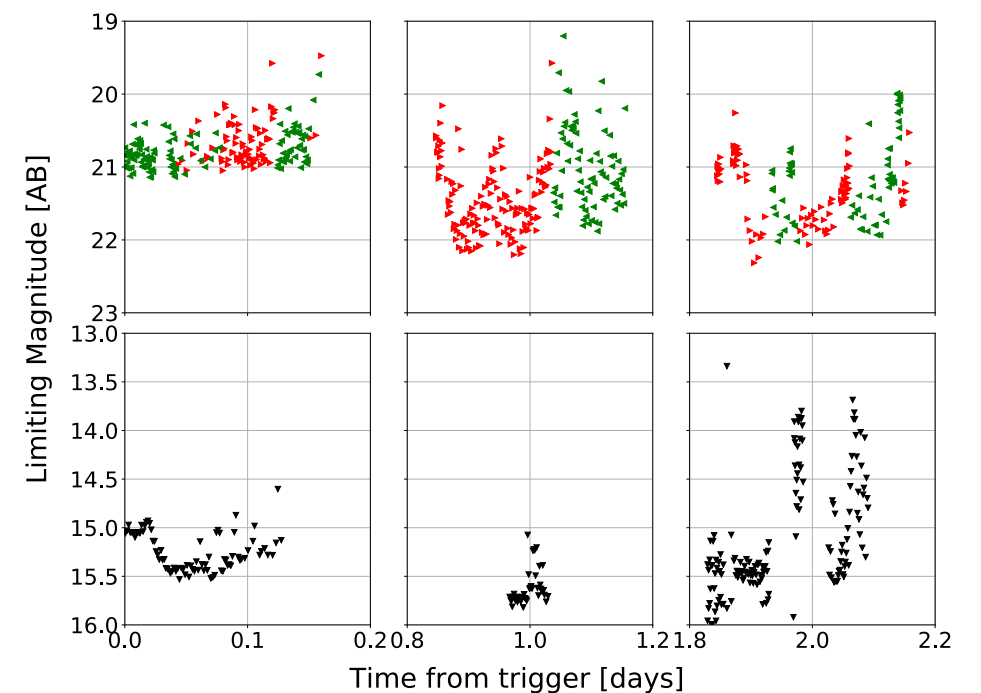
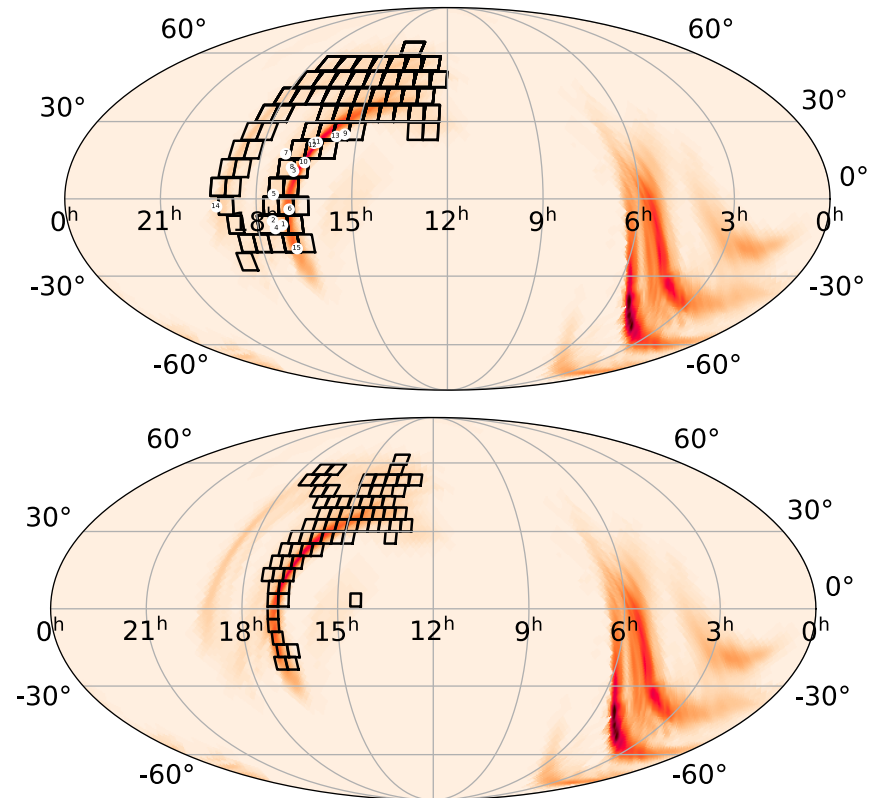
# Second NS-NS: GW190425



	Low-spin prior ( $\chi < 0.05$ )	High-spin prior ( $\chi < 0.89$ )
Primary mass $m_1$	$1.62 - 1.88 M_\odot$	$1.61 - 2.52 M_\odot$
Secondary mass $m_2$	$1.45 - 1.69 M_\odot$	$1.12 - 1.68 M_\odot$
Chirp mass $\mathcal{M}$	$1.44^{+0.02}_{-0.02} M_\odot$	$1.44^{+0.02}_{-0.02} M_\odot$
Detector-frame chirp mass	$1.4868^{+0.0003}_{-0.0003} M_\odot$	$1.4873^{+0.0008}_{-0.0006} M_\odot$
Mass ratio $m_2/m_1$	$0.8 - 1.0$	$0.4 - 1.0$
Total mass $m_{\text{tot}}$	$3.3^{+0.1}_{-0.1} M_\odot$	$3.4^{+0.3}_{-0.1} M_\odot$
Effective inspiral spin parameter $\chi_{\text{eff}}$	$0.013^{+0.01}_{-0.01}$	$0.058^{+0.11}_{-0.05}$
Luminosity distance $D_L$	$161^{+67}_{-73} \text{ Mpc}$	$159^{+69}_{-71} \text{ Mpc}$
Combined dimensionless tidal deformability $\tilde{\Lambda}$	$\leq 600$	$\leq 1100$

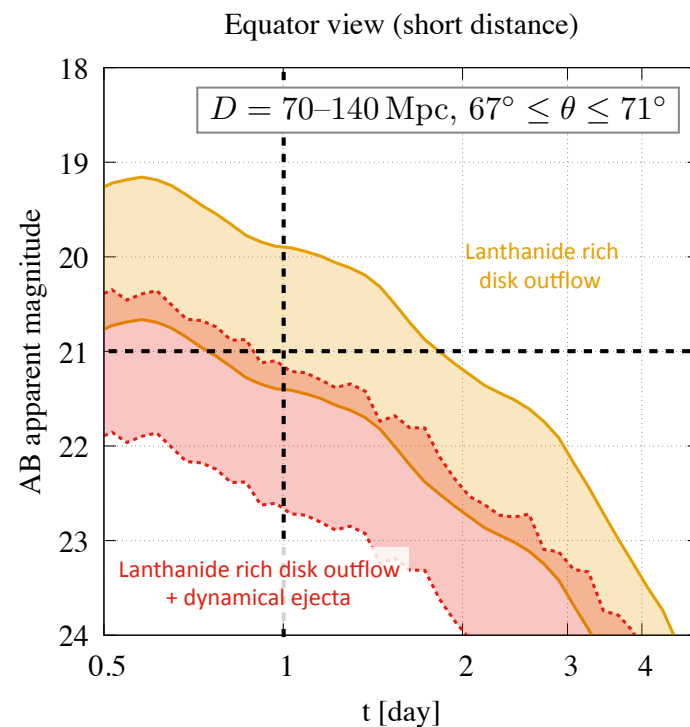
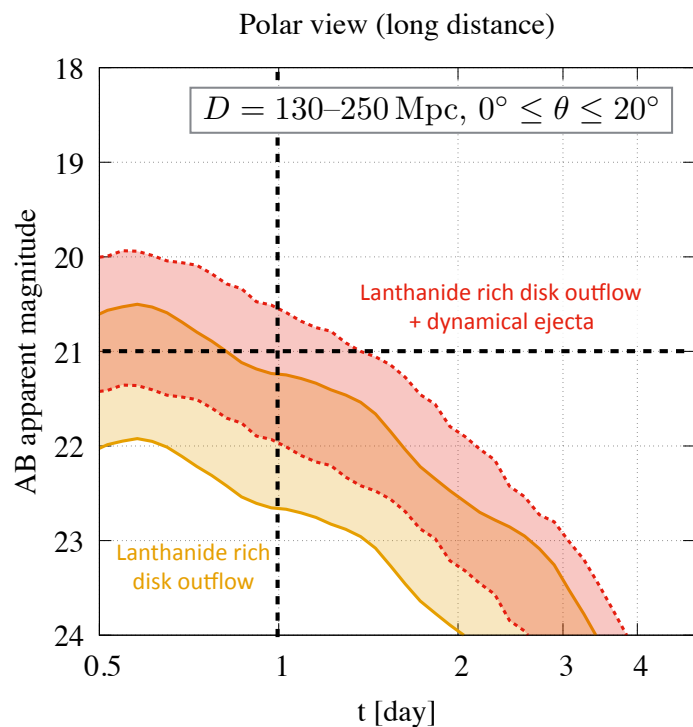
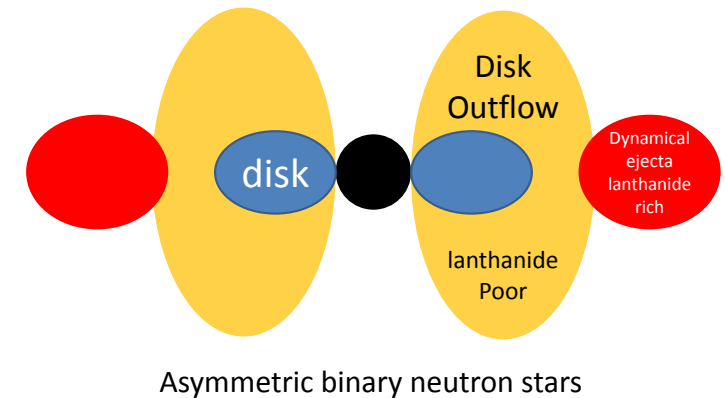
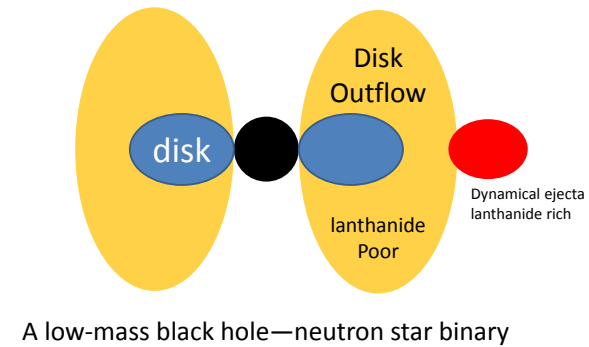
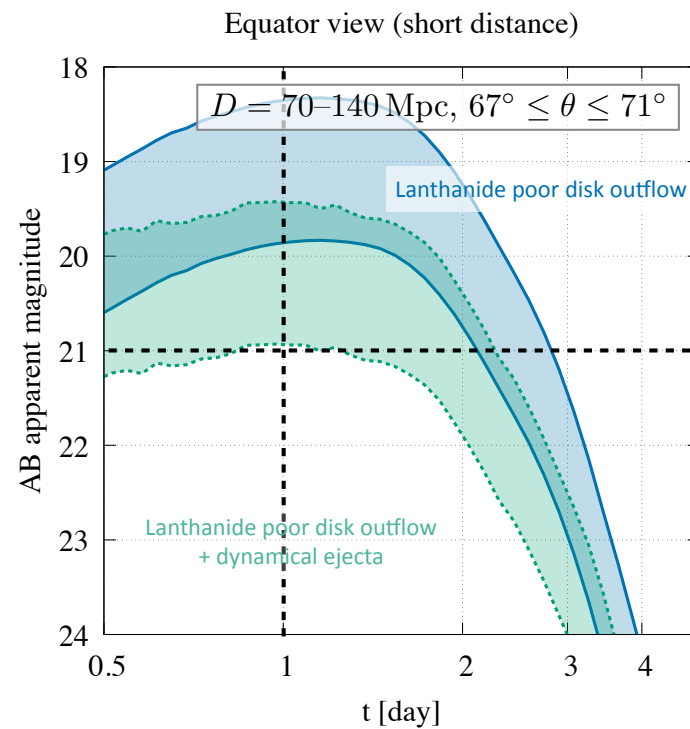
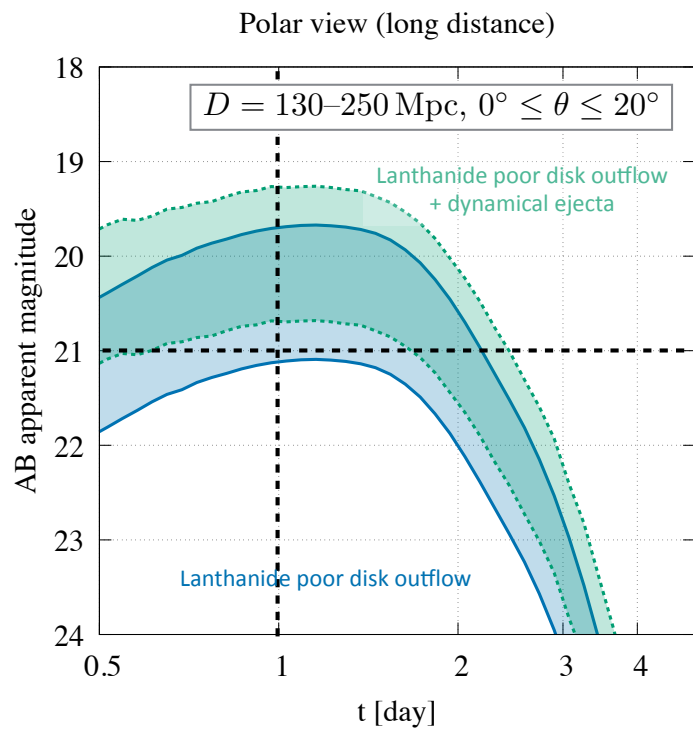
# EM followup

- GW190425
  - **D=156±41Mpc (Initial announce)**
  - 10,000 deg<sup>2</sup> (A:BAYESTAR)  
->7,500 deg<sup>2</sup>(B:LALInference)
- GROWTH:1907.12645
  - ZTF: g & r band
    - 1st Night: ~0.1days  
~>20.4 mag (median?) (A: 36% B:19%)
    - **2nd Night: ~1days**  
**~>21 mag (average?median?) (A: 46% B:21%)**
    - 3rd Night: ~2 days  
~>21 mag? (median) (A: 46% B:21% ?)
  - Palomar Gattini-IR: J band
    - ~> 15.5 mag (median)





# GW190425: NS-NS? BH-NS?



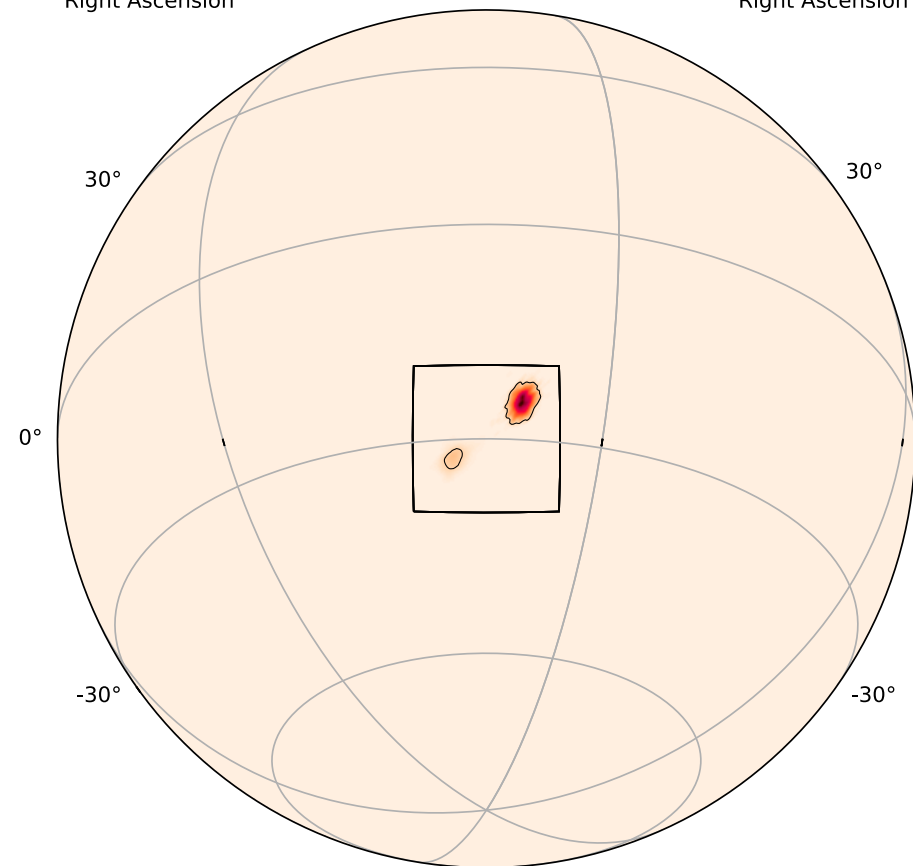
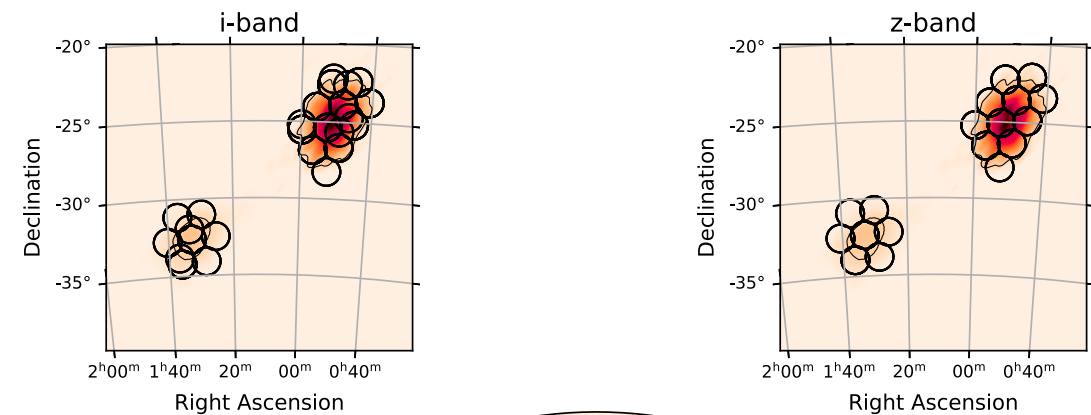
Symmetric binary neutron stars  
A low-mass black hole—small-radius neutron star binary

Binary type <sup>a</sup>	Merger Outcome <sup>b</sup>	Detectable? <sup>c</sup>
low-mass BH-NS	La-poor disk	YES
	La-poor disk+La-rich dyn.	≈YES
	La-rich disk	YES if equatorial
	La-rich disk+La-rich dyn.	YES if polar
asymmetric NS-NS	weak/no disruption (small radius)	NO
	La-poor disk+La-rich dyn.	YES if polar
symmetric NS-NS	La-rich disk+La-rich dyn.	YES if polar
	massive neutron star (large maximum mass) prompt collapse	YES if polar NO

Ref) [Kyutoku et al. \(2020\)](#)

# S190814bv: a BH-NS merger candidate

- Aug. 14, 2019 21:10:39 UTC, detection of a BH-NS merger candidates has been reported
- False alarm rate:  $\sim 1 / 10^{25}$  yrs.
- Distance:  $\sim 267 \pm 52$  Mpc (c.f. GW170817:  $\sim 40$  Mpc)
- Sky localization:  $23 \text{ deg}^2$  (90%)
- **No electromagnetic counterpart has been found**



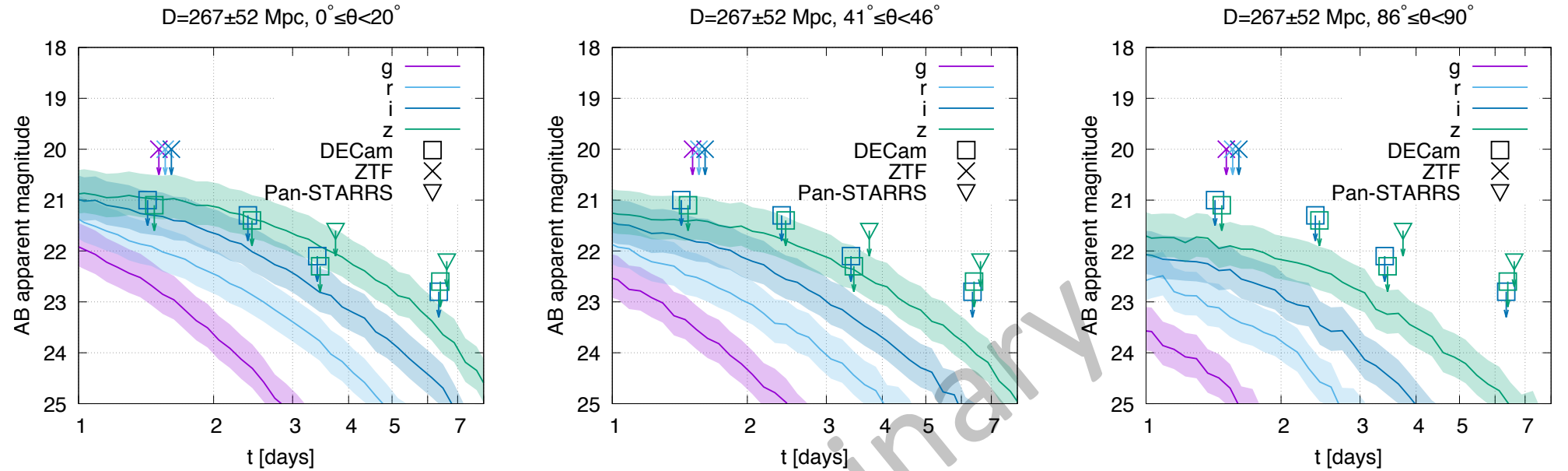
Ref) [Andreoni et al. \(2019\)](#)

**Can we constrain the binary parameters from EM upper limits?**

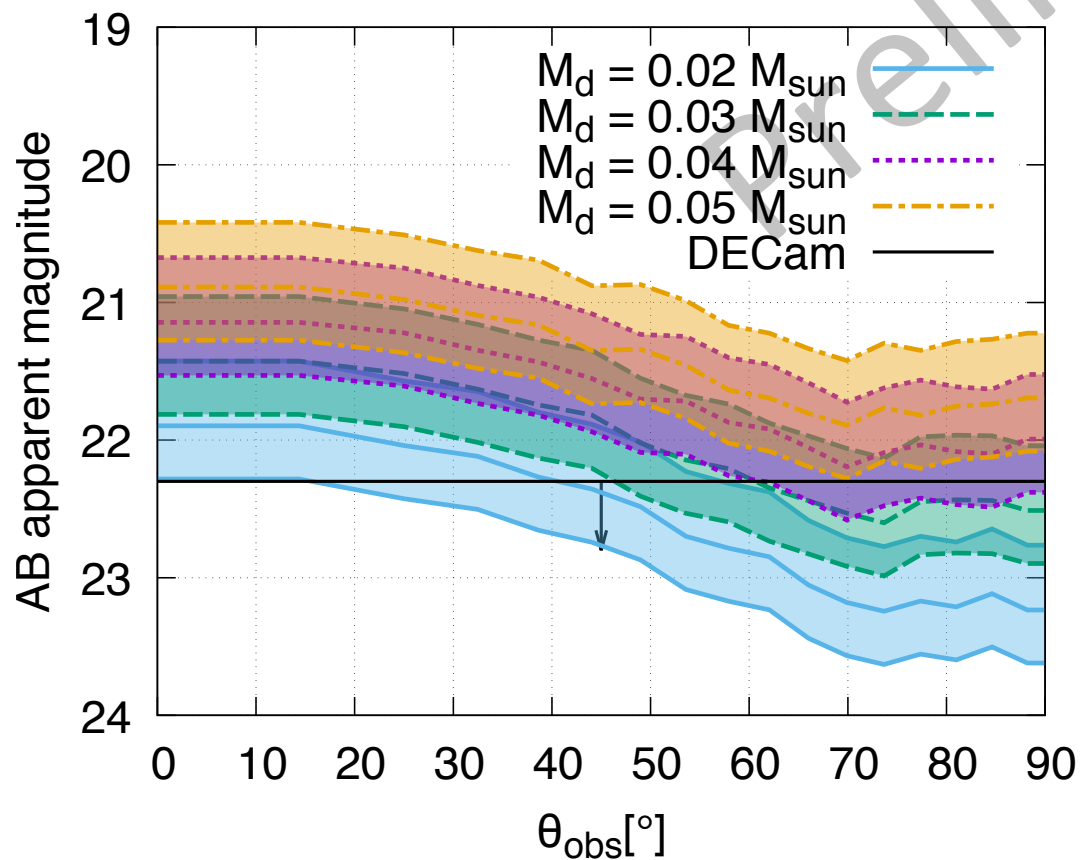
# Constraint on the ejecta mass

$$m_d = 0.02 M_\odot$$

$$m_{pm} = 0.02 M_\odot$$

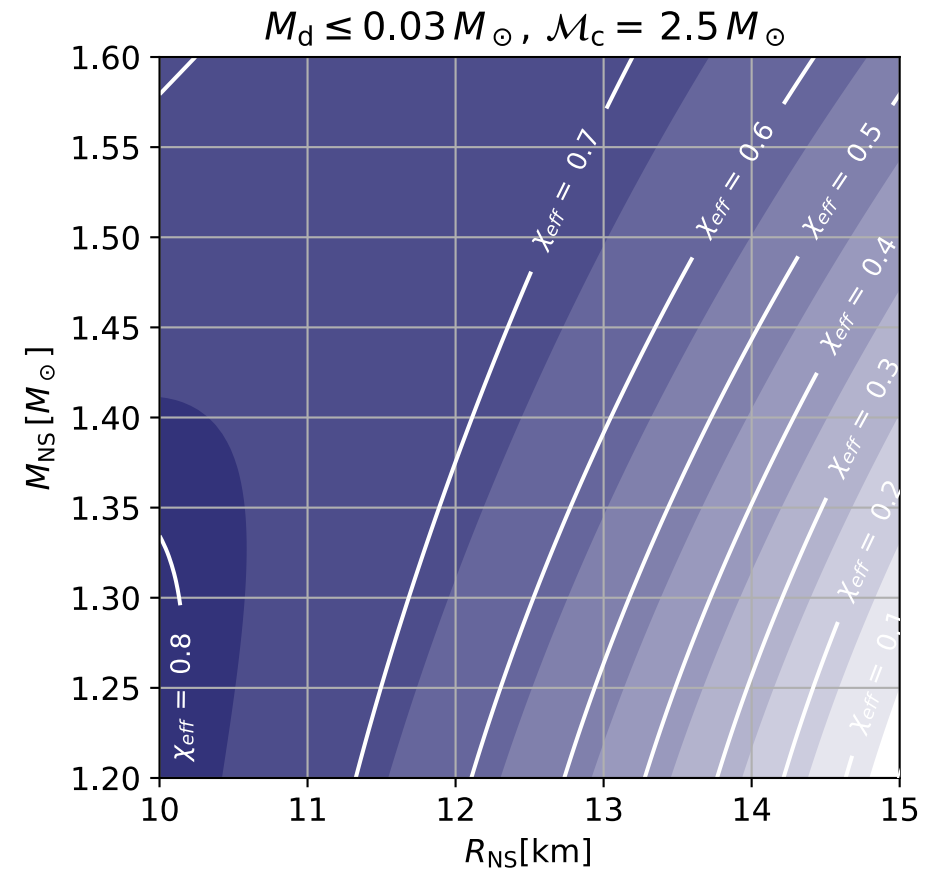


$D=267\pm 52$  Mpc, z band,  $t=3.43$  d  
 $M_{pm} = M_d$



**$M_d \leq M_{pm}$  is assumed**  
 since the remnant torus mass is typically much larger than the dynamical ejecta mass (see e.g., Kyutoku et al. 2015)

Shaded regions denote the uncertainty due to the error bar in the distance measurement



# Summary

- Analytical/numerical studies for compact binary mergers have been enable us to achieve comprehensive understanding of observations.
- GW170817 achieved the measurement of the NS tidal deformability and confirmed that GW observation has a great impact on NS physics.
- The simultaneous observation of EM counterparts to GW170817 marked up the beginning of multi-messenger astronomy era.
- More and more GW events with more precise measurements of physical parameters would be achieved in the future.
- Further theoretical investigation is needed to maximize the scientific returns from the GW/EM events.

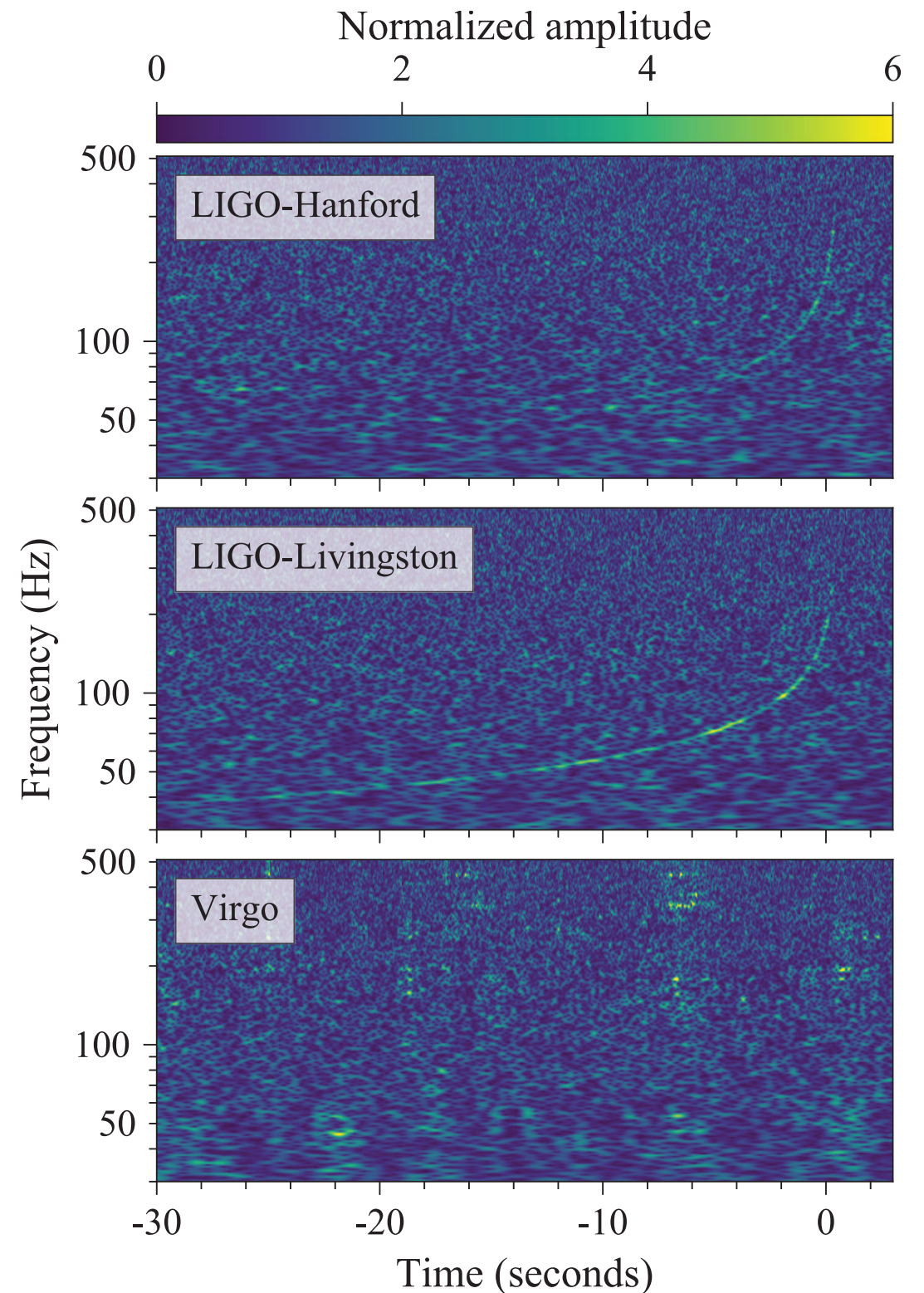
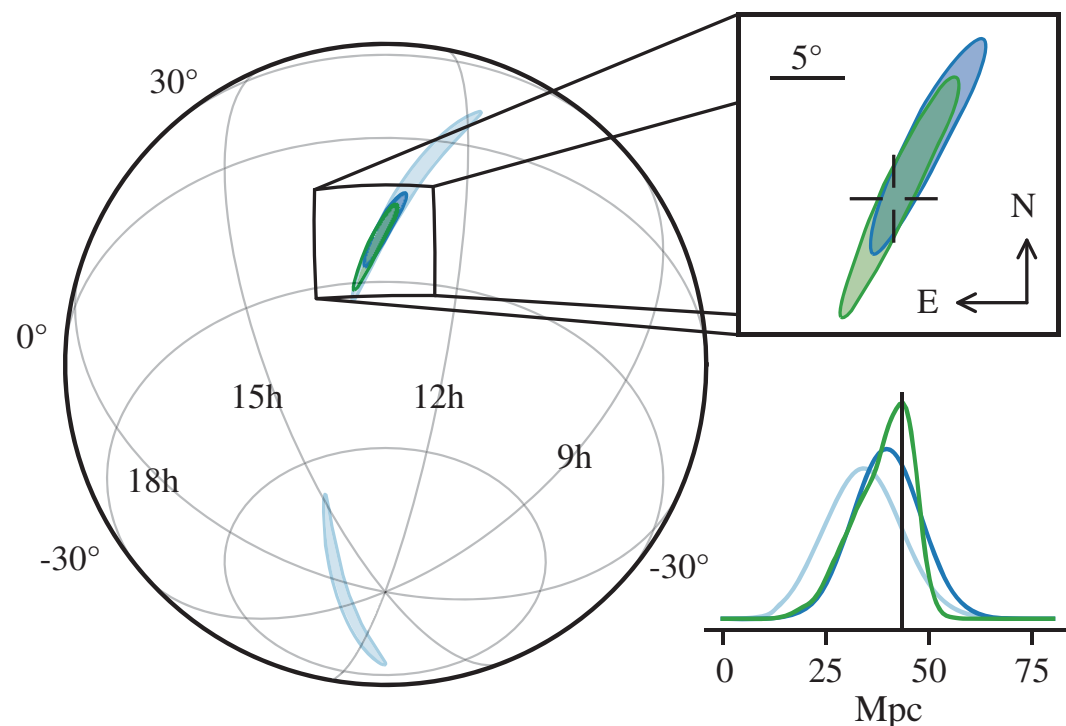
# Appendix



The first NS-NS merger event:  
GW170817

# GW170817

- On 17th of August 2017, LIGO and Virgo reported the first detection of gravitational waves from a binary NS (BNS; NS+NS binary) merger
- SNR=32.4
- Distance  $\sim 40$  Mpc
- Sky localization:  $28 \text{ deg}^2$

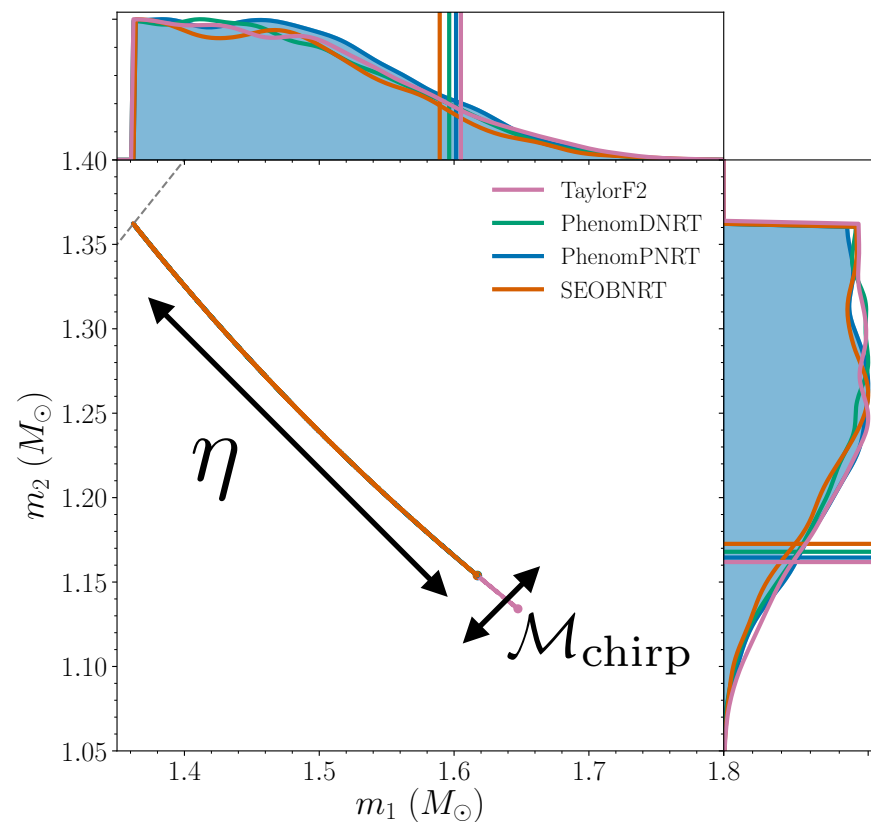


# GW170817: Constraints on binary parameters

- Binary parameters were constrained tightly as ever was (SNR~32), and **the tidal deformability** is indeed measured (constrained) in this event

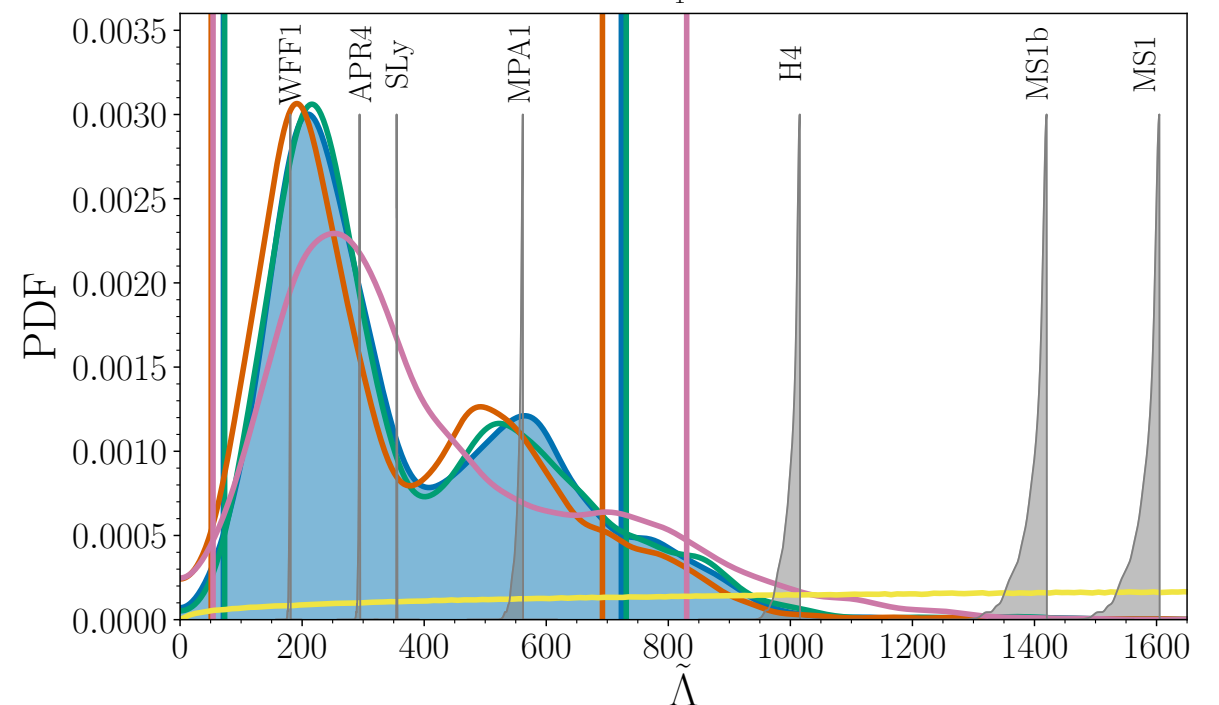
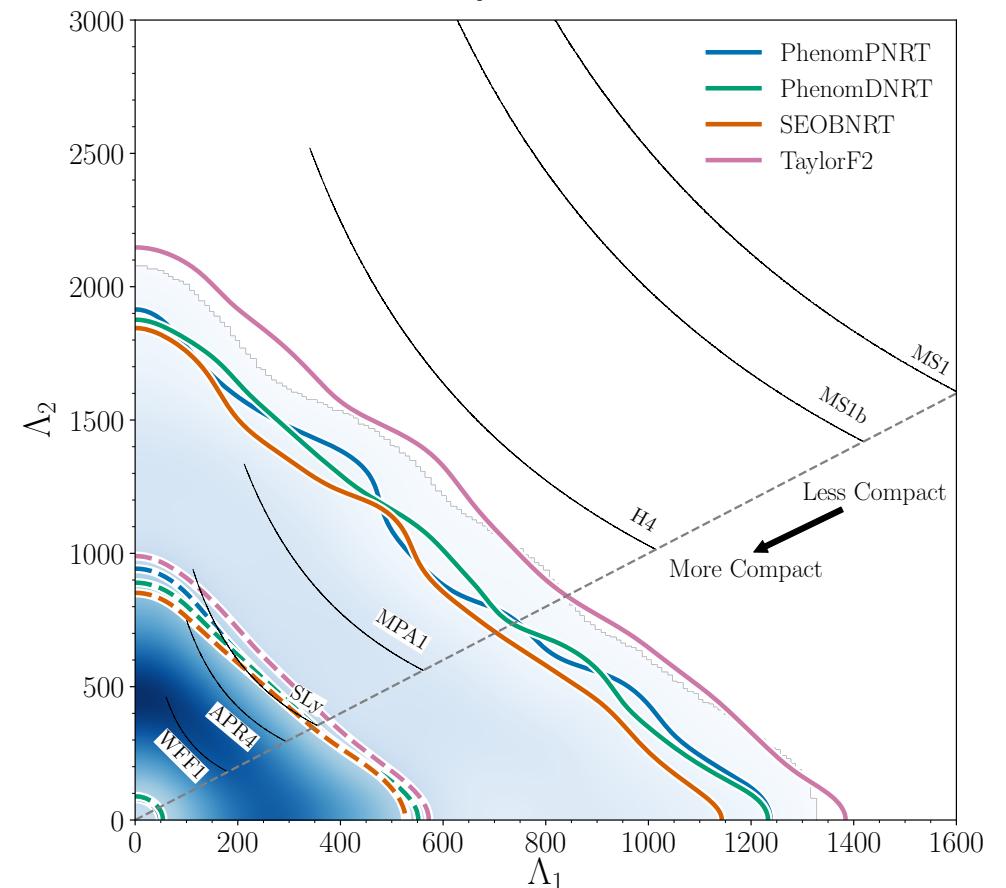
$$\tilde{\Lambda} = \frac{16}{13(1+q)^5} [(1+12q)\Lambda_1 + (12+q)q^4\Lambda_2]$$

Masses of the binary components



Tidal deformability

Ref: LIGO/Virgo 2017,2018



# GW170817: Constraints on binary parameters

Ref: LIGO/Virgo 2018

	Low-spin prior ( $\chi \leq 0.05$ )	High-spin prior ( $\chi \leq 0.89$ )
Binary inclination $\theta_{\text{JN}}$	$146_{-27}^{+25}$ deg	$152_{-27}^{+21}$ deg
Binary inclination $\theta_{\text{JN}}$ using EM distance constraint [104]	$151_{-11}^{+15}$ deg	$153_{-11}^{+15}$ deg
Detector frame chirp mass $\mathcal{M}^{\text{det}}$	$1.1975_{-0.0001}^{+0.0001} M_{\odot}$	$1.1976_{-0.0002}^{+0.0004} M_{\odot}$
Chirp mass $\mathcal{M}$	$1.186_{-0.001}^{+0.001} M_{\odot}$	$1.186_{-0.001}^{+0.001} M_{\odot}$
Primary mass $m_1$	(1.36, 1.60) $M_{\odot}$	(1.36, 1.89) $M_{\odot}$
Secondary mass $m_2$	(1.16, 1.36) $M_{\odot}$	(1.00, 1.36) $M_{\odot}$
Total mass $m$	$2.73_{-0.01}^{+0.04} M_{\odot}$	$2.77_{-0.05}^{+0.22} M_{\odot}$
Mass ratio $q$	(0.73, 1.00)	(0.53, 1.00)
Effective spin $\chi_{\text{eff}}$	$0.00_{-0.01}^{+0.02}$	$0.02_{-0.02}^{+0.08}$
Primary dimensionless spin $\chi_1$	(0.00, 0.04)	(0.00, 0.50)
Secondary dimensionless spin $\chi_2$	(0.00, 0.04)	(0.00, 0.61)
Tidal deformability $\tilde{\Lambda}$ with flat prior	$300_{-190}^{+500}$ (symmetric) / $300_{-230}^{+420}$ (HPD)	
		(0, 630)

- Chirp mass gives rigid lower limit to the total mass

$$m = \mathcal{M}_{\text{chirp}} \eta^{-3/5} \geq 2.72 M_{\odot}$$

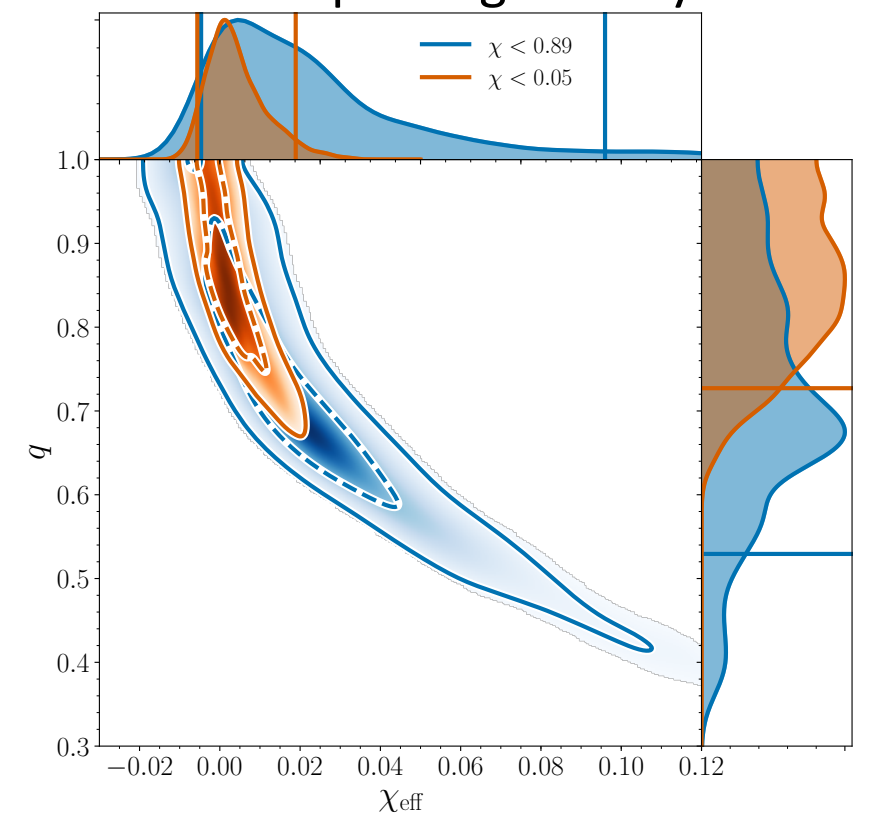
- Tidal deformability:  $\tilde{\Lambda} < 800$  (90%)

or

$$\Lambda_{1.4} < 800 \text{ (90\%)}$$

※  $\tilde{\Lambda}$  depends only weakly on the mass ratio for fixed chirp mass

Mass ratio-spin degeneracy

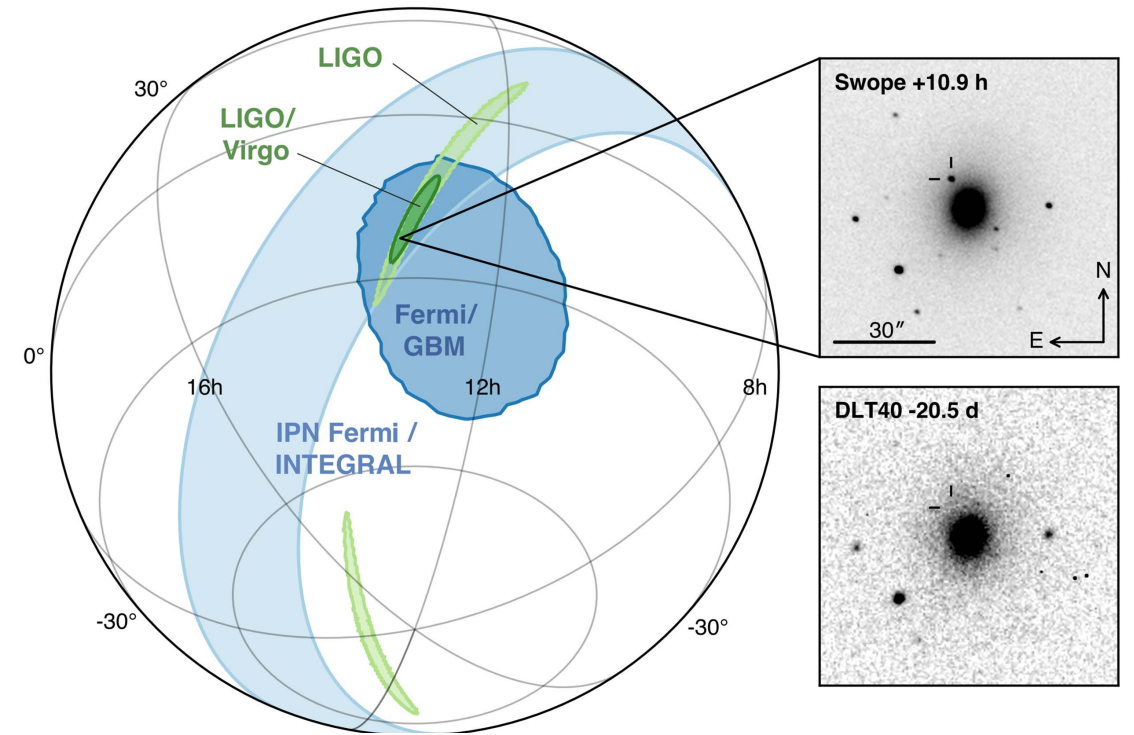




# GW170817:

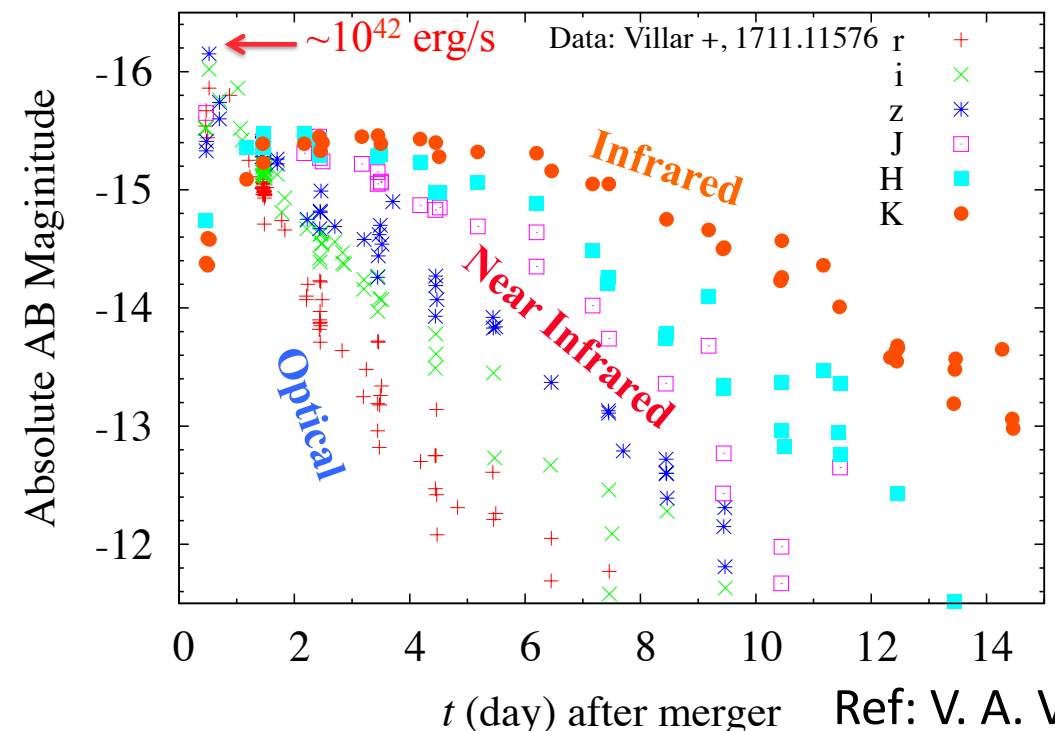
## Electromagnetic Counterparts

- Electromagnetic (EM) counterparts to GW170817 were observed simultaneously over the entire wavelength range (from radio to gamma wavelengths)
- The follow-up observation of the electromagnetic counterparts allowed us to identify the host galaxy (NGC4993:  $\sim 40$  Mpc)
- Observed lightcurves and spectra provided the physical implication to the merger  $\sim$  post-merger dynamics of the system (property of merger remnant, **r-process nucleosynthesis**, existence of relativistic jets,...)



Ref: P. S. Cowperthwaite 2017

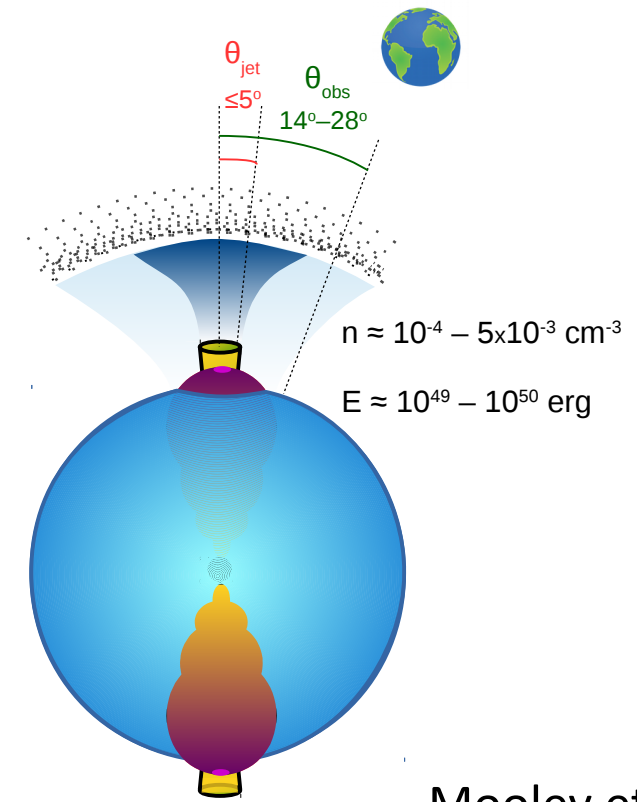
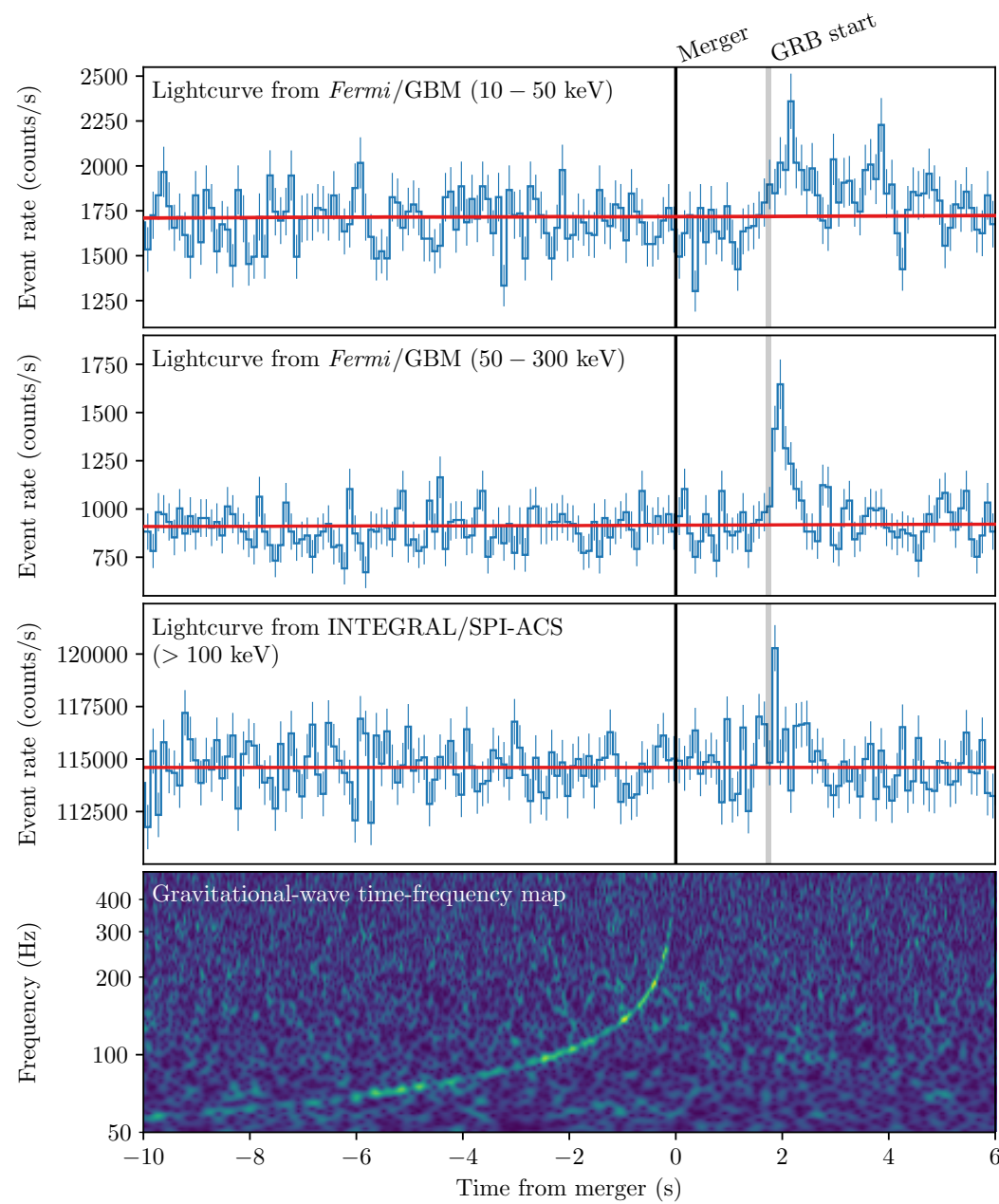
### Optical-IR EM counterparts of GW170817





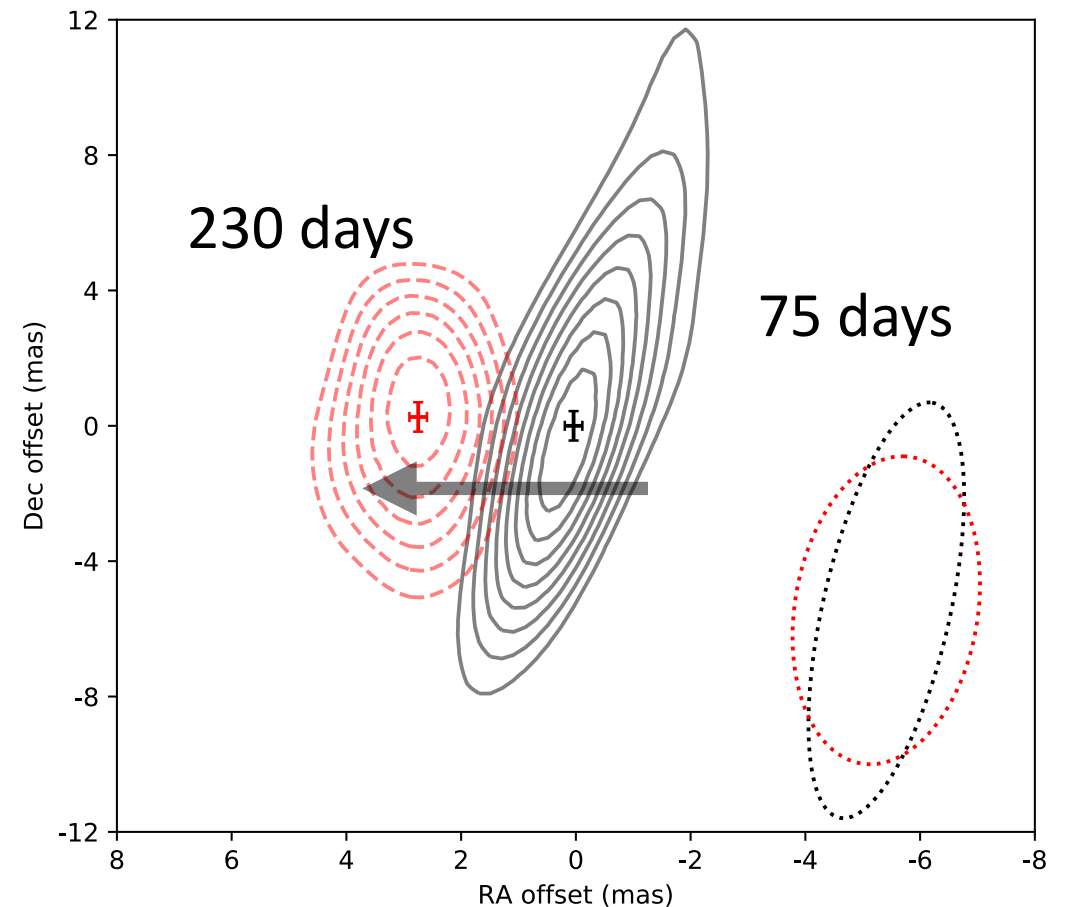
# Gamma ray burst?

Ref: LIGO/Virgo/Fermi/INTEGRAL 2017



Mooley et al. 2018

Radio observation (VLBI)

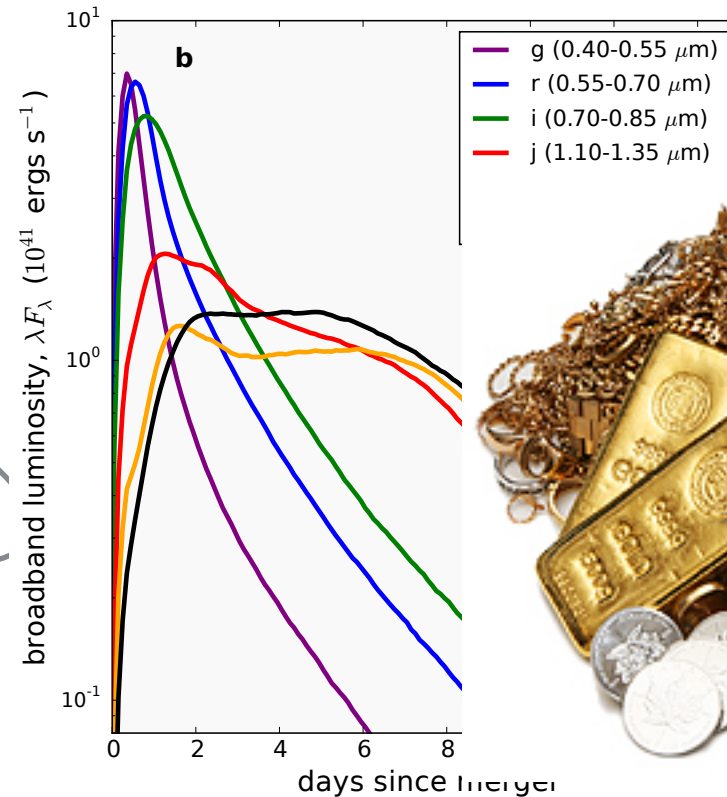
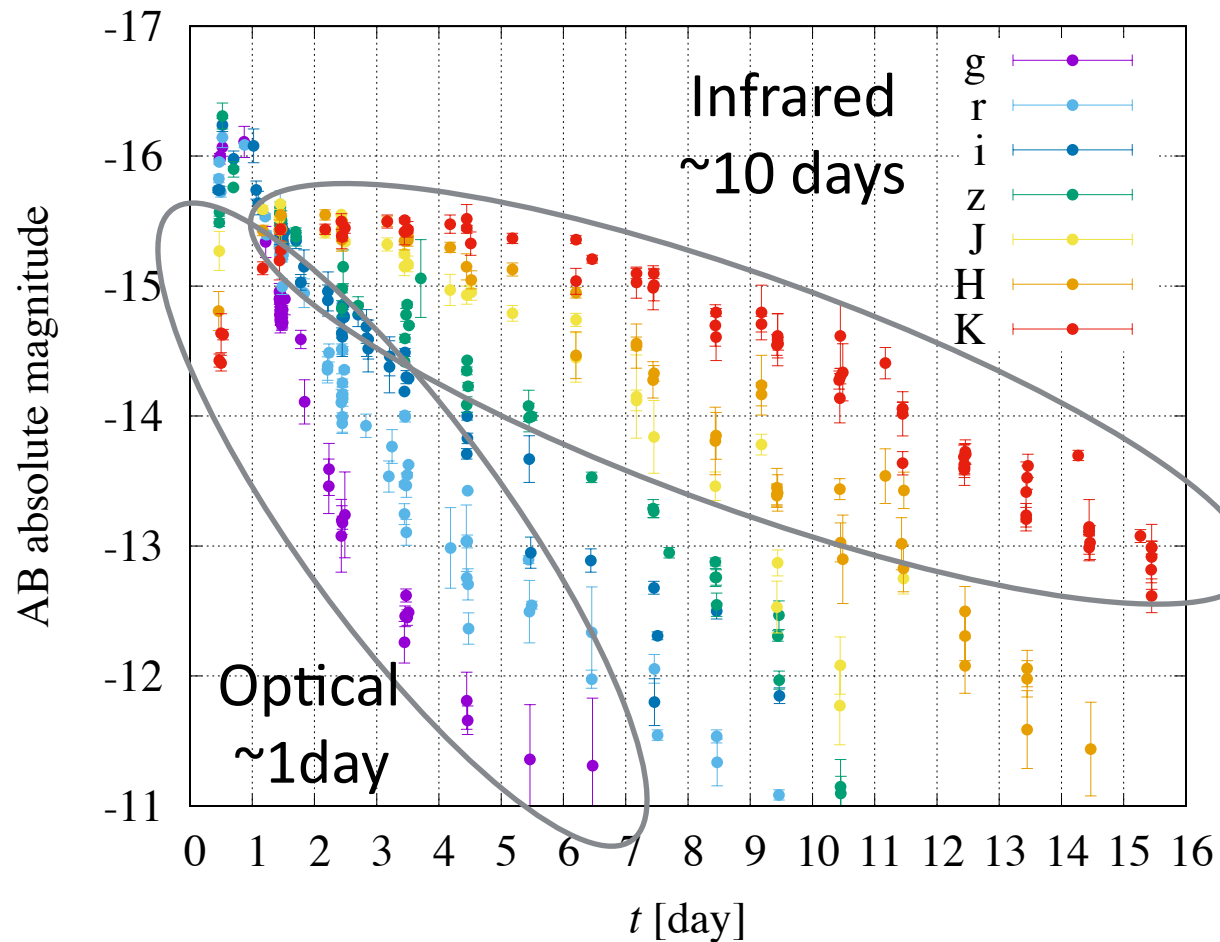


- Gamma ray signal was detected 1.7s after the GW trigger ...however, not typical short hard GRB?
- Superluminal motion of the radio counterpart → existence of a relativistic jet

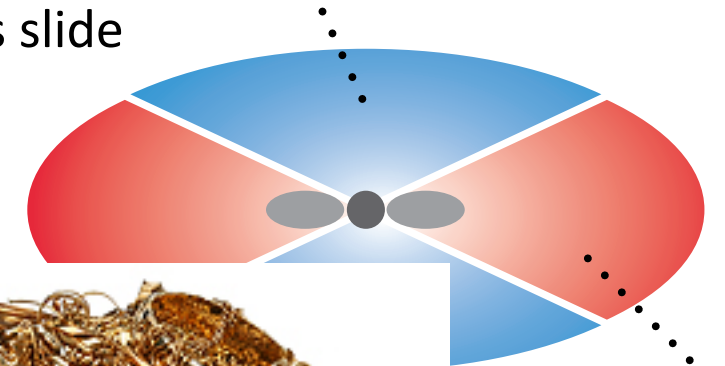
# GW170817:

## Kilonova/macronova with multiple components

Data: Summarized in Villar et al. 2017  
D=40 Mpc



Blue (lanthanide-free)  
ref) Masaomi's slide



lanthanide-rich



ref) D. Kasen et al. 2017

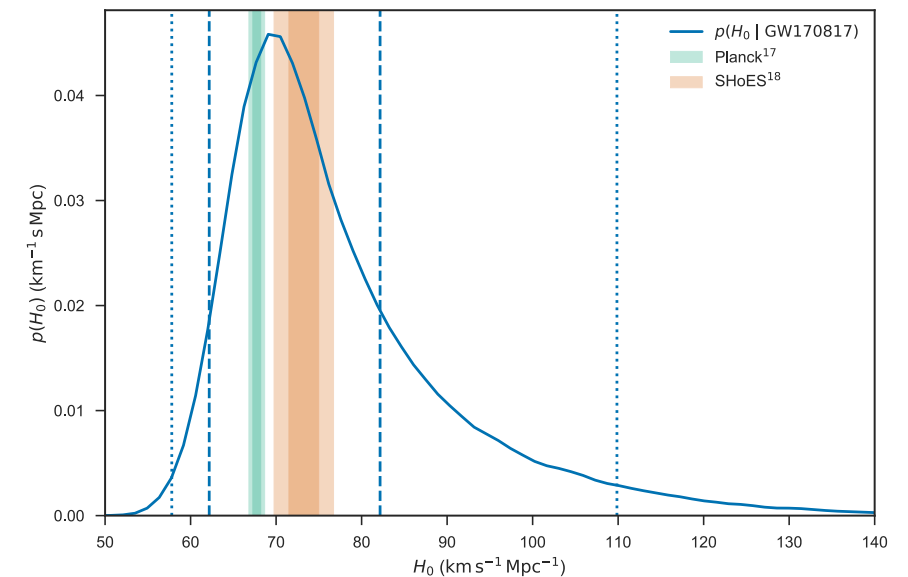
• **A Kilonova/macronova model with multiple components well interprets the optical-Infrared observation** (see e.g., Kasliwal et al. 2017, Cowperthwaite et al. 2017, Kasen et al. 2017, Villar et al. 2017)

- early-blue component (~1day) from **lanthanide-free ejecta** (~0.01  $M_{\text{sun}}$ , opacity ~0.1-1  $\text{cm}^2/\text{g}$ )  
+ long-lasting red component (~10days) from **lanthanide-rich ejecta** (~0.04  $M_{\text{sun}}$ , opacity ~10  $\text{cm}^2/\text{g}$ )

✳radiation transfer effect among the multiple ejecta components would change the ejecta mass estimation

# Multi-messenger Astronomy

- The first opportunity of **multi-messenger astronomy** with the combination GW and EM observation
- Host galaxy + GW luminosity distance  
→ Hubble parameter
- Time delay of Gamma ray observation:  
→ GW propagation speed
- Tidal deformability + EM Constraint  
→ Tighter limit on the NS property  
(e.g. Radice & Dai 2018, Kiuchi et al. 2019)

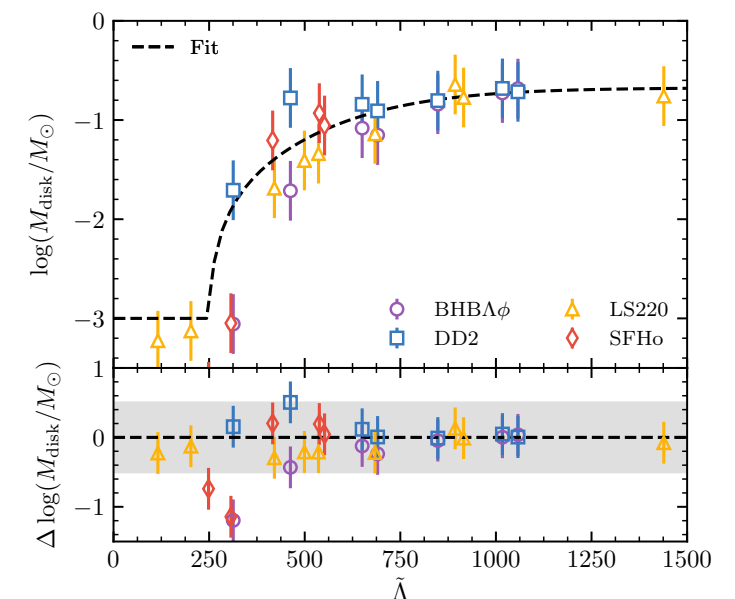


Ref: LIGO/Virgo 2017

$$-3 \times 10^{-15} \leq \frac{\Delta v}{v_{EM}} \leq +7 \times 10^{-16}$$

$$\Delta v = v_{GW} - v_{EM}$$

Ref: LIGO/Virgo/Fermi/INTEGRAL 2017



Ref: Radice & Dai 2018

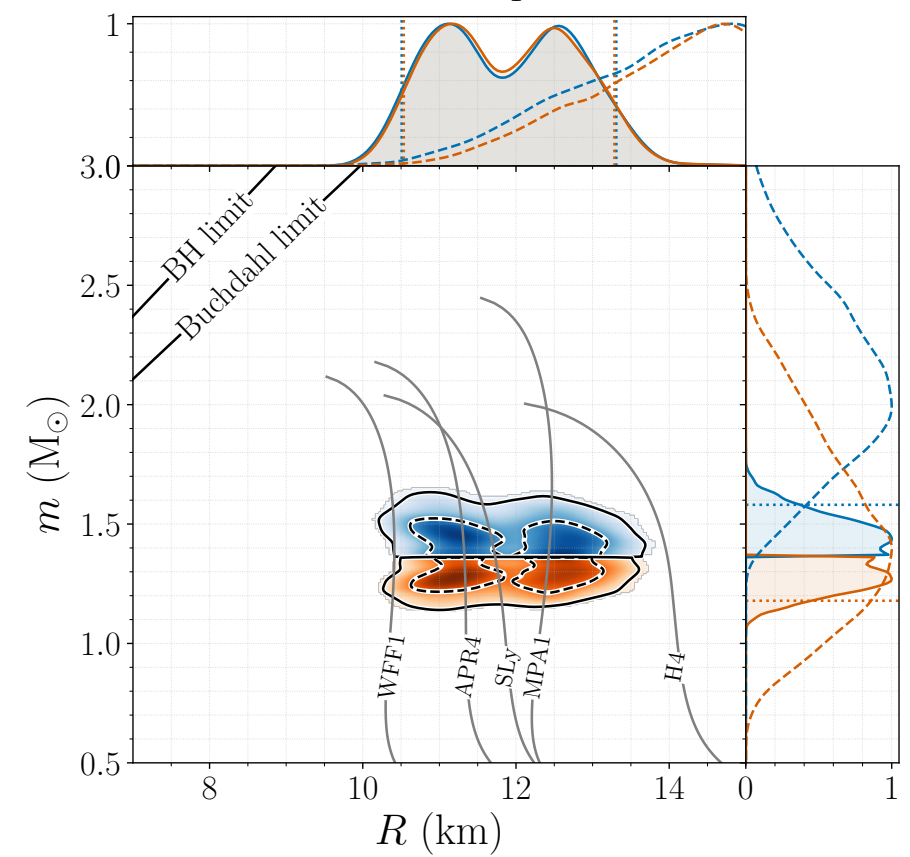
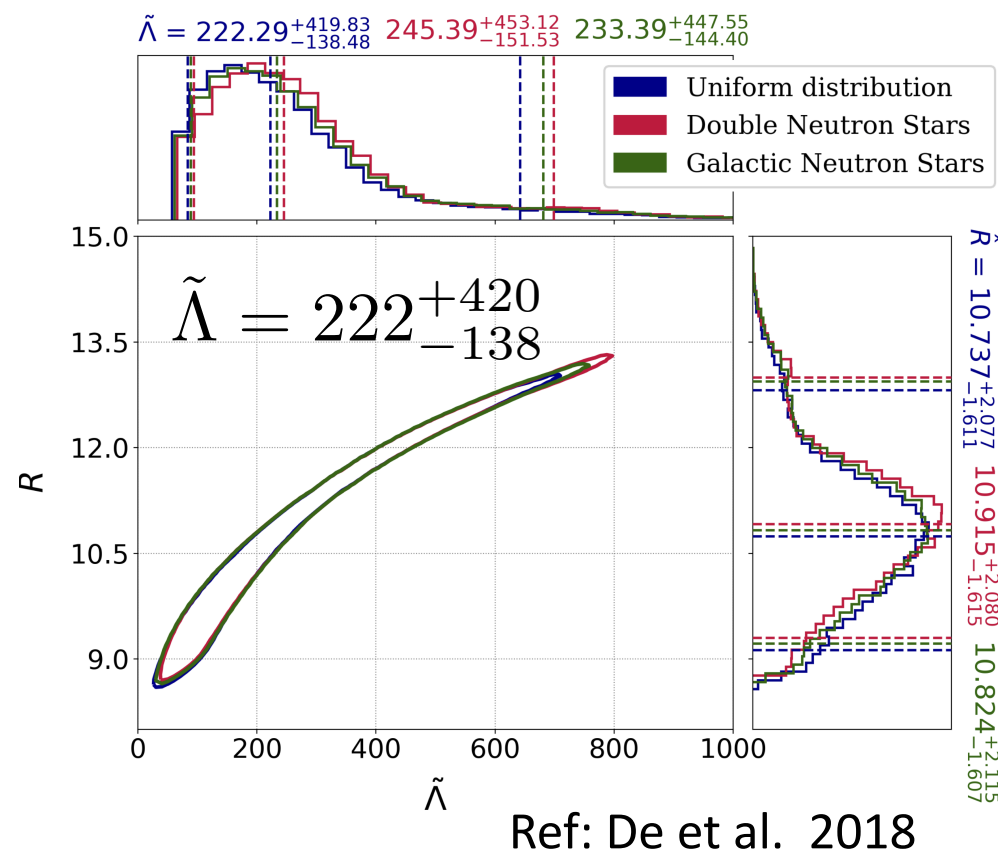
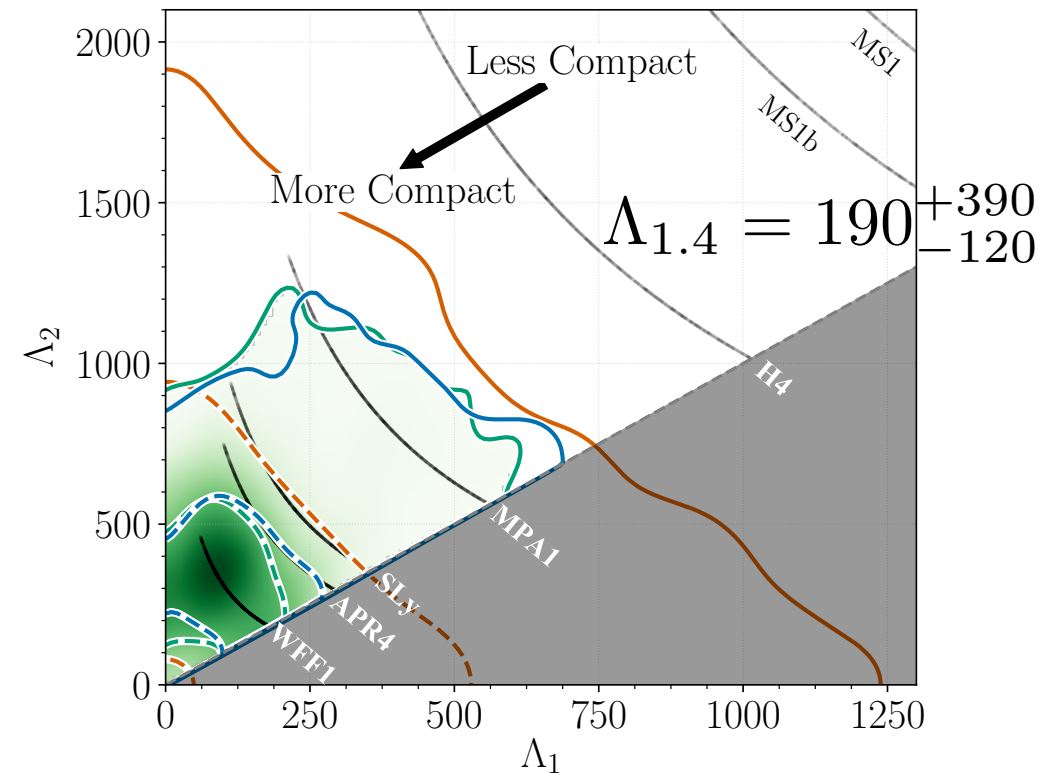
# GW170817: Further constraints on $\Lambda$ /Radius/Maximum mass

- Analysis of GW data with further assumptions
- Lower limit on the NS tidal deformability / radius based on EM observation
- Upper limit on the maximum mass based on EM observation

# Analysis of GW data with further assumptions

- Tighter constraints on the NS tidal deformability and radius are obtained by considering
  - the same NS EoS for two objects (c.f. twin stars)
  - current lower limit for the NS maximum mass ( $M_{\text{max}} > 1.97 M_{\text{sun}}$  : Antoniadis et al. 2013)

Ref: LIGO/Virgo 2018

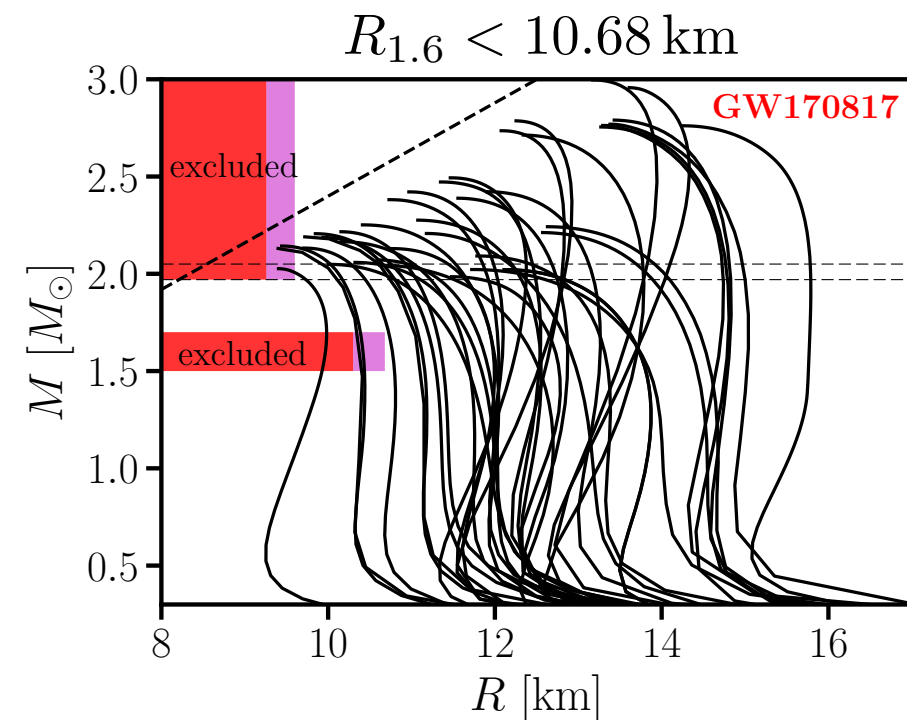
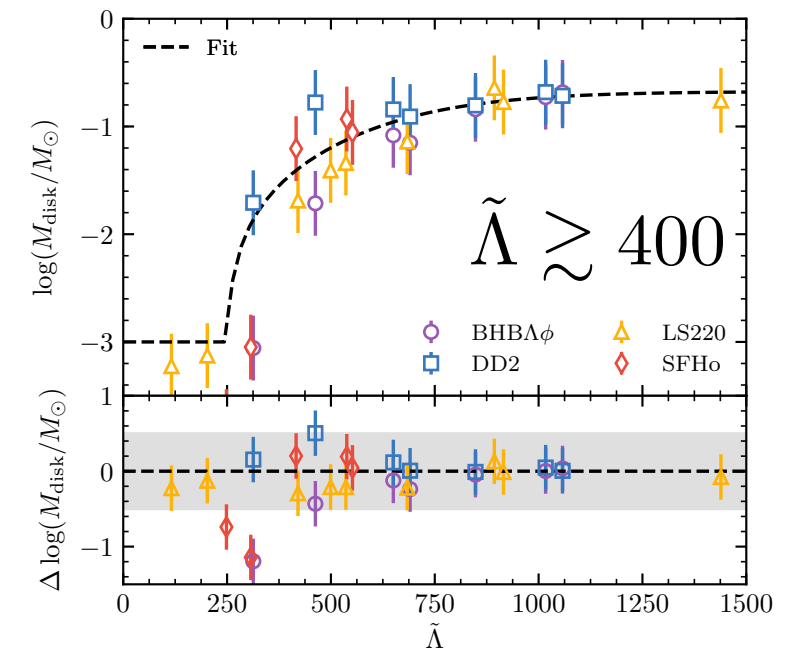




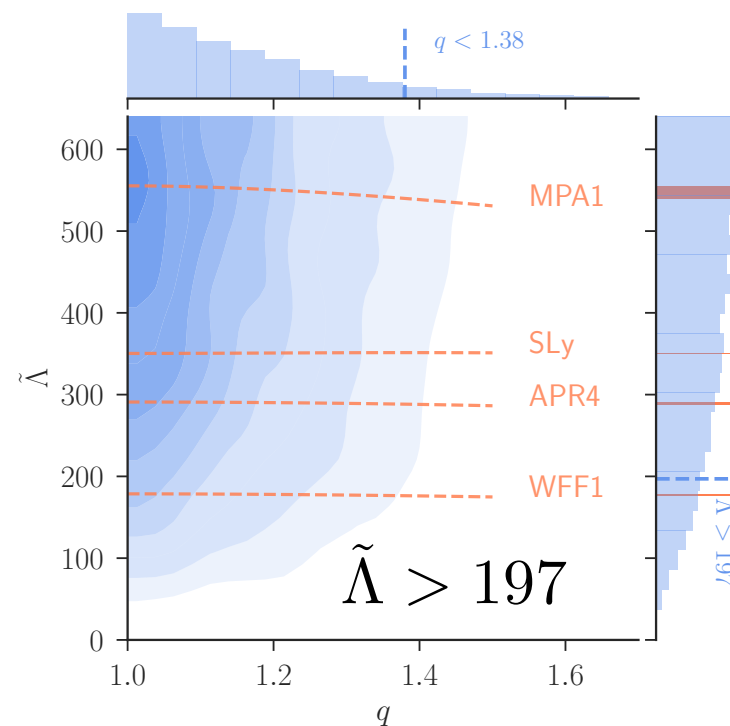
# Lower limit on the NS tidal deformability / radius

Ref: Radice & Dai 2018

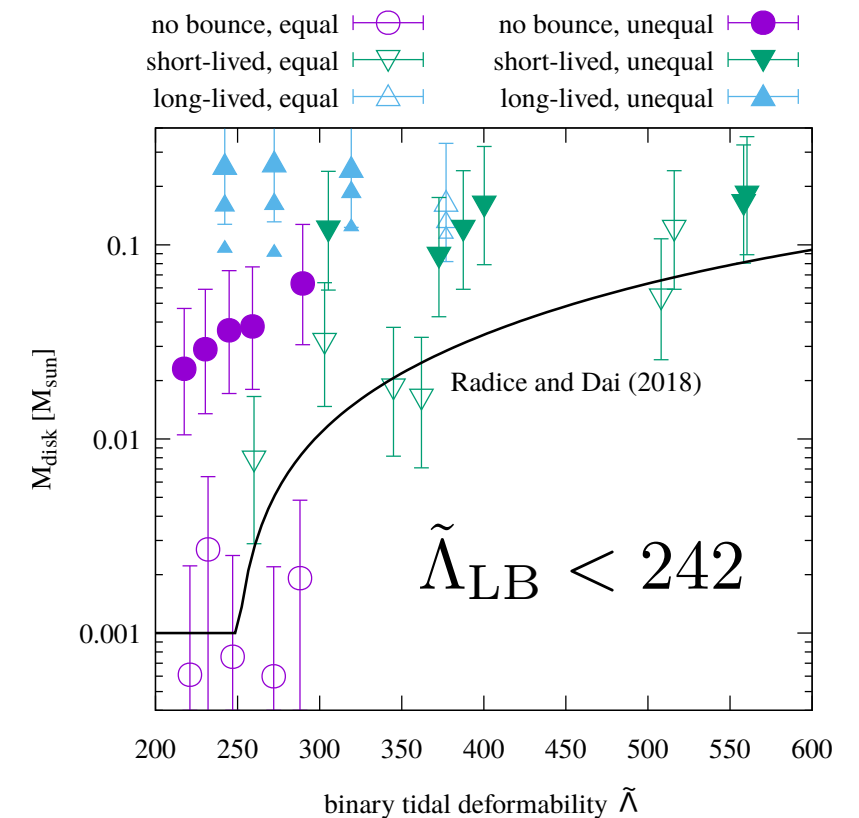
- Constraints from the fact that EM counterparts are observed
- Lower limit on the NS tidal deformability / radius based on the prediction of numerical relativity simulations



Ref: Bauswein et al. 2017



Ref: Coughlin et al. 2018

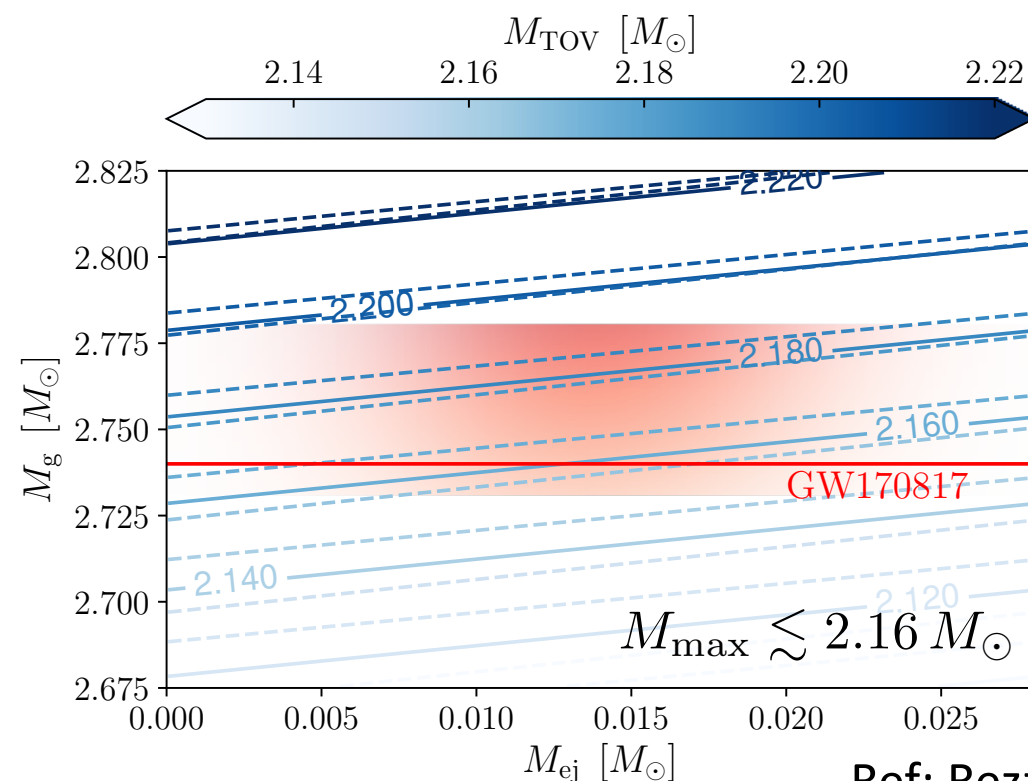


Ref: Kiuchi et al. 2019

# Upper limit on the NS maximum mass

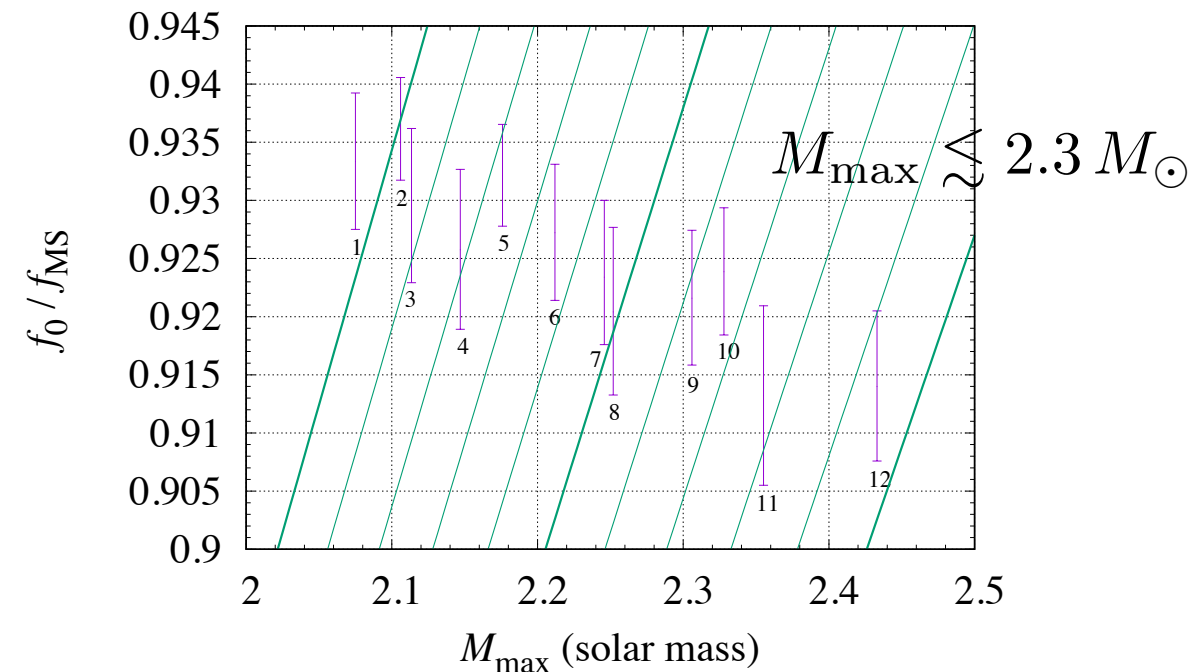
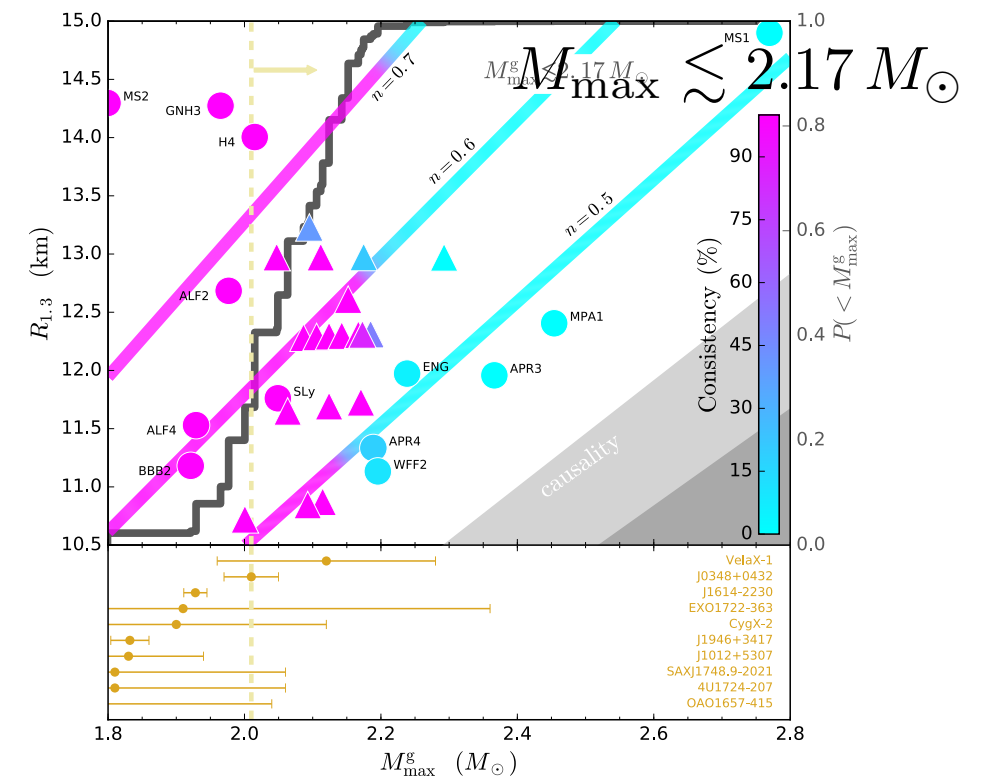
- Upper limit on the NS maximum mass from the fact that the remnant NS is likely to be temporarily survived and collapsed eventually to a BH
- Presence of EM counterparts
- No observation of magnetor-like activity
- GRB association

$$M_{\max, \text{rot}} \approx 1.2 M_{\max}$$



Ref: Rezzolla et al. 2018

Ref: Margalit & Metzger 2017



Ref: Shibata et al. 2019